8-2013

Modulation of Bax/Bak Dependent Apoptosis by Sirtuin 3 and Mitochondrial Permeability Transition by Sirtuin 4

Manish Verma
Rowan University

MANISH VERMA

MODULATION OF BAX/BAK DEPENDENT APOPTOSIS BY SIRTUIN 3 AND MITOCHONDRIAL PERMEABILITY TRANSITION BY SIRTUIN 4

MODULATION OF BAX/BAK DEPENDENT APOPTOSIS BY SIRTUIN 3 AND MITOCHONDRIAL PERMEABILITY TRANSITION BY SIRTUIN 4

Manish Verma B.S., M.S.

A Dissertation submitted to the Graduate School of Biomedical Sciences, Rowan University in partial fulfillment of the requirements of the Ph.D. Degree.

Stratford, New Jersey 08084

August 2013

Table of Contents

Acknowledgements

Firstly, I would like to thanks my parents for their constant support. Secondly, I would like to thank my lab members, specially, my mentor Dr. John G. Pastorino. Without his support and constant guidance this work would not have been possible. I would also like to thank Dr. Catherine Neary and Nataly Shulga for helping me with experiments and troubleshooting them. I would also like to thank my committee members, Dr. Michael Henry, Dr. Robert Nagele, Dr. Gary Goldberg and Dr. Venkat Venkataraman for taking time off from their busy schedule and attend the committee meetings and always making sure that I was on the right track and making progress. I would also like to thank the Graduate School of Biomedical Sciences at UMDNJ-SOM and our program director Dr. Diane Worrad for giving me an opportunity and accepting me into the Ph.D. program.

Lastly, the studies presented here were supported by grants from National Cancer Institute (5RO1CA118356) and National Institute of Alcohol Abuse and Alcoholism (5RO1AA01287)

Abstract

Mitochondria are dynamic organelles that regulate a myriad of cellular functions, including energy production and metabolic regulation. Mitochondria are also a critical regulator of cell death signaling cascades modulating both apoptotic and necrotic cell death. However, what determines which cell death pathway is activated is still unclear. The mitochondrial/intrinsic pathway of apoptosis is dependent on the activation of pro-apoptotic proteins, Bax and Bak, which induce mitochondrial outer membrane permeabilization (MOMP). Once the integrity of outer mitochondrial membrane (OMM) is compromised, pro-apoptotic intermembrane space proteins like cytochrome c, Smac/Diablo, Omi/HtrA2 and AIF are released into the cytoplasm, which activates the post-mitochondrial phase of apoptosis.

In humans, there are seven sirtuins (Sirt1-7), three of which are localized to the mitochondria (Sirt3-5). Sirt3 and Sirt5 have acetyltransferase activity, whereas Sirt4 has ADP-ribosyltransferase activity. Sirt3 is the major deacetylase in the mitochondrial matrix, and regulates various metabolic pathways by modulating the acetylation status of key metabolic enzymes. Although, metabolic regulation by Sirt3 has been studied extensively, the role of Sirt3 in cancer progression and regulation of the apoptotic pathway remains unclear.

To sustain their rapid growth, cancer cells have a high glycolytic rate. This is achieved by overexpression of a key glycolytic enzyme, hexokinase II (HKII), which attaches to the OMM. HKII binding to the OMM transmembrane voltage-dependent anion channel (VDAC) protein renders cancer cells resistant to a variety of cell death stimuli (e.g. DNA damage, oxidative stress and TNFα) by inhibiting activation of

Bax/Bak. In this thesis, I present evidence that Sirt3 acts a mitochondrial localized tumor suppressor by modulating the binding of HKII on the OMM. Sirt3 dependent dissociation of HKII from the OMM increases activation of pro apoptotic protein Bax/Bak in response to pro death stimuli, t-Bid and cisplatin.

In contrast to apoptosis, opening of a multiprotein mitochondrial permeability transition pore (MPTP) by oxidative stress or mitochondrial calcium overload leads to necrotic cell death. The constituents of the MPTP, though controversial, consist of cyclophilin-D in the matrix, adenine nucleotide translocator (ANT) in the inner mitochondrial membrane, and VDAC on the OMM. Sirt4-mediated ribosylation of glutamate dehydrogenase-1 (GDH-1) inhibits its activity. In the second part of this thesis, I demonstrate that Sirt4 regulates the induction of the permeability transition by regulating the activity of GDH-1. Downregulation of Sirt4 inhibits PTP induction by calcium overload and the thiol reactive agent phenylarsine oxide by increasing GDH-1 activity. Similarly, in intact cells, depletion of Sirt4 protected against PTP induction by cytotoxic drugs like TNFα and doxorubicin. The evidences presented here demonstrate possible mechanisms by which mitochondria, more specifically, Sirt3 and Sirt4 modulate apoptotic and necrotic cell death respectively

Introduction

Mitochondria are dynamic cellular organelles long considered the powerhouse of the cell, involved in generation of ATP, the energy currency of the cell. Mitochondria are intimately involved in cellular homeostasis. In the last 50 years, significant progress has been made in mitochondrial research, such that mitochondria are now considered to be more than just ATP generators. Apart from generating energy for the cell, they participate in intracellular signaling and apoptosis, intermediary metabolism, and in the metabolism of amino acids, lipids, cholesterol, steroids and nucleotides. Structurally, mitochondria contain two membranes that separate two distinct compartments: intermembrane space and matrix. The inner membrane is highly folded into cristae, which house the complexes of the electron transport chain and ATP synthase.

The first indications that mitochondria participated in the regulation of apoptosis came from the study of *Caenorhabditis elegans*. The worm Ced-9 protein (an ortholog of human B cell lymphoma 2), a component of core apoptotic machinery, was found to be attached to the mitochondrial outer membrane (Hengartner et al., 1992). Subsequent studies in a wide variety of organisms made it clear that mitochondria actively participate in regulation of the programmed cell death (Kroemer et al., 2007). It also became evident that mitochondrial outer membrane permeabilization (MOMP) is a near universal event that marks the point of no return of multiple signal transduction cascades leading to cell death, including apoptosis and necrosis (Galluzzi et al., 2012a). These experiments established that mitochondria occupy a central position in the regulation of cell death (Tait and Green, 2010).

The discovery that dissipation of the mitochondrial transmembrane potential ($\Delta\Psi_m$) constitutes an early and irreversible step in the cascade of events leading to apoptotic cell death demonstrated that mitochondria are not simply a metabolic organelle (Zamzami et al., 1995). Mitochondria not only modulate apoptosis triggered by alteration in the intracellular milieu (intrinsic apoptosis) but also participate in the regulation of the apoptotic response to external stimuli (extrinsic apoptosis) (Tait and Green, 2010). Mitochondria also control non-apoptotic cell death, like necrosis (Vitale et al., 2011).

Mitochondria and Apoptosis

The term apoptosis was first coined in 1972 by Kerr *et al* (Kerr et al., 1972). Later, studies in the nematode *C. elegans* led to our understanding that apoptosis is a controlled process important for the development of this organism. For example, 131 of 1090 somatic cells undergo apoptosis or programmed cell death (Horvitz, 1999). Even though apoptosis is a controlled process, there is heterogeneity within a population of cells when they are challenged with apoptotic stimuli. When populations of cells are treated with death-inducing ligands, some cells may undergo apoptosis, some might be affected only slightly, while others are unaffected. In some cases, the strength of the stimulus dictates the mechanism of cell death. At low doses, various stimuli, such as heat, radiation, hypoxia and cytotoxic drugs, can induce apoptosis. If the same stimulus is given at higher doses, cell death can be due to necrosis (described later). Apoptosis is a controlled and energy-dependent process that requires activation of cysteine aspartate proteases (caspases) which leading to a complex cascade of events and ultimately cell death.

Morphology of Apoptosis

Apoptosis is characterized by cell shrinkage and pyknosis. Cells decrease in size and the cytoplasm appears more condensed due to tight packing of the cytoplasmic organelles. Pyknosis is irreversible chromatin condensation in the nucleus. There is also extensive plasma membrane blebbing, followed by karyorrhexis and separation of the cell fragments into apoptotic bodies in a process called budding. These bodies consist of cytoplasm with tightly packed organelles with or without nuclear fragments. These bodies are phagocytosed by macrophages, parenchymal cells or neoplastic cells and degraded within phagolysosomes. During apoptosis, there is no inflammatory response because: (1) the process is controlled and there is no release of cytoplasmic contents into the surrounding interstitial tissue; (2) apoptotic cells are destroyed by phagocytosis thereby preventing the occurrence of secondary necrosis; and, (3) the phagocytes themselves do not produce any anti-inflammatory cytokines (Kerr et al., 1972).

Biochemical features of Apoptosis

Biochemical modifications associated with apoptosis include protein cleavage (caspases), protein cross-linking and DNA fragmentation. Caspases are expressed as inactive zymogens, and once activated, they further activate themselves (feedback loop) to cleave and activate other caspases. This proteolytic caspase cascade in which one caspase activates other caspases amplifies the apoptotic signaling pathway and leads to cell death. Once caspases are activated there is an irreversible commitment towards cell death. To date, 10 major caspases have been identified and are categorized as either

initiators (caspase -2,-8,-9,-10), effectors/executioners (caspase-3,-6,-7) or inflammatory caspases (caspase-1,-4,-5) (Cohen, 1997; Rai et al., 2005).

During apoptosis, activation of endonucleases results in DNA fragments of 180 to 200 base pairs. On agarose gel electrophoresis, a characteristic DNA ladder is visualized with ethidium bromide and ultraviolet illumination. Early exposure of cell surface markers during apoptosis results in early phagocytosis of apoptotic cells by macrophages, thus preventing damage to the surrounding tissues. This is achieved by the movement of the normally inward-facing phospholipid phosphatidylserine (PS), in the inner leaflet of the plasma membrane bilayer to the outer leaflet (Bratton et al., 1997). This externalization of PS marks the cell for engulfment by phagocytes.

Mechanisms of Apoptosis

Apoptosis is a highly controlled, sophisticated energy-dependent cascade of events. Generally, the pathways can be divided into two: the extrinsic or death receptor pathway, and the intrinsic or the mitochondrial pathway. Although these two pathways are distinct in a number of ways, there is a cross talk between them. The extrinsic and intrinsic pathways both result in DNA fragmentation, degradation of cytoskeletal and nuclear proteins, cross-linking of proteins, formation of apoptotic bodies, expression of ligands for phagocytic cell receptors, and, finally, engulfment by phagocytic cells (Igney and Krammer, 2002).

Extrinsic Apoptotic pathway

As the name suggests, the extrinsic apoptotic pathway originates from transmembrane receptor-mediated interactions at the plasma membrane. These receptors belong to the tumor necrosis factor (TNF) receptor gene superfamily (Locksley et al., 2001). They all share a similar cysteine-rich extracellular domain and an 80 residue cytoplasmic region called the death domain (DD) (Ashkenazi and Dixit, 1998). Mutations in these receptors inhibit extrinsic apoptosis demonstrating that these DDs are critical for transmission of extra cellular death signals (i.e. CD95L, TNFα or TRAIL) from the cell surface to the intracellular pathways since mutations in these receptors inhibit extrinsic apoptosis (Zamzami et al., 1997).

The sequence of events for the extrinsic pathway is best characterized for the FasL/FasR and TNF-α/TNFR1 models. In these models, there is a clustering of receptors upon binding with the homologous trimeric ligand. Upon ligand binding, the cytoplasmic adapter proteins are recruited on the cytosolic face of the receptors. For example, Fas ligand binding to the Fas receptor results in binding of the adapter protein FADD, whereas TNF ligand binding to the TNF receptor results in binding of the adapter protein TRADD, with the subsequent recruitment of FADD and RIP (Hsu et al., 1995). FADD then associates with procaspase-8 to form the death inducing signaling complex (DISC). This results in the auto-catalytic activation of procaspase-8 to caspase 8. Activated caspase 8 then cleaves and activates procaspase-3 to caspase 3, leading to activation of the execution phase of extrinsic apoptosis.

Intrinsic Apoptotic pathway

The intrinsic/mitochondrial pathway, involves a diverse range of non-receptor-mediated stimuli that produce intracellular signals to initiate cell death. The signals that initiate this pathway fall into categories, negative and positive (Brenner and Mak, 2009). Negative signals include the absence of growth factors such as hormones and cytokines, that lead to de-repression of the apoptotic program. Positive signals directly activate the cell death program, and include radiation, free radicals, hypoxia and toxins. In the intrinsic pathway, caspases play a critical role. Their activation is dependent on the permeabilization of the outer mitochondrial membrane (OMM), which in turn, is influenced by an array of factors. These include members of the Bcl-2 family of proteins, mitochondrial lipids, proteins regulating bioenergetic metabolic flux, and components of mitochondrial permeability transition pore complex (Tait and Green, 2012).

Disruption of the OMM leads to the release of apoptogenic intermembrane space (IMS) proteins into the cytoplasm. These proteins include cytochrome c, Smac/DIABLO, Omi/HtrA2, apoptosis-inducing factor (AIF) and endonuclease G (Wallace, 2012). Once in the cytoplasm, these proteins trigger the execution phase of the cell death program by activating caspases (Jourdain and Martinou, 2009). However, caspase independent pathways have also been reported (Galluzzi et al., 2012b). Of the various pro apoptotic proteins released from the IMS, the role of cytochrome c is the best understood. Once in the cytoplasm, it binds to apoptotic protease activating factor 1 (Apaf-1) (Hüttemann et al., 2011). This protein contains an N-terminal caspase recruitment domain (CARD), a nucleotide binding domain and a C-terminal domain containing 12-13 WD-40 repeats (Zou et al., 1997). Cytochrome c binding to Apaf-1 facilitates the recruitment of dATP

through its nucleotide binding domain, which then exposes the N-terminal CARD domain, allowing recruitment of pro-caspase 9 to form the apoptosome complex. Finally, the executioner pro-caspase 3 is recruited to the apoptosome complex, where it is activated to caspase 3 leading to cleavage of many cellular proteins and ultimately apoptosis (Adrain et al., 1999).

Other IMS proteins also have a significant role in the intrinsic pathway. In contrast to cytochrome c, Smac/DIABLO and Omi/HtrA2 neutralize the endogenous caspase inhibitors known as inhibitor of apoptosis proteins (IAPs). Smac is a nuclear encoded protein with a mitochondrial targeting sequence. After cleavage in the mitochondria, the imported protein is about 23 kDa (Du et al., 2000) and binds to XIAP, cIAP1, cXIAP2 and survivin. Omi/HtrA2 is also a nuclear encoded, 49 kDa protein with N-terminal mitochondrial localization signal that mediates its translocation into the IMS (Suzuki et al., 2001). It is processed in the IMS into a 37 kDa mature form and, once released, promotes cell death similarly to Smac/DIABLO in a caspase-dependent manner by neutralizing IAPs (Saelens et al., 2004).

Post mitochondrial or Execution Phase

The extrinsic and the intrinsic pathways converge on a common pathway called the execution phase. Here, the activated caspases degrade the nuclear and cytoplasmic proteins. Caspase 3, caspase 6 and caspase 7 act as executioner caspases cleaving substrates ranging from PARP to plasma membrane-associated proteins, resulting in the collapse of cellular structure (Slee et al., 2001). One of the most important executioner caspases is caspase 3. This caspase cleaves and activates caspase activated DNAse

(CAD) which then degrades nuclear DNA. Caspase 3 is activated by initiator caspases, which include caspase 8, caspase 9 and caspase 10.

Bcl-2 family of proteins and regulation of apoptosis

The signaling cascade linking MOMP to the execution of apoptosis has been extensively characterized (for review see (Jourdain and Martinou, 2009)). Importantly, the interplay between pro- and anti- apoptotic members of the Bcl-2 protein family has been found to control MOMP. The identification of Bcl-2 as a cell death regulator was first determined from cytogenetic analysis of human B cell lymphomas. In this work a strong correlation was observed between t[14:18] chromosomal translocation and B cell lymphomas. This rearrangement placed bcl-2 (B cell lymphoma-2) expression under the control of the immunoglobulin heavy chain gene enhancer Eμ (Tsujimoto et al., 1984). Later, the pro-survival function of bcl-2 was confirmed by Vaux *et al.* Using retroviral transduction, they introduced bcl-2 cDNA into bone marrow cells of wild type or c-myc transgenic mice. Bcl-2 was found to cooperate with c-myc to induce proliferation of B-cell precursors, some of which became tumorigenic. In lymphoid and myeloid cell lines which require interleukin-3 (IL-3) growth factor for survival, the absence of bcl-2 promoted the survival upon IL-3 withdrawal (Strasser et al., 1990; Vaux et al., 1988). These were the first studies to implicate bcl-2 as an oncogene and showed that co-expression with c-myc had a synergistic effect in tumorigenesis.

The discovery that bcl-2 could function as a tumor promoter opened a new avenue of cancer research. Bcl-2 was found to be a member of a family of proteins which are capable of regulating apoptosis (Davids and Letai, 2012). The Bcl-2 family is divided

into three main sub-classes, defined in part by the homology shared with the four conserved regions termed Bcl-2 homology (BH) 1-4 domains. The anti-apoptotic members include Bcl-2, Bcl-X_L, Mcl-1, A1 and Bcl-w. The pro-apoptotic members containing BH1-3 domains include the effecter proteins Bax and Bak. Interestingly, both proteins require are activated and function as a rheostat to regulate the apoptotic process. Finally, the BH3-only protein subclass, includes Bid, Bim, Bad, Puma, Noxa, Hrk, Bmf, and Bik. These proteins are the most apical regulators of death signaling cascades and are activated by multiple internal and external stimuli to initiate the apoptotic response. Their BH3 domain binds either multidomain anti- or pro-apoptotic Bcl-2 family members. This interaction either antagonizes the survival activity of anti-apoptotic proteins or activates pro-apoptotic Bax and Bak proteins, resulting in MOMP.

Activation of Bax and Bak and MOMP

Two models of Bax and Bak activation have been put forward. The indirect activator or neutralization model proposes that Bax and Bak are bound in a constitutively active state by anti-apoptotic Bcl-2 proteins. A competitive interaction of BH3-only proteins with anti-apoptotic Bcl-2 family members is sufficient to release active Bax and Bak. The direct activator or derepressor model proposes that Bax and Bak are inactivate and only activated following interactions with a subset of BH3-only proteins known as direct activators. Anti-apoptotic Bcl-2 proteins prevent MOMP either by sequestering the activating BH3-only proteins or by inhibiting activated Bax and Bak. A second subset of BH3-only proteins, known as sensitizers, cannot directly activate Bax and Bak but neutralize anti-apoptotic Bcl-2 proteins (Letai et al., 2002; Willis et al., 2005). Bax and

Bak activity is largely controlled through interactions with other Bcl-2 proteins (Wei et al., 2001). Activation of Bax and Bak occurs through similar mechanisms, though Bax requires an additional step due to its cytoplasmic localization (Kim et al., 2009). Upon activation, Bax and Bak undergo conformational changes leading to mitochondrial targeting of Bax, and homo-oligomerization of Bak and Bax (Eskes et al., 2000; Hsu et al., 1997; Wei et al., 2000). Oligomerization of Bax and Bak is an essential step, as mutants that fail to undergo oligomerization do not induce MOMP (George et al., 2007). MOMP results in rapid release of cytochrome c and other soluble proteins into the cytoplasm; rapid caspase activation ensues and results in the cleavage of hundreds of proteins and ultimately, apoptosis (Chipuk et al., 2006). Thus, MOMP functions as the point of no return for the cell.

Various studies have now proposed a model for Bak activation and oligomerization. Bak activation leads to exposure of the BH3 domain and its insertion into the hydrophobic groove of an adjacent, activated Bak molecule. This interaction leads to the formation of a symmetrical Bak homodimer. Higher order oligomers of Bak are formed by dimer-dimer interactions mediated through interfaces that are exposed following Bak activation. These oligomers form a channel on the OMM that leads to the release of IMS proteins (Dewson et al., 2009).

Mitochondria and Necrosis

Necrosis is a toxic process where the cell is a passive victim, and follows an energy-independent mode of cell death. Compared to apoptosis, which is a controlled, energy-dependent process affecting either a single cell or a cluster of cells; necrosis is an uncontrolled and passive process that usually affects a large field of cells. During necrosis, there is cell swelling, formation of cytoplasmic vacuoles, distension of the endoplasmic reticulum, formation of cytoplasmic blebs, as well as condensed, swollen or ruptured mitochondria, disaggregation and detachment of ribosomes, disrupted organelle membranes, swollen and ruptured lysosomes, and eventually disruption of the cell membrane (Kerr et al., 1972; Majno and Joris, 1995; Trump et al., 1997). The loss of cell membrane integrity results in the release of the cytoplasmic contents into the surrounding tissue, sending chemotactic signals that recruit inflammatory cells. Since apoptotic cells do not release their cellular contents into the surrounding interstitial tissue and are quickly phagocytosed by macrophages or adjacent normal cells. there is essentially no inflammatory response (Savill and Fadok, 2000). Importantly, cell death that occurs with apoptotic morphology can be shifted to a more necrotic phenotype when caspase activation is inhibited by pharmacological inhibitors or by elimination of essential caspase activators such as Apaf-1 (Pedersen, 1999).

Activation of the necrotic pathway is preceded by loss of the permeability of the inner mitochondrial membrane (IMM), known as mitochondrial membrane permeabilization (MMP). IMM permeabilization implies the formation of pores or channels that dissipate $\Delta\Psi_m$ built across the inner membrane due to the activity of the

electron transport chain. The proteins responsible for formation of the channel is a multi-protein complex known as the mitochondrial permeability transition pore (MPTP).

Mitochondrial permeability transition (MPT) and necrosis

Mitochondrial permeability transition (MPT) is defined as the sudden increase in the permeability of the IMM to solutes of molecular mass of less than 1500 Da. This loss in permeability results in loss of $\Delta\Psi_m$, mitochondrial swelling and rupture of the OMM. It was first reported by Hunter *et al.* that the MPT is a consequence of Ca^{2+} induced increased IMM permeability that is characterized by simultaneous stimulation of ATPase, uncoupling of oxidative phosphorylation, and, finally, loss of respiratory control (Hunter et al., 1976). It was first considered an artifact, but later the authors suggested that it may have physiological relevance, and that mitochondria have protective mechanisms to guard against this induction. Further experimentation solidified the idea that MPT is not a consequence of non-specific mitochondrial membrane damage but, instead, is the result of opening of a pore or megachannel, known as the MPTP (Crompton and Costi, 1988; Hunter and Haworth, 1979). The best studied example of MPT involvement in necrotic cell death is in reperfusion injury in the heart. During the ischemic phase of the insult, calcium concentrations rise and production of reactive oxygen species (ROS) increases, resulting in oxidative stress. Increased calcium and ROS are potent inducers of the MPT, but in this phase, due to enhanced glycolysis, accumulation of lactic acid results in decreased intracellular pH. This prevents MPTP opening, which is progressively inhibited as the pH drops below 7. However, upon reperfusion, there is a burst of ROS

formation and the pH returns to normal, stimulating pore opening and increased cell death (Halestrap et al., 1998; Halestrap et al., 2004).

Mitochondrial Permeability Transition Pore (MPTP) structure

In the last three decades, intensive research has been carried out to identify the constituents of the MPT megachannel. On a molecular basis the MPT pore consists of voltage dependent anion channel (VDAC), an unspecific pore protein also known as porin, in the OMM (Roos et al., 1982). In the IMM, the channel consists of a specific ATP/ADP transporter called the adenine nucleotide translocator (ANT). Directly associated with the ANT in the matrix of mitochondria is cyclophilin D (Cyp-D), a chaperone with peptidylprolyl isomerase (PPIase) activity (Tanveer et al., 1996). With advances in transgenic mouse technology, the contributions of each of the constituents of the MPTP are becoming better defined.

Mammalian VDAC is a 31 kDa protein with three isoforms (VDAC1-3). The generation of isoform-specific VDAC deficient mice allowed the assessment of the role of individual VDAC isoforms in the MPT pore structure. Mice lacking VDAC1 and VDAC3 were viable, whereas elimination of VDAC2 resulted in embryonic lethality, suggesting that VDAC2 is important for embryonic development. Though VDAC is considered to be a constituent of the MPTP, recent studies have shown that it might be dispensable for MPT induction. MPT properties in mitochondria from VDAC $1^{-/-}$ mice were indistinguishable from those of wild type mice (Krauskopf et al., 2006). More convincingly, Baines *et al* showed that mitochondria from $VDAC1^{-/-}$, $VDAC3^{-/-}$ or $VDAC1^{-/-}/VDAC3^{-/-}$ mice or fibroblasts lacking all three isoforms exhibited oxidative

stress induced MPT, which was indistinguishable from wild type (Baines et al., 2007). These results suggest that VDAC, instead of having a direct effect, may have an accessory role in induction of MPT.

Mammals have three isoforms of ANT (ANT1-3), another constituent of the MPTP, which are expressed in a tissue specific pattern. Genetic knockout of ANT in mouse liver demonstrated that MPT could still be induced in the mitochondria by Ca^{2+}, albeit, at a higher concentration. Furthermore, inhibitor studies proved that ANT in a constituent of the MPTP. Atractyloside induced opening of MPTP, whereas bongkrekic acid inhibited pore opening in mitochondria overloaded with Ca^{2+} (Hunter and Haworth, 1979).

Genetic studies with Cyp-D knockout mice confirmed its role in the regulation of MPTP machinery. Cyclopsorin A (CsA) inhibits MPTP opening by inhibiting the PPIase activity of Cyp-D (Crompton et al., 1988) and mitochodria from Cyp-D knockout mice did not exhibit CsA-sensitive MPTP opening. Similar to ANT-deficient mitochondria, Cyp-$D^{-/-}$ mitochondria also showed more resistance to Ca^{2+}_{i} induced MPT induction (Baines et al., 2005).

Sirtuins: regulation of cellular physiology and cell death

The silent information regulator (Sir) proteins were first identified in the budding yeast *S. cerevisiae* and function in genomic silencing, cell cycle progression and maintenance of chromosome stability (Brachmann et al., 1995). In yeast, the Sir family comprises four proteins: Sir1, Sir2, Sir3 and Sir4. Of the four, Sir2 is the most widely studied and is associated with an extension of replicative lifespan. Sir2 deletion mutants showed shorter life spans, whereas increasing the gene dosage extended the life span in wild type cells (Kaeberlein et al., 1999). Sir2 promoted longevity in yeast by suppressing the formation of toxic extrachromosomal rDNA circles (ERCs) (Sinclair and Guarente, 1997). Initially, Sir2 was found to have ADP-ribosyltransferase activity; this enzymatic activity was essential for its genome silencing function (Tanny et al., 1999). However, further studies showed that Sir2 was actually a deacetylase, because active Sir2 catalyzed an NAD^+ dependent deacetylation of histones, and mutations of a histidine residue in the core enzymatic domain abolished the enzymatic activity (Landry et al., 2000).

Calorie restriction (CR) was first described as a reduction in food intake in rats of 30-40% of ad libitum levels that would extend their lifespan by up to 50%. CR extends life span in a wide variety of organisms, although the mechanism is still unclear (Barger et al., 2003). CR in yeast also extended life span; this extension of life span was dependent on Sir2 and its deacetylase activity, which required NAD^+ (Imai et al., 2000; Lin et al., 2000).

Sirtuins and Evolutionary History

Sir2 is considered the founding member of the histone deacetylases (HDACs), which are involved in, cell cycle progression, chromosome stability and the repair of the double stranded DNA breaks (Brachmann et al., 1995). Sirtuins are conserved proteins found in bacteria to mammals (Frye, 1999; Frye, 2000). The hallmark of the family is a domain of approximately 260 amino acids that has a high degree of sequence similarity in all sirtuins. They are further divided into five classes (I-IV and U) on the basis of phylogenetic analyses of 60 sirtuins from a wide variety of organisms (Fig. 1). The human genome encode 7 sirtuins (Sirt1-Sirt7) (Frye, 2000).

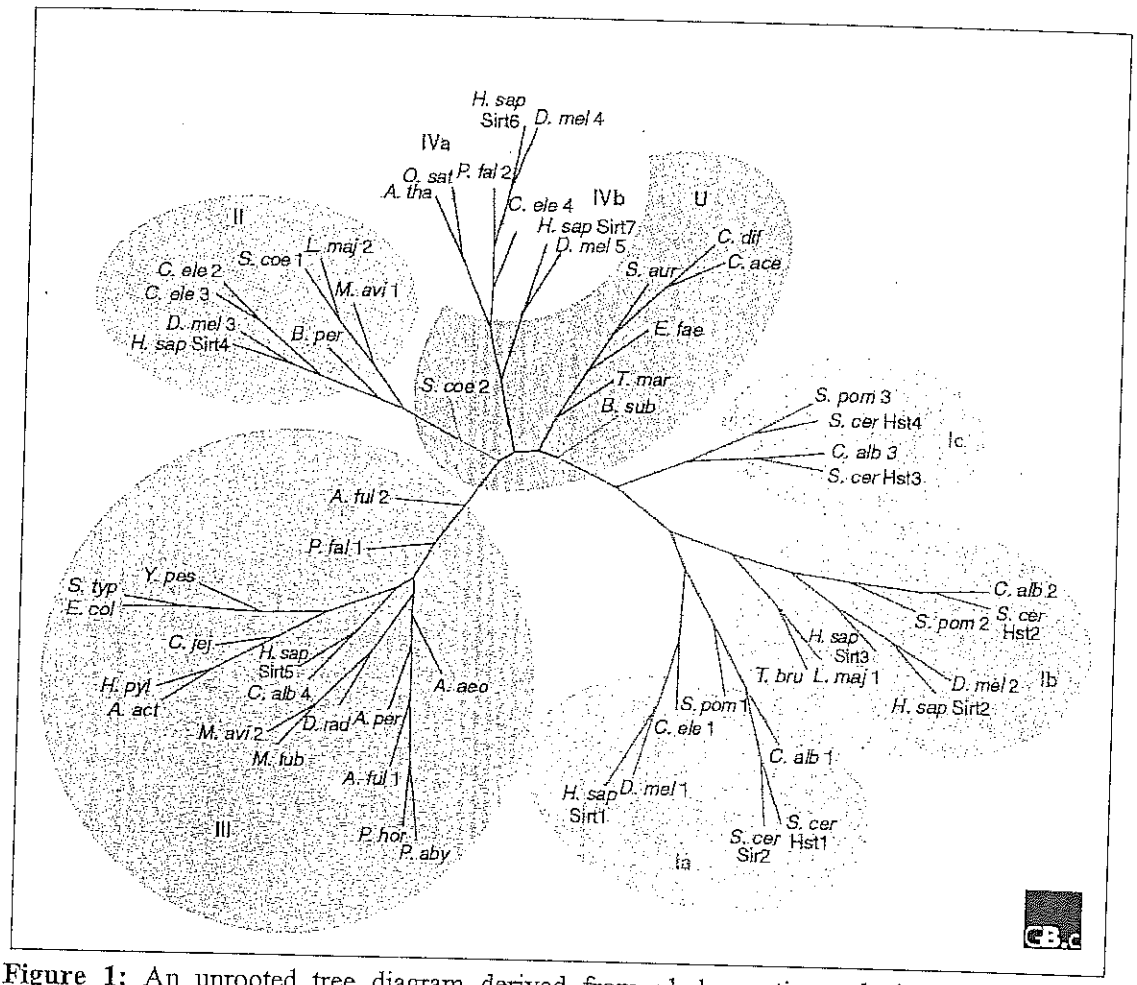

Figure 1: An unrooted tree diagram derived from phylogenetic analysis of the conserved domains of 60 sirtuin sequences from all sirtuin classes. Classes I, II, III, IV, and U and subdivisions of classes I and IV are indicated. Organism abbreviations: A. act, *Actinobacillus actinomycetemcomitans*; A. aeo, *Aquifex aeolicus*; A. ful, *Archaeoglobus fulgidus*; A. per, *Aeropyrum pernix*; A. tha, *Arabidopsis thaliana*; B. per, *Bordetella pertussis*; B. sub, *Bacillus subtilis*; C. ace, *Clostridium acetabutylicum*; C. alb, *Candida albicans*; C. dif, *Clostridium difficile*; C. ele, *Caenorhabditis elegans*; C. jej, *Campylobacter jejuni*; D. mel, *Drosophila melanogaster*; D. rad, *Deinococcus radiodurans*; E. col, *Escherichia coli*; E. fae, *Enterococcus faecalis*; H. sap, *Homo sapiens*; H. pyl, *Helicobacter pylori*; L. maj, *Leishmania major*; M. avi, *Mycobacterium avium*; M. tub, *Mycobacterium tuberculosis*; O. sat, *Oryza sativa*; P. aby, *Pyrococcus abyssi*; P. fal, *Plasmodium falciparum*; P. hor, *Pyrococcus horikoshii*; S. aur, *Staphylococcus aureus*; S. coe, *Streptomyces coelicolor*; S. pom, *Schizosaccharomyces pombe*, S. typ, *Salmonella typhimurium*; S. cer, *Saccharomyces cerevisiae*; T. bru, *Trypanosoma brucei*; T. mar, *Thermotoga maritima*; Y. pes, *Yersinia pestis*.

Mammalian Sirtuins

The seven mammalian sirtuins have significant sequence homology and are also homologous with yeast Sir2. Based on the phylogenetic analysis of 60 sirtuins in wide variety of organisms they are divided into five classes (I-IV and U) (Fig 1). They contain a central, conserved catalytic domain where acetyl transferase or ADP-ribosyl transferase enzymatic activity resides, and a NAD^+ binding domain (Table 1) (Fig 2). The sirtuin protein has been found in a wide variety of subcellular compartment. Three sirtuins, Sirt1, Sirt6 and Sirt7, are nuclear proteins. Sirt2 localizes to cytoplasm. The remaining three sirtuins, Sirt3, Sirt4 and Sirt5, are present in the mitochondria. (Michishita et al., 2005).

Table 1: Classification, localization and enzymatic activity of mammalian sirtuins

Sirtuin	Class	Localization	Activity	Targets
Sirt1	I	Nucleus	Deacetylation	PGC1α,FOXO1, FOXO3, p53
Sirt2	I	Cytosol	Deacetylation	Tubulin, FOXO1, PEPCK
Sirt3	I	Mitochondria	Deacetylation	LCAD, GDH, AceCS2
Sirt4	II	Mitochondria	ADP-ribosylation	GDH
Sirt5	III	Mitochondria	Deacetylation, demalonylation, desuccinylation	CPS1
Sirt6	IV	Nucleus	Deacetylation, ADP-ribosylation	H3K9, H3K56
Sirt7	IV	Nucleolus	Deacetylation	Unknown

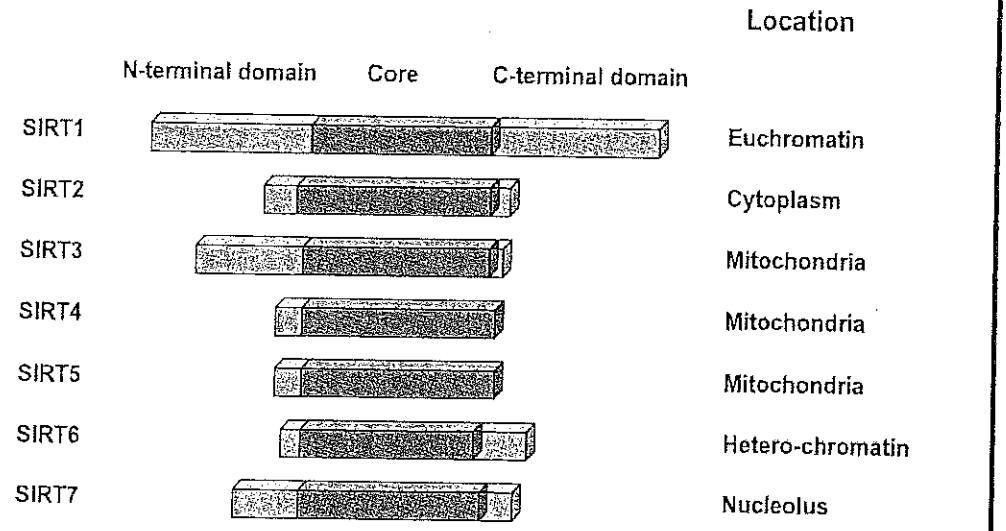

Figure 2: Homology between human sirtuins. The dark grey block represents the core catalytic domain. The light grey regions represent the N- and C- terminal domains

Enzymatic activity of mammalian sirtuins

The deacetylase or ADP-ribosyltransferase activities of mammalian sirtuins require NAD^+ as a cofactor. During deacetylation, sirtuins use an acetylated protein and one molecule of NAD^+ as substrate to give nicotinamide (NAM), 2'-O-acetyl-ADP-ribose and a deacetylated protein as products. During the ADP-ribosylation reaction, an ADP ribose is transferred from NAD^+ to a target protein to form NAM and the ADP-ribosylated protein (Fig 3). The enzymatic activity of sirtuins is regulated by the cellular $[NAD^+]/[NADH]$ ratio. NAD^+ acts as an activator whereas NAM and reduced nicotinamide adenine dinucleotide (NADH) inhibit their activity (Lin et al., 2004). Based on their enzymatic activity mammalian sirtuins are classified as either deacetylases (Sirt1, Sirt2, Sirt3, Sirt5 and Sirt7) or ADP-ribosyltransferases (Sirt4 and Sirt6).

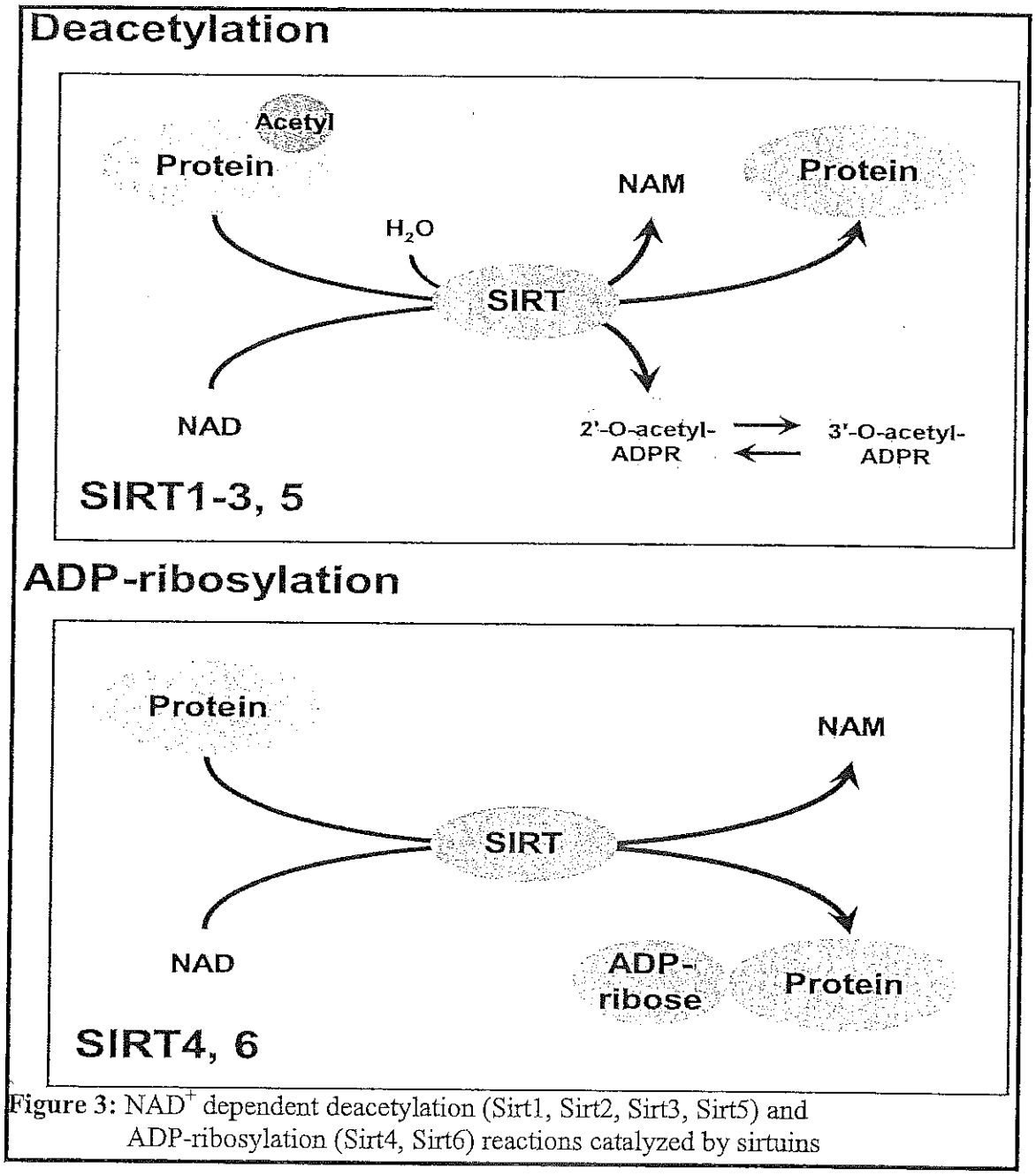

Figure 3: NAD^+ dependent deacetylation (Sirt1, Sirt2, Sirt3, Sirt5) and ADP-ribosylation (Sirt4, Sirt6) reactions catalyzed by sirtuins

Sirtuins: Aging and cancer

There is a strong correlation between aging and cancer incidence. During aging, mutations arise from errors in DNA replication, environmental insults or accumulation

intracellular ROS (Balaban et al., 2005). In many organisms decreased intracellular ROS correlates with increased lifespan (Barger et al., 2003). Since Sir2 was implicated in aging, it was postulated that Sir2 may also have an important role in cancer progression. In fact, Sir2 negatively regulates p53-dependent apoptosis in yeast during oxidative stress. Sir2p physically associates with p53 and induced its deacetylation, therby suppressing p53-dependent apoptosis in response to DNA damage and oxidative stress (Luo et al., 2001).

Various mammalian sirtuins have a role in cancer pathogenesis. However, studies have shown that mammalian sirtuins can both suppress and promote tumor formation. For example, Sirt1 promotes cell survival under a CR diet in rats, an effect which requires its deacetylase activity (Cohen et al., 2004b) and also promotes survival of tumor cells (Huffman et al., 2007). Mitochondrial Sirt3 also has both pro- and anti-apoptotic functions depending on the cell and tumor type. Understanding the mechanistic differences in tumor types will enhance our knowledge of the complex biology of sirtuins in cancer and will be beneficial in developing better anti-cancer drugs.

Nuclear Sirtuins

Sirtuin 1

Sirtuin 1 (Sirt1) is the most studied protein of the sirtuin family and its increased expression has been observed in a number of cancers (Herranz and Serrano, 2010; Huffman et al., 2007; Pfluger et al., 2008). One possible mechanism by which Sirt1 could promote tumors is by loss or inactivation of its transcriptional repressors (e.g. p53). Sirt1 promoters have two p53 binding sites. Under oxidative stress, FOXO3a translocates to

the nucleus from the cytoplasm where it interacts with p53. This interaction inhibits the tumor suppressive function of p53, leading to increased expression of Sirt1. Also, Sirt1 levels are usually high in tumors that lack functional p53 (Nemoto et al., 2004).

Hypermethylated in cancer 1 (HIC1), is a zinc finger transcription factor that cooperates with p53 to prevent tumor development in mice (Dehennaut and Leprince, 2009). Recently, HIC1 has also been shown to regulate Sirt1 expression (Naqvi et al., 2010). HIC1 interacts with Sirt1 to form a transcriptional repression complex that binds to a Sirt1 promoter, forming a negative feedback loop and further inhibiting its function. In $HIC1^{-/-}$ mice, Sirt1 inactivated p53 by deacetylation and allowed cells to bypass apoptosis during DNA damage (Chen et al., 2005; Huffman et al., 2007).

Another target of Sirt1 is Ku70. Ku70 localizes mainly to the nucleus and is involved in DNA damage repair (Ahmed et al., 2013). Increased Sirt1 expression promotes deacetylation of Ku70 at lysines 539 and 542, which increases its interaction with Bax and prevents apoptosis. Mutations which mimic K539 and/or K542 acetylation, or treatment with deacetylase inhibitors, prevented the ability of Ku70 to suppress Bax mediated apoptosis (Cohen et al., 2004a).

Forkhead box O (FOXO) proteins are important transcription factors that regulate the expression of proapoptotic genes such as Bim and FasL (Fu and Tindall, 2008). FOXO factors are key regulators of stress response, longevity and oncogenesis (Charitou and M Th Burgering, 2012). FOXO1, a member of the family, interacts with Sirt1. Sirt1-mediated FOXO1 deacetylation inhibited its transcriptional function and promoted prostate tumorigenesis in response to stress (Kojima et al., 2008; Yang et al., 2005).

Treatment of lung cancer (H1299) and breast cancer (MCF-7) cell lines with the Sirt1 inhibitor sirtinol induced senescence-like growth arrest. This arrest was accompanied by inactivation of the MAPK pathway and decreased levels of active Ras, a protooncogene, indicating that Sirt1 is oncogenic through the MAPK-Ras pathway (Ota et al., 2006). Similarly, in another lung cancer cell line (A549) Sirt1 knockdown induced G1 arrest and apoptosis. The latter effect was dependent on increased p53 acetylation and Bax expression (Sun et al., 2007). Apart from its role in cancer, Sirt1 also has an important physiological role in various tissues (Fig 4).

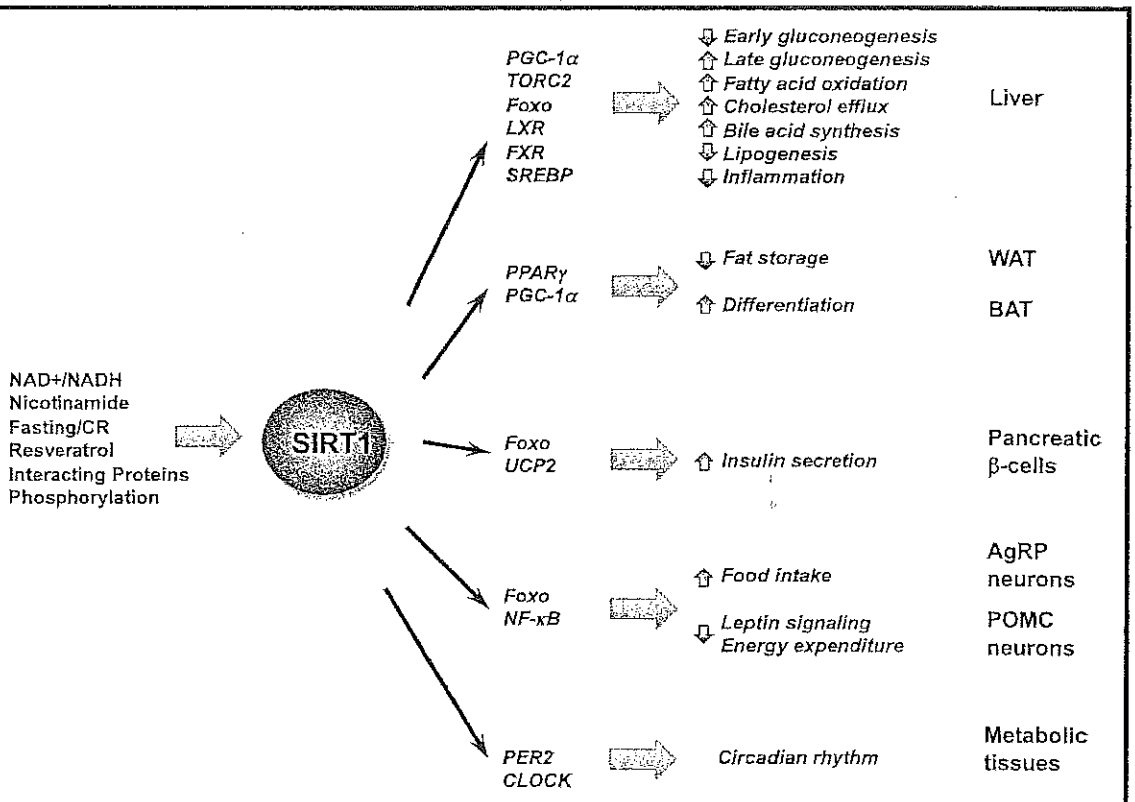

Figure 4: Sirtuin 1 regulates various functions in different tissues

Sirtuin 6 (Sirt6)

Sirt6 is a nuclear localized sirtuin possessing a ADP-ribosyltransferase activity (Liszt et al., 2005). Within the nucleus it has a nucleolar localization where it associates with heterochromatin (Michishita et al., 2005). Functionally, Sirt6 suppresses genomic instability by promoting resistance to DNA damage (Jia et al., 2012; Van Meter et al., 2011a). Sirt6 knockout mice presented with an aging-like phenotype, such as lymphopenia, loss of subcutaneous fat, and severe metabolic defects suggesting that Sirt6 has important role in regulation of metabolism (Mostoslavsky et al., 2006). This phenotype observed in Sirt6 knockout mice was due to lack of interaction of Sirt6 with NF-κB subunit RelA (Kawahara et al., 2009). Sirt6-deficient cells showed hyperacetylation of H3K9 causing increased RelA promoter occupancy and enhanced NF-κB dependent modulation of gene expression. This leads to decreased apoptosis and cellular senescence. Additionally, Sirt6 knockout cells are more resistance to apoptosis activated by the pro-death ligand TNFα (Kawahara et al., 2009).

Oxidative stress induces DNA double strand breaks (DSB) and repair of these DSBs is critical to prevent accumulation of mutations and the genome instability. Sirt6 is recruited to DSB sites and stimulates DSB repair. DSB repair by Sirt6 was stimulated by its interaction with PARP1, a DNA repair enzyme. Sirt6 mono-ADP-ribosylates PARP1 on lysine residue 521, that enhances its activity and DSB repair capability under oxidative stress. These results show that Sirt6 has tumor suppressive functions (Mao et al., 2011).

Pro-apoptotic Sirt6 activity has been shown in different cancer cell lines. Overexpression of Sirt6 in HeLa, HCC1954, and MDA-MB-231 cancer cell lines induced

massive apoptosis compared to non-cancerous HCA2 and HMEC1 cells (Sebastián et al., 2012). In cancer cell lines, Sirt6 overexpression induced activation of the proapoptotic proteins p53 and p73. Inhibition of the ATM signaling cascade using wortmann attenuated Sirt6-induced cytotoxicity in cancer cells. Interestingly, the pro-apoptotic activity of Sirt6 seems to be dependent on its ADP-ribosyltransferase activity (Van Meter et al., 2011b). Although most studies suggests that Sirt6 lacks any deacetylase activity (Liszt et al., 2005) other suggests that it might possess a dual enzymatic activity depending on its tissue expression (Cardus et al., 2013; Gil et al., 2013; Zhong et al., 2010).

The Cytosolic Sirtuin

Sirtuin 2

Sirtuin 2 (Sirt2) is a cytosolic NAD^+-dependent protein deacetylase that co-localizes with microtubules. Sirt2 deacetylates Lys-40 of α-tubulin and its knockdown with siRNA results in tubulin hyperacetylation. The consequences of tubulin acetylation/deacetylation are not completely understood, but may affect tubulin stability (North et al., 2003). Sirt2 arrests the cell cycle in normal cells, but has a pro-survival role in cancer cells (Park et al., 2012). Sirt2 knockdown was sufficient to induce apoptosis in HeLa cells (Li et al., 2011). The mechanism by which Sirt2 functions as a tumor promoter is incompletely understood. One study by Li *et al.* suggested that apoptosis induced by Sirt2 knockdown depended on stabilization and accumulation of p53. Its accumulation was attributed to degradation of MDM2 by activation of the MAPK signaling cascade (Li et al., 2011). Similarly, studies in gliomas indicated a pro-survival

role for Sirt2, as Sirt2 knockdown induced apoptosis of C6 glioma cells in a caspase 3-dependent manner (He et al., 2012).

Sirt2 expression was also positively correlated with invasiveness in hepatocellular carcinoma. Depletion of Sirt2 led to the regression of epithelial to mesenchymal transition phenotype, whereas Sirt2 overexpression immortalized the hepatocyte cell line LO2. Mechanistically, Sirt2 regulates deacetylation and inactivation of Akt and GSK-3β signaling pathway to promote tumor cell survival (Chen et al., 2013).

Mitochondrial Sirtuins

Mitochondria are dynamic organelles that regulate nutrient utilization to provide the cell with energy even during dramatic changes in diet and development. Mitochondria also have a critical role in mediating apoptosis in response to DNA damage or oxidative stress. Three sirtuins localize to the mitochondria (Sirt3-5); they are involved in the regulation of metabolism, the oxidative stress response, and nutrient utilization. Mitochondria have an important role in cell death by the activation of MOMP or by the induction of MPTP. Despite the central role of mitochondria in cell death, very little is known about how mitochondrial sirtuins participate in and/or regulate cell death. The following section describes some aspects by which mitochondrial sirtuins regulate metabolism. However, evidence is beginning to emerge about how these sirtuins could modulate the mitochondrial mode of cell death.

Sirtuin 3 and regulation of metabolism

The prototype sirtuin (Sirt1) regulates energy homeostasis. Sirt1 regulates various metabolic responses to insulin secretion, by cycles of acetylation/deacetylation of nuclear transcription factors (Herranz and Serrano, 2010; Pfluger et al., 2008). Hence, it was predicted that if Sirt1 could regulate metabolic pathways, then the mitochondrial Sirt3 might also regulate various energy pathways. Indeed, almost 20% of the proteins isolated from mouse liver mitochondria were are acetylated, indicating that acetylases could regulate metabolic pathways (Kim et al., 2006). Another study in *Salmonella* showed that the majority of metabolic pathways, such as the tricarboxylic acid (TCA) cycle, fatty acid β-oxidation, urea cycle, carbohydrate metabolism, and oxidative phosphorylation, were regulated through lysine acetylation and (Wang et al., 2010). Though protein modification can regulate metabolic pathways, some studies showed that nutritional status also regulates the mitochondrial acetylation status. These include , CR, a high fat diet, fasting and ethanol intoxication (Hirschey et al., 2011b; Kim et al., 2006; Picklo, 2008; Schwer et al., 2009). One key tool for studying the role of Sirt3 in metabolism was to analyse the acetylation status of mitochondrial proteins in Sirt3 KO mice. Although these mice were physiologically indistinguishable from wild type, their mitochondrial proteins had increased acetylation. This increase was not observed in Sirt4 and Sirt5 (other mitochondrial sirtuins) KO mice. Moreover, when mitochondrial extracts from Sirt3 KO mice were incubated with recombinant Sirt3 *in vitro*, the acetylation status was reversed. This study confirmed that Sirt3 is the major deacetylase in the mitochondria (Lombard et al., 2007).

Sirtuin 3 and regulation of energy status

Sirt3 KO mice also have decreased levels of ATP in their tissues, which can be rescued by exogenously overexpressing wild type Sirt3 (Lombard et al., 2007). In tissues such as heart, liver, kidneys and skeletal muscles, which normally show high expression of Sirt3, its depletion caused decreased ATP production, oxygen consumption, disruption of the electron transport chain (ETC), decreased mitochondrial membrane potential, and increased ROS production (Ahn et al., 2008). Decreased ETC activity was attributed to an increase in acetylated ETC proteins. In fact, Sirt3 deletion decreased complex I activity by hyperacetylation of NDUFA9 (Ahn et al., 2008). Sirt3 also interacts and regulates the activity of succinate dehydrogenase, a component of complex II (Finley et al., 2011a). Additionally, Sirt3 KO mice have decreased complex III and IV activity, though the mechanisms are still unclear (Kendrick et al., 2011).

Apart from its direct regulation of the ETC, Sirt3 also exerts an indirect regulation of the ETC and oxidative phosphorylation. Sirt3-mediated deacetylation of CyP-D, a mitochondrial matrix protein involved in the regulation of MPTP, induced its dissociation from ANT-1 in the IMM. This dissociation induces the redistribution of HKII to the cytoplasm from the OMM, where it interacts with VDAC. This redistribution of HKII results in increased oxidative phosphorylation and increased ATP production (Shulga et al., 2010).

Sirt3 also regulates activities of various metabolic enzymes. One of the first Sirt3 substrate to be identified was acetyl CoA synthetase II (AceCSII) (Schwer et al., 2006). AceCS has two isoforms; cytosolic AceCSI and mitochondrial AceCSII. AceSCI is expressed in liver and kidney and is regulated by Sirt1 and AceCSII by Sirt3 (Hirschey et

al., 2011a). AceCS catalyzes the conversion of acetate to acetyl CoA, which is used for oxidation in the TCA cycle or for fatty acid synthesis. During CR, Sirt3 ensures that sufficient acetyl CoA is provided for oxidation by TCA for the maintenance of energy homeostasis. In addition, Sirt3 deletion causes hyperacetylation of glutamate dehydrogenase 1 (GDH-1), a metabolic enzyme that regulates the conversion of glutamate to α-ketoglutarate. Increased acetylation inhibits the enzymatic activity and deacetylation by Sirt3 increases its activity (Colman and Frieden, 1966). In fact, during CR, GDH-1 increased in a manner that correlated with increased Sirt3 expression (Haigis et al., 2006).

Sirtuin 3 and Hepatic metabolism

Urea cycle is most active in the liver (Morris, 2002). Sirt3 has been shown to regulate the urea cycle by regulating the rate limiting enzyme ornithine transcarbamylase (OTC) during fasting. As a consequence, Sirt3 knock outs show an accumulation of urea cycle intermediates such as ornithine, aspartate and uracil (Hallows et al., 2011). Similar to CR, fasting has been shown to increase Sirt3 expression. In Sirt3 KO mice, fasting increased the accumulation of long chain acyl carnitines and triglycerides (Hirschey et al., 2010). This accumulation was the result of inefficient fatty acid oxidation due to increased acetylation of long chain acyl-CoA dehydrogenase (LCAD) which catalyzes the oxidation of long chain fatty acids in the liver leading to fatty liver (Kendrick et al., 2011). Similarly, Sirt3 $^{-/-}$ mice placed on a high fat diet (HFD) showed increased obesity, insulin resistance, hyperlipidemia and steatohepatitis compared to wild type mice. This result indicates that Sirt3 loss can lead to metabolic syndrome (Hirschey et al., 2011b).

HFD also leads to decreased expression of Sirt3 in skeletal muscles (Palacios et al., 2009). Additionally, during fasting, Sirt3 $^{-/-}$ mice showed increased acetylation of 3-hydroxy-3-methylglutaryl-CoA synthase 2 (HMGCS2), which catalyzes the production of β-hydroxybutyrate. Also, Sirt3 deacetylated HMGSC2 *in vitro* (Shimazu et al., 2010).

Sirtuin 3 and The Heart

Cardiac hypertrophy is defined as restructuring of the cardiomyocytes in response to stress. The short term benefit of hypertrophy is protection of the heart from oxidative damage, but long term hypertrophy can lead to fibrosis, heart failure, and eventually, death of cardiomyocytes by either apoptosis or necrosis (Frey et al., 2004). Sirt3 is highly expressed in the heart tissue. Sirt3 $^{-/-}$ mice have a severe hypertrophic response 8 weeks after birth, accompanied by increased ROS production. In these mice overexpression of Sirt3 protected the heart from hypertrophy. Sirt3 activates Forkhead box O3a (FOXO3a)-dependent gene expression of anti-oxidant enzymes, mitochondrial manganese superoxide dismutase and catalase. These anti-oxidant enzymes act as ROS scavengers and suppress activation of Ras oncoprotein and preventing hypertrophy (Sundaresan et al., 2009).

Another ailment associated with the aging heart is cardiac failure. Though the exact mechanisms are still unclear, the role of MPTP cannot be ruled out. Sirt3-mediated deacetylation of CyP-D at Lys166 (Hafner et al., 2010) or Lys145 (Shulga and Pastorino, 2010) renders cells more resistant to the permeability transition induced by various signals (Elrod et al., 2010).

Sirtuin 3, Mitochondria and Reactive Oxygen Species

Mitochondria are the main source of ROS, specifically, superoxide anion (O_2^-). According to some estimates, almost 80% of superoxide in a cell is generated by mitochondria. There is always a balance between the generation and detoxification of ROS. Any imbalance can lead to serious cellular damage, including damage to DNA, RNA, proteins and lipids and genome instability. The main site for ROS/O_2^- generation in the mitochondria is the ETC. Under physiological conditions, minor leakage of electrons from the ETC during oxidative phosphorylation generates basal levels of ROS (Fig 5). This small amount of ROS acts as a critical signaling molecule within the cell (Hamanaka and Chandel, 2010). However, increased ROS production can lead to decreased cellular function, aging, and aging-associated disorders (Balaban et al., 2005). Since the ETC is the main site for O_2^- generation and Sirt3 regulates the activity of the ETC, it was speculated that Sirt3 might regulate ROS generation in mitochondria (Ahn et al., 2008). A correlation between ROS and mitochondrial Sirt3 is beginning to emerge.

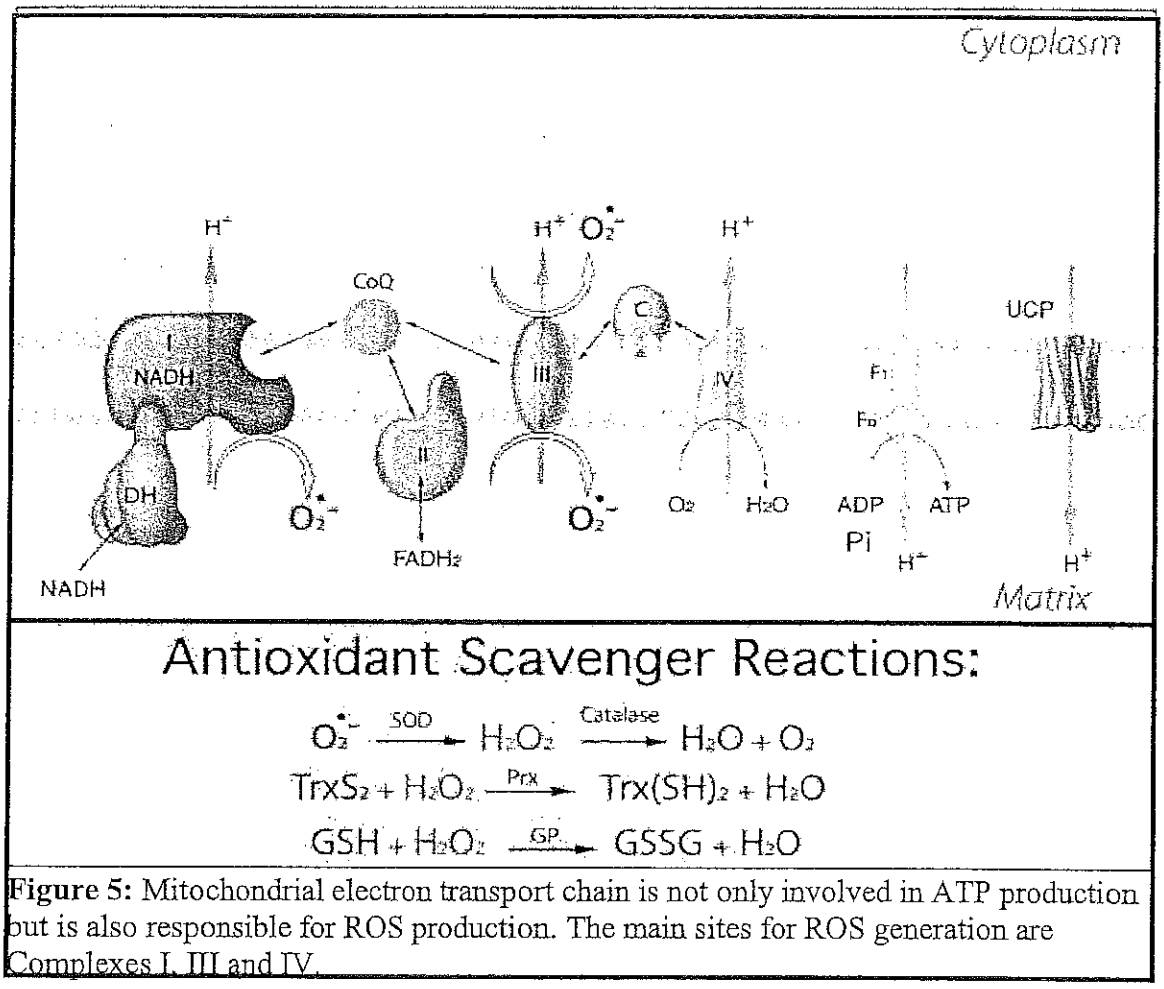

Figure 5: Mitochondrial electron transport chain is not only involved in ATP production but is also responsible for ROS production. The main sites for ROS generation are Complexes I, III and IV.

A. Sirtuin 3 and ROS generation

The primary role of the ETC is to generate a proton gradient ($\Delta\Psi_m$) across the IMM by pumping protons (H^+) into the IMS. As electrons travel through the ETC the sites of H^+ generation are complexes I, III and IV. Finally, the electrons are used by the ATP synthase (Complex V) in concert with the proton gradient to generate ATP. Under physiological conditions, there is a slight leakage of electron at these complexes, which results in basal levels of ROS generation. Any dysregulation of the ETC can elevate ROS generation.

i) Sirt3, Complex I and ROS

Sirt3 interacts with complex I of the ETC, specifically, with a 39 kDa subunit, NDUFA9. Proteomic analysis showed that this subunit was acetylated in $Sirt3^{-/-}$ mice and inactive. This acetylation increased ROS generation, which could be reversed by overexpression of wild type Sirt3. Thus, demonstrating a direct relationship between Sirt3 regulation of complex I activity and ROS generation (Ahn et al., 2008).

ii) Sirt 3 and Complex III

Another important site for ROS generation in the mitochondria is complex III. $Sirt3^{-/-}$ mice show hyperacetylation of various proteins in this complex and elevated ROS production. The exact target of Sirt3 in this complex is still unknown (Kim et al., 2006). Following increased ROS production $Sirt3^{-/-}$ mouse embryonic fibroblasts displayed an increase in replicative lifespan. This tumor-associated phenotype was associated with stabilized hypoxia inducible factor 1α (HIF1α). Under hypoxic conditions, observed in the tumor microenvironment, HIF1α stabilizes, translocates to the nucleus and binds to HIF response elements within target genes. Among HIF1α transcription targets are genes involved in glucose metabolism, angiogenesis and metastasis (Semenza, 2009). Stabilization of HIF1α is dependent on ROS generated by complex III. Inhibition of complex III by the specific inhibitor, stigmatellin, or treating the cells with an anti-oxidant (N-acetyl cysteine), decreased the ROS levels which attenuated HIF1α levels in Sirt3 knock down cells (Bell et al., 2011; Finley et al., 2011b).

B. Sirtuin 3 and defense against ROS

Sirt3 regulates detoxification of ROS by directly deacetylating and activating enzymes such as manganese superoxide dismutase 2 (MnSOD2), isocitrate dehydrogenase 2 (IDH2) and thioredoxin 2, or indirectly through transcriptional regulation of PGC1α or FOXO3a.

i) MnSOD2

Mitochondrial MnSOD2 catalyses the conversion of superoxide to less toxic hydrogen peroxide which is converted to water by catalase (Iborra et al., 2011). Sirt3 directly interacts with MnSOD2 (Tao et al., 2010). Deacetylation of MnSOD2 by Sirt3 increases its activity and decreases cellular ROS production (Tao et al., 2010).

ii) IDH2

IDH2 is a matrix protein and a major source of NADPH which is used by glutathione reductase for the detoxification of ROS (Reitman and Yan, 2010). IDH2 directly interacts with Sirt3 (Someya et al., 2010). During CR conditions, Sirt3-mediated deacetylation of IDH2 increases its activity, which in turn, exerts a protective effect by increasing the levels of reduced glutathione (Yu et al., 2012)

iii) Stress response by transcriptional regulation

One of the best studied transcription factors in the stress response is FOXO3a (for review see (Storz, 2011)). Sirt3 directly interacts with FOXO3a and deacetylates it,

which increases its DNA binding capacity. Increased DNA binding by FOXO3a increases MnSOD2 gene expression which, in turn, decreases ROS levels (Jacobs et al., 2008).

Sirtuin 3 and Cancer

Sirt3 plays an important role in regulation of metabolism and ROS production under CR conditions and fasting. These important functions of Sirt3 regulate aging (Hall et al., 2013). In fact, Sirt3 was initially identified as a homolog of yeast sirtuin (Silent information regulator 2, *Sir2*), which increases the replicative lifespan (Chen and Guarente, 2007). The incidence of cancer also increases with aging (López-Otín et al., 2013). Therefore, it is possible that if Sirt3 delays the aging process, then it may also have a role in cancer pathogenesis. In the past few years, Sirt3 has been shown to be involved in numerous oncogenic pathways (Allison and Milner, 2007; Haigis et al., 2012a; Shulga et al., 2010). However, a controversy exists whether Sirt3 is a tumor promoter or tumor suppressor (Alhazzazi et al., 2011b).

Sirt3 and tumorigenesis or cell survival

Tumor cells have a high metabolic requirement to maintain their growth rate. One particular molecule required in higher concentration by cancer cells is NAD^+, which regulates various metabolic pathways. One study showed that prostate cancer cells generate a higher NAD^+ concentration by increasing the expression of NAMPT. Inhibition of NAMPT in these cells reduced ATP levels and activated the AMPK pathway (Bowlby et al., 2012). Another study showed that rodents had increased Sirt3-regulated NAMPT activity during a 48 hour fasting (Shackelford et al., 2013). Under

genotoxic stress, Sirt3 was required to prevent cell death in HEK293 and fibrosarcoma cell lines by maintaining the cellular NAD^+ levels (Yang et al., 2007).

p53, a well known tumor suppressor, induces cell cycle arrest and cell death under stress conditions (McCubrey and Demidenko, 2012). p53 is a Sirt3 target and rescues p53-induced growth arrest in human bladder cancer derived cell lines (EJ/p53) (Li et al., 2010). Sirt3 was expressed higher in oral squamous cell carcinoma (OSCC) cell lines and human breast cancer tissues (Alhazzazi et al., 2011a; Ashraf et al., 2006). Sirt3 also has a role in anoikis, apoptotic cell death triggered by loss of extra cellular matrix contacts, in OSCC cell lines. In this study, stable suppression of receptor interacting protein (RIP) increased Sirt3 expression, which increased resistance to anoikis. Also, higher Sirt3 expression in OSCC cells increased tumor burden and incidence in mice that was reversed by stable suppression of Sirt3 (Kamarajan et al., 2012).

Sirtuin 3 and cell death

Based on the above studies, Sirt3 is considered to be pro-survival and protects various cancer cells against induction of apoptosis. In a few studies, Sirt3 has also been shown to be pro-apoptotic (Alhazzazi et al., 2011a; Giralt and Villarroya, 2012; Haigis et al., 2012b). Sirt3 expression positively correlates with growth arrest and apoptosis colorectal and osteosarcoma cancer cell lines. Also, Sirt3 rescued apoptosis induced by a loss of Bcl-2 (Allison and Milner, 2007). Moreover, treatment with kaempferol induced cell death by Akt inactivation, increased Bax and Sirt3 expression and caspase 3-dependent mitochondrial dysfunction (Marfe et al., 2009).

A tumor suppressive function of Sirt3 was shown in $Sirt3^{-/-}$ MEFs. In one study, $Sirt3^{-/-}$ MEFs expressing either Myc or Ras underwent spontaneous immortalization and possessed a tumorigenic phenotype (Kim et al., 2010). In contrast, wild type MEFs required expression of both oncogenes. $Sirt3^{-/-}$ mice also developed breast cancer after 24 months (Kim et al., 2010). In another study, $Sirt3^{-/-}$ MEFs transfected with Ras or E1a oncogenes grew more aggressively in a mouse xenograft model. Bell *et al* also demonstrated that Sirt3 suppressed tumor growth by inhibiting HIF1α stabilization and decreased mitochondrial ROS production (Bell et al., 2011). Sirt3 also deacetylates Cyp-D, which in turn regulates hexokinase II (HKII) binding to VDAC on the outer mitochondrial membrane (OMM). Sirt3 mediated deacetylation of Cyp-D is required for dissociation of HKII from OMM (Shulga et al., 2010), which sensitizes cells to Bax mediated apoptosis (Pastorino et al., 2002).

Expression levels of Sirt3 were also downregulated in head and neck squamous cell carcinoma (Lai et al., 2013), hepatocellular carcinoma (Zhang et al., 2012) and breast cancer (Sastre-Serra et al., 2013) cell lines. Aberrant Skp2 signaling is implicated in tumorigenesis (Chan et al., 2010). In breast and prostrate cancers, Skp2 was acetylated by p300 which leads to its activation and increases its oncogenic properties. Sirt3-mediated deacetylation of Skp2 decreases its stability and activity, thus providing evidence that Sirt3 acts as a tumor suppressor in breast cancer (Inuzuka et al., 2012).

Sirtuin 4

Sirtuin 4 (Sirt4) is another mitochondrial sirtuin that lacks deacetylase activity but possesses ADP-ribosyltransferase activity. Sirt4 has an important role in regulating amino acid stimulation of insulin secretion in pancreatic β-cells by ADP-ribosylating and

inhibiting glutamate dehydrogenase (GDH). Sirt4-mediated inhibition of GDH reduces the ATP generation from the catabolism of glutamate and glutamine (Haigis et al., 2006). Very little is known about the role of Sirt4 in the regulation of cell death. Interestingly, a recent study demonstrated that Sirt4 could function as a tumor suppressor in response to DNA damage (Csibi et al., 2013). Additionally, loss of Sirt4 increased glutamine-dependent tumor cell proliferation and spontaneous tumor development in Sirt4 KO mice (Jeong et al., 2013). However, the role of Sirt4 in the regulation of cell death pathways is still unclear.

Sirtuin 5

Sirtuin 5 (Sirt5) is another mitochondrial matrix localized sirtuin. It possesses weak deacetylase activity. Recent studies have shown that Sirt5 possesses lysine dessuccinylase and demalonylase activity *in vitro*, but the physiological significance is still unclear (Du et al., 2011). One of the first Sirt5 targets to be identified was carbamoyl phosphate synthase 1 (CPS1), an enzyme that catalyzes the rate limiting step of the urea cycle for detoxification and disposal of ammonia. Sirt5 deacetylated CPS1 and increased its enzymatic activity as $Sirt5^{-/-}$ mice failed to upregulate CPS1 activity (Nakagawa et al., 2009). These mice had elevated blood ammonia during fasting suggesting an impaired urea cycle (Nakagawa et al., 2009; Ogura et al., 2010). Another target indentified for Sirt5 was urate oxidase (UOX). In Sirt5 overexpression transgenic mice, UOX acetylation levels were almost half of those in wild type mice and UOX activity was significantly higher (Nakamura et al., 2012). Thus, it seems that Sirt5 like Sirt1, Sirt2 and Sirt3, has a major metabolic regulatory function. However, the role of Sirt5 in cancer is

yet to be determined. One study showed that Sirt5 overexpression in cerebellar granulae neurons (CGN) promoted neuronal cell death suggesting that Sirt5 could function as a tumor suppressor, at least in neurons (Pfister et al., 2008)

Materials and Method

Reagents

TransIT-TKO® Transfection reagent was purchased from Mirus (Madison,WI). Phenylarsine oxide and carbonyl cyanide 3-chlorophenylhydrazone (CCCP) were purchased from Sigma. Cyclosporin A was from Biomol Research Laboratories. Digitonin was from Calbiochem. Tetramethylrhodamine Methyl Ester Perchlorate (TMRM) was from Molecular Probes (Life Technologies).

Cell culture and treatment

HeLa, U2OS, MDA-MB231 and L929 cells (all from American Type Culture Collection, Manassas, VA) were maintained in 25 cm^2 flasks (Corning Costar, Corning, NY) with 5 ml Dulbecco's modified Eagle's medium (Gibco) containing 100 U/ml penicillin, 0.1 mg/ml streptomycin and 10% heat-inactivated fetal bovine serum and incubated at 37 °C under an atmosphere of 95% air and 5% CO_2. Where indicated, cells were transferred to DMEM containing galactose at 4.5 g/l.

For time lapse fluorescent microscopy, cells were plated in Labtek® 8 well chamber slides™ (Nunc, Rochester, NY) at 25,000 cells/well in DMEM containing glucose or galactose at 4.5 g/l. Treatments with cyclosporine A (10 μM) or leucine (1 mM) were done for 5 minutes before start of image acquisition.

Isolation of Mitochondria

Following treatments, cells from four individual wells (~400,000 cells total) were harvested by trypsinization and centrifuged at 600 *g* from 10 minutes at 4 °C. The cell pellets were washed once in phosphate buffered saline (PBS) and then resuspended in

three volumes of isolation buffer (20 mM HEPES, pH 7.4, 10 mM KCl, 1.5 mM $MgCl_2$, 1 mM sodium EDTA, 1 mM dithiothreitol and 10 mM phenylmenthylsulfonyl fluoride, 10 μM leupeptin, 10 μM aprotonin) in 250 mM sucrose. After chilling on ice for 3 minutes, the cells were disrupted by 40 strokes of glass homogenizer. The homogenate was centrifuged twice at 1500 *g* at 4 °C to remove unbroken cells and the nuclei. The mitochondria-enriched fraction (heavy membrane fraction) was then pelleted by centrifugation at 12,000 *g* for 30 minutes. Mitochondrial integrity was determined by the respiratory control ratio as oxygen consumption in state 3 and state 4 of respiration using a Clark oxygen electrode with 1 mM glutamate and 1 mM malate as respiratory substrates. The supernatant was removed and filtered through 0.2 μM and then 0.1 μM Ultrafree MC filters (Millipore) to give cytosolic protein.

RNA interference and plasmid Transfection

siRNAs targeting sirtuin-3 (sirt3), sirtuin-4 (sirt4), sirtuin-5 (sirt5), Mcl-1, Bcl-XL, Bak, Bax, Hexokinase-II (HKII), cyclophilin-D (CyP-D), glutamate dehydrogenase-1 (GDH-1) and non-target control were delivered into the cells using TransIT-TKO at the final concentration of 50 nM. Twenty-four hours after plating cells, siRNA-liposome complexes were added and incubated for 24 hours, after which the cells were washed twice with PBS and fresh complete medium was added. Where indicated, the cells were incubated for additional 24 hours.

For transfection of plasmids, U2OS cells were plated at 50,000 cells per well in 24 well plates. Following 24 hours, the cells were co-transfected with plasmid encoding enhanced green fluorescent protein (EGFP, Addgene) and the mammalian expression

vector pcDNA 3.1 containing sirt-3 (Addgene-13814) or sirt-3 mutant (sirt-3 [H248Y], Addgene-24492). Following 24 hours, the cells were either un-treated or treated with 30 μM of cisplatin. After 16 hours exposure to cisplatin, the cells were harvested and the number of EGFP expressing cells staining for Yo-Pro-1 was determined on a Cellometer Vision.

Measurement of cell viability

Cell viability was determined utilizing Yo-Pro-1, which is, selectively taken up by apoptotic cells (Boffa et al., 2005; Idziorek et al., 1995) and propidium iodide. Following treatments, floating and attached were harvested and centrifuged at 700 *g*. The cell pellet was washed twice with phosphate buffered saline and resuspended in PBS. 5 μM of Yo-Pro-1 and 5 μM was added and incubated for 5 minutes. After incubation, the cells were pelleted and resuspended in PBS. The percentage of viable cells was determined utilizing a Cellometer (Nexelom) as the ratio of the number of cells in the fluorescent images (green for Yo-Pro-1 and red for propidium iodide) to the bright field images.

Determination of caspase activity and phosphatidylserine exposure

Caspase activity was determined using NucView 488 Caspase-3 activity kit (Biotium, Hayward, CA). Forty-eight hours after siRNA transfection, floating and attached cells were collected and resuspended in DMEM containing 5 μM of the NucView 488 substrate and then incubated at room temperature for 30 minutes protected from light. After incubation, the cells were washed once with ice cold PBS, and then resuspended in PBS. Caspase activity was detected by an increase in the intensity of the

DNA binding dye using Cellometer Vision. For determination of phosphatidylserine (PS) exposure, forty-eight hours after siRNA transfection, floating and attached cells were collected and resuspended in 100 µl of binding buffer at 1.0 x 10^6 cells per ml. AnnexinV-FITC (5 µl) was added, and the cells were incubated at room temperature for 15 minutes protected from light. PS positive cells were determined using Accuri C6 flow cytometer.

Mitochondrial membrane potential and reactive oxygen species (ROS) determination

Mitochondrial membrane potential after treatment or transfection with siRNA was determined using potentiometric dye TMRM. MitoTracker green was used to determine mitochondrial mass since its uptake is independent of mitochondrial membrane potential and dependent on mitochondrial membrane integrity. Forty-eight hours after siRNA transfection, 200 nM TMRM and 200nM of MitoTracker green was added to each well and cells were incubated at 37 ˚C for 30 minutes. After incubation, floating and attached cells were collected and washed twice with ice cold PBS. The cells were then suspended in ice cold PBS and analyzed immediately using flow cytometery. For ROS determination, MitoSOX and DCFDA [5-(and-6)-carboxy-2',7'-dichlorodihydrofluorescein diacetate] (both from Life Technologies) were utilized. Forty-eight hours after siRNA transfection, 5 µM MitoSOX or 10 µM of DCFDA was added to each well and the cells were incubated for 30 minutes at 37 ˚C. After incubation, floating and attached cells were collected and washed twice with ice cold PBS. After final wash,

the cells were resuspended in ice cold PBS and analyzed immediately utilizing Accuri C6 Flow Cytometer.

Determination of Bax and Bak activation

For Bax activation, cells were plated on 12 mm coverslips at 5.0 X 10^4 density and allowed to attach overnight. The cells were transfected with the indicated siRNAs for 24 h. Following siRNA transfection, the cells were washed twice with PBS, fixed with 3.7% formaldehyde in PBS for 5 min, and then permeabilized with 0.2% CHAPS in PBS for 10 min. Non-specific antibody binding was blocked with 5% goat serum and 1% bovine serum albumin in PBS for 30 min. Following another wash, cells were incubated for 1 hour in primary antibody solution (1:100, mouse anti-BAX, clone 6A7; Sigma). The cells were then incubated in the secondary antibody solution (1:750 Alexa 488-conjugated goat anti-mouse IgG) for 1 hour. For nuclear staining, the coverslips were incubated with 2 μg/ml Hoechst 33342 in PBS for 10 min. The coverslips were mounted on glass slides using 80% glycerol in PBS. The stained cells were viewed on an Olympus IX51 (Olympus, Center Valley, PA). Images were captured with a Hamamatsu C-10600-10B camera (Hamamatsu, Bridgewater, NJ) and SlideBook software (Intelligent Imaging Innovations, Denver, CO). Quantification was done by drawing a region of interest around each cell in the acquired images. The intensity was determined by the SlideBook software, and was expressed as the percentage of Bax activation and staining induced by the Triton X-100.

For Bak oligomerization, mitochondria were isolated from approximately 400,000 cells. Briefly, cell pellets were washed once with phosphate-buffered saline and then

resuspended in 3 volumes of isolation buffer (20 mM HEPES (pH 7.4), 10 mM KCl, 1.5 mM $MgCl_2$, 1 mM sodium EDTA, 1 mM dithiothreitol, 10 mM phenylmethylsulfonyl fluoride, 10 μM leupeptin, and 10 μM aprotinin) in 250 mM sucrose. The cells were disrupted in a glass homogenizer and centrifuged twice at 1500 × g at 4 °C to remove unbroken cells and nuclei. The mitochondrial fraction was then pelleted by centrifugation at 12,000 × g for 30 min. Cellular fractionation was assessed for cross contamination by utilizing lamin A/C (1:1,000 Cell Signaling), prohibitin (1:1000,EMD) and GADPH (1:1,000 Cell Signaling) as nuclear, mitochondrial and cytosolic markers, respectively. After various treatments in intact cells and isolated mitochondria, Bak oligomerization was determined by incubating isolated mitochondria with 0.1mM bismaleimidohexane (BMH) for 30 minutes at room temperature. The samples were then separated on Novex 10% Tris/Glycine precast gels in the XCell II module with MagicMark XP (all from Invitrogen) as the molecular weight marker. Proteins were immune-blotted onto PVDF membrane and probed with anti-Bak antibody (Cell Signaling).

Time lapse fluorescence microscopy

HeLa cells or U2OS cells were plated in 8 well chamber slides (Nunc, Rochester, NY) at 25,000 cells per well. Cells were transfected with siRNA as described above. Where indicated, cells were pre-treated with cyclosporin A or clotrimazole for 10 minutes before the start of image acquisition. For determination of mitochondrial energization, cells were loaded with 200 nM TMRM for 30 min. For determination of ROS formation, cells were loaded with 200nM of MitoSOX for 30 minutes. The cells were then washed twice with was buffer (50 mM Tris, 1 mM EGTA, pH 7.5). The cells

were placed in respiratory medium containing 0.5 mM EGTA, 3 mM $MgCl_2$, 60 mM potassium lactobionate, 20 mM taurine, 10 mM KH_2PO_4, 20 mM HEPES, 110 mM sucrose, 1 g/l BSA, 2 μM oligomycin, 1mM of succinate and either 20nM of TMRM or 20nM of MitoSOX. The cells were then incubated in the respiratory medium for 5 min on a heated stage maintained at 37°C. Digitonin (2.5μg/ml) was added to permeabilize the plasma membrane. Images containing 200-250 cells were taken at 1 min intervals for 20 min on the Olympus IX51 microscope using a 20X objective. Recombinant truncated Bid (tBid), phenylarsine oxide or calcium was added after 2 min, and CCCP was added after 18 min to induce complete depolarization. For superoxide anion production, cells were loaded with 5 μM MitoSOX for 30 minutes. Treatment and image acquisition was similar to TMRM except that an increase in ROS dependent MitoSOX fluorescence was measured over 20 minutes. Images were analyzed using Slidebook software. For TMRM, regions of interest were drawn around cells in the acquired images, pixel intensities were measured and averaged for each image. A line graph for each condition was drawn in SigmaPlot using the formula: **% Intensity** = (Observed Intensity-Final Image Intensity)/(First Image Intensity-Final Image Intensity)*100. to provide more clarity to the graphs, a constant was added or subtracted from data sets of each condition to prevent the traces from overlapping. For MitoSOX, intensity measurements were done similar to TMRM experiments. The increase in fluorescence intensity at one minute intervals was compared to the intensity of the first image acquired (at zero minute time point) and represented as percent using the formula: **% increase in fluorescence intensity** = (Observed image intensity-first Image intensity)/(first image intensity)*100. A bar graph was made for the 3 and 20 min time points. At the end of each experiment,

the cells from 4 wells per condition were collected and used to determine cytochrome c retention.

Western blotting

Protein samples (20 μg/lane) were separated on Novex 10% Tris/Glycine precast gels in the XCell II module with MagicMark XP (all from Invitrogen) as the molecular weight marker. Proteins were immuno-blotted onto PVDF membranes using the XCell II Blot module (Invitrogen). Mcl-1, Bcl-X_L, Sirtuin-3, Hexokinase II, VDAC-1, tubulin, UACRC-1, prohibitin, lamin A/C, βactin, GAPDH and PARP were detected using mouse monoclonal antibodies (from Sigma, Cell Signaling and MitoSciences) at 1:1000 dilution. Bak monoclonal antibody (Cell Signalin) was also used at 1:1000 dilution. Cytochrome c in the pellets collected after time lapse fluorescence microscopy was detected using mouse monoclonal anti-cytochrome c antibody (BD Pharmingen) at 1:1000 dilution. Appropriate horseradish peroxidase labeled secondary antibodies (1:10,000 dilution) was used to detect the relevant proteins by enhanced chemiluminescence.

Microplate assay from mitochondrial depolarization and H_2O_2 production

HeLa cells were plated at 50,000 cells per well in 24 well plates and transfected with the indicated siRNAs. After forty-eight hours, the cells were loaded with 200 nM TMRM in DMEM for 30 minutes. After loading, the cells were washed once with wash buffer. After washing, cells were incubated further for 5 minutes in the respiratory buffer containing 2.5 μg/ml digitonin and 20 nM of TMRM. Fluorescence intensity was

measured using a Synergy HT microplate reader with an excitation wavelength at 550 nm and emission wavelength at 573 nm at 37 °C for 30 seconds interval. After 4 minutes, either phenylarsine oxide or Ca^{2+} was added at the indicated concentrations with fluorescence measured over 20 minutes. For complete depolarization 2.5 μM of CCCP was added after 4 minutes. The results are presented as percent of TMRM retained in the non-treated cells transfected with non-target siRNA at the 20 minute time point. For Amplex red assay, HeLa cells were plated and then transfected with siRNAs targeting sirt-4 and CyP-D either individually or in tandem with siRNA targeting GDH-1. following 48 hours, cells were placed in the respiratory buffer and permeabilized with digitonin (2.5 μg/ml). Amplex red reagent was added at 5 μM along with 10 U/ml horseradish peroxidase. Following addition of Ca2+ or phenylarsine oxide, Fluorescence intensity was measure using Synergy HT microplate reader with an excitation of 570 nm and emission at 585 nm at 37 °C at 1 minute intervals.

Measurement of Glutamate Dehydrogenase-1 activity

Glutamate dehydrogenase-1 (GDH-1) activity in HeLa cells was measured using the GDH activity assay kit from BioVision (Mountain View, CA). Briefly, 50,000 cells per well were plated in 24 well plates. Transfection was carried out as described above. Forty-eight hours after transfection, cells from four wells were harvested by trypsinization and washed twice with ice cold PBS. Mitochondria were isolated and lysates prepared as described above. Optical density at 450 nm was measured with Synergy HT microplate reader (BioTek, Winooski, VT) at 37 °C at 3 minute intervals for

1 hour. The results are expressed as the percentage increase or decrease in activity compared to non-treated cells transfected with non-target control siRNA.

Measurement of mitochondrial glutathione levels

Glutathione (GSH) was estimated using monobromobimane fluorochrome based assay according to the manufactures instruction (Millipore, Billerica, MA). Briefly, 50,000 cells per well were plated in 24 well plate. Transfection was carried out as described above. Forty-eight hours after transfection, cells from four wells were harvested by trypsinization and washed twice with ice cold PBS. All procedures were done on ice and as rapidly as possible to prevent GSH oxidation. Mitochondria were isolated and lysates were prepared. The supernatant was used to determine the GSH content. Fluorescence was measured at excitation of 308 nm and emission of 460 nm using Synergy HT microplate reader. The results are presented as percentage of GSH content compared to non-treated and non target transfected cells.

Determination of mitochondrial Ca^{2+} retention capacity

The Ca^{2+} retention capacity was measured fluorimetrically on a microplate reader at 37 ˚C in the presence of the Ca^{2+} indicator Calcium Green-5N (1 μM; excitation: 505 nm; emission: 535 nm; Molecular Probes). Whole cells were placed in the respiratory buffer containing 1 mM succinate and permeabilized with digitonin. Calcium was added in pulses 10 μM and uptake measured as decrease of Calcium Green-5N fluorescence. Calcium was added in pulses until onset of the PTP occurred as indicated by a rapid rise of calcium-green 5N fluorescence. To allow calculation of medium Ca^{2+} from the

measured fluorescence values, each experiment was ended by the addition of 10 μM of the uncoupler CCCP followed by 400 μM EGTA, to be in excess of Ca^{2+} added during the study to determine the minimum fluorescence intensity (F_{min}) value, followed by 4 mM $CaCl_2$ to determine the maximum fluorescence intensity (F_{max}) value. The results are average of three independent experiments.

EXPERIMENTAL RESULTS

Sirtuin 3 modulates Bax/Bak dependent apoptosis

Rationale

The mitochondrial deacetylase, sirtuin-3, controls multiple aspects of mitochondrial function. Sirtuin-3 deacetylates a number of mitochondrial matrix proteins including constituents of the respiratory chain complexes and anti-oxidant effectors such as isocitrate dehydrogenase-2 (IDH2) and mitochondrial manganese superoxide dismutase (MnSOD) (Ahn et al., 2008; Tao et al., 2010; Yu et al., 2012). The increased acetylation of respiratory chain components by depletion of sirt-3 brings about a decrease in oxidative phosphorylation. Similarly, the increased acetylation of MnSOD and IDH2 in sirt-3 depleted cells inhibits their activity as anti-oxidants. These two effects of sirt-3 depletion conspire to elevate ROS levels. The increased ROS is thought to promote tumorigenesis in part by generating genomic instability (Kim et al., 2010). Additionally, once transformed, the stimulation of ROS due to sirt-3 depletion helps to promote glycolysis, a characteristic of transformed cells, by increasing the stability of hypoxia-inducible factor-1α (HIF-1α) (Bell et al., 2011; Schumacker, 2011). Elevated levels of HIF-1α bring about increased expression of glycolytic enzymes including hexokinase II, which is a rate limiting step of glycolysis (Marín-Hernández et al., 2009; Mathupala et al., 2001; Riddle et al., 2000) Moreover, suppression of sirtuin-3 expression also promotes the binding of hexokinase II to the mitochondria by stimulating the activity of cyclophilin-D (Shulga et al., 2010).

Cyclophilin-D is localized to the mitochondrial matrix and is best known as a positive modulator of the mitochondrial permeability transition pore (Baines et al., 2005; Basso et al., 2005). Onset of the permeability transition is a critical event in necrotic cell

death, with knock-down of cyclophilin-D preventing necrosis. As in necrosis, mitochondrial injury is also a central mediator of apoptotic cell death, but with the mechanisms differing vastly. In contrast to necrosis some studies indicate that cyclophilin-D prevents apoptotic cell death (Li et al., 2004; Lin and Lechleiter, 2002; Schubert and Grimm, 2004). The duality of cyclophilin-D effects in necrosis versus apoptosis may lie in the ability of cyclophilin-D to modulate the binding of hexokinase II to the mitochondria (Machida et al., 2006). We and others have demonstrated that mitochondrial bound hexokinase II prevents mitochondrial injury during apoptosis by inhibiting the ability of pro-apoptotic proteins Bak and Bax from disrupting the integrity of the outer mitochondrial membrane (Gall et al., 2011; Majewski et al., 2004a; Majewski et al., 2004b; Pastorino et al., 2002)

The aims of the study are:

1. Does Sirt3 function as a tumor suppressor or a tumor promoter?
2. How does Sirt3, which is a mitochondrial matrix protein modulates the events of apoptotic cell death on the outer mitochondrial membrane?
3. How does expression of Sirt3 correlates with hexokinase II binding on the outer mitochondrial membrane and activation of the apoptotic cell death program?

6. Sirt-3 modulates loss of cell viability induced by Mcl-1 and Bcl-X_L depletion

Mcl-1 and Bcl-X_L are critical anti-apoptotic proteins localized to the outer mitochondrial membrane. As shown in Fig. 6A, siRNAs targeting Mcl-1 or Bcl-X_L are able to selectively suppress their respective targets, with tandem transfection suppressing expression of both Mcl-1 and Bcl-X_L. Fig. 6B demonstrates that downregulation of Mcl-1 and Bcl-X_L separately gave little loss of cell viability as assessed by Yo-Pro-1 staining, which selectively stains apoptotic cells (Boffa et al., 2005; Idziorek et al., 1995). However, the tandem suppression of Mcl-1 and Bcl-X_L expression resulted in 78% of the cell undergoing apoptosis following 48 hours (Fig. 6B). These results agree with previous studies indicating that suppression of both Mcl-1 and Bcl-X_L are required to induce mitochondrial injury and subsequent apoptosis. Bak and Bax are pro-apoptotic proteins localized to the outer mitochondrial membrane and kept in a tonic state of inhibition by interaction with Mcl-1 and Bcl-X_L. We wanted to determine if cell death induced by depletion of Mcl-1 and Bcl-X_L was dependent on Bak/Bax. As shown in Fig. 6C, left panel, siRNAs targeting Bak and Bax are able to selectively suppress the expression of their respective targets, with tandem transfection lowering the levels of both Bak and Bax. Significantly, concomitant suppression of Bak and Bax expression prevented induction of cell death induced by Mcl-1 and Bcl-X_L depletion, with only an 18% loss of cell viability after 48 hours (Fig. 6B). Importantly, as shown in Fig. 6C, middle panel, lane 1, simultaneous transfection with siRNAs targeting Bak/Bax did not interfere with the ability of siRNAs to target and deplete Mcl-1 and Bcl-X_L.

Sirtuin-3 (sirt-3) has been proposed to be a tumor suppressor, whose depletion enhances cancer cell survival. We wanted to determine if sirt-3 expression had any effect on the Bak/Bax dependent cell death brought about by depletion of Mcl-1 and Bcl-X_L. As shown in Fig. 6B, concurrent transfection with siRNA targeting sirt-3 prevented the loss of cell viability brought about by depletion of Mcl-1 and Bcl-X_L to the same degree as did suppression of Bak/Bax expression. Importantly, depletion of sirt-3 had no effect on the ability to suppress expression of Mcl-1 and Bcl-X_L when utilizing their respective siRNAs (Fig. 6C, middle panel, lane 2). Intriguingly, the protective effect exerted by suppression of sirt-3 is not mediated by depletion of Bak or Bax. As demonstrated in Fig. 6C, right panel, lane no. 2, transfection with siRNAs targeting sirt-3 in combination with siRNAs against Mcl-1 and Bcl-X_L had no effect on the level of Bak or Bax expression. In contrast to sirt-3, suppression of sirtuin-4 or sirtuin-5 expression, both localized to the mitochondria, did not prevent cell death induced by Mcl-1 and Bcl-X_L depletion (Fig. 6B).

Figure 6. Sirt-3 modulates Bak/Bax dependent apoptosis induced by Mcl-1 and Bcl-X_L depletion.

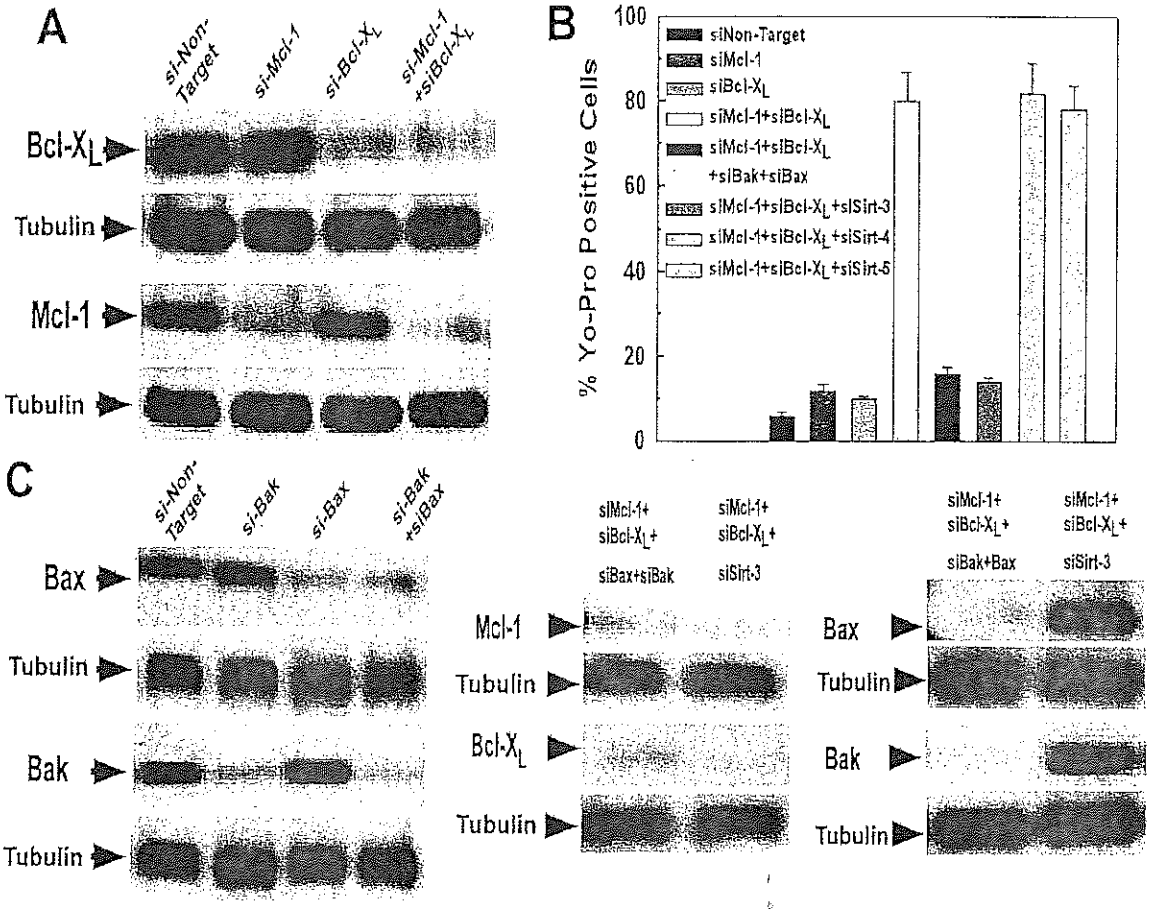

(A) HeLa cells were transfected with 50 nM of a non-targeting control siRNA or siRNAs targeting Mcl-1 or Bcl-X_L, either alone or in tandem. Following 24 hours incubation, the cells were harvested and the levels of Mcl-1, Bcl-X_L and tubulin were determined by western blotting. The results are typical of three independent experiments.

(B) HeLa cells were transfected with 50 nM of the indicated siRNAs, either individually or in tandem. Following 48 hours, the cells were harvested and the degree of apoptosis determined by staining with Yo-Pro-1 as described in Materials and Methods. Values are the means of three independent experiments with the error bars indicating standard deviations.

(C) HeLa cells were transfected with 50 nM of a non-targeting control siRNA or siRNAs targeting Bak, Bax, sirtuin-3, Mcl-1 or Bcl-X_L, either alone or in tandem. Following 24 hours incubation, the cells were harvested and the levels of Bak, Bax, Mcl-1, Bcl-X_L and

tubulin were determined by western blotting. The results are typical of three independent experiments.

7. Depletion of sirt-3 prevented Bax activation and Bak oligomerization

When unrestrained by Mcl-1 or Bcl-X_L, Bak undergoes activation and oligomerization. As show in Fig. 7A, lane 2, depletion of Mcl-1 and Bcl-X_L induced Bak oligomerization that was not prevented by concomitant transfection with a non-targeting siRNA, but was prevented by depletion of sirt-3 (lane 3). Similarly, when activated, Bax undergoes a conformational alteration that exposes it N-terminus, making it detectable utilizing the Bax6A7 antibody. As shown by immunostaining and quantification, cells transfected with non-targeting control siRNA displayed minimal Bax activation (Fig. 7B, left micrograph). However, there was robust immunostaining 24 hours following transfection with siRNAs targeting Mcl-1 and Bcl-X_L (Fig. 7B, middle micrograph). Importantly, like Bak activation, depletion of sirtuin-3 also inhibited the activation of Bax induced by suppression of Mcl-1 and Bcl-X_L expression (Fig. 7B, right micrograph).

Figure 7. Mcl-1 and Bcl-X_L knockdown induced Bak and Bax activation is prevented by depletion of Sirt-3

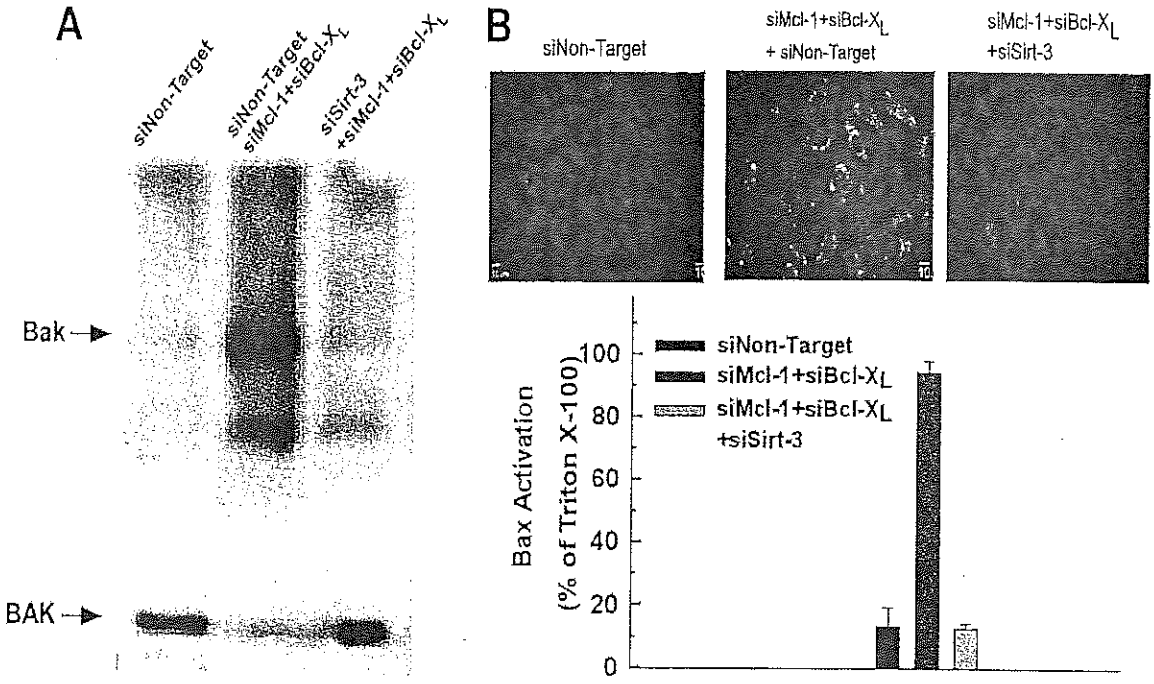

(A) HeLa cells were transfected with 50 nM of the indicated siRNAs. Following 24 hours incubation, the cells from four wells were harvested and the mitochondrial fraction isolated. The isolated mitochondria were incubated with 0.1 mM of the cross-linking reagent BMH for 30 minutes. The samples were then run out on 12% SDS-PAGE gels and Bak oligomerization was assessed by western blotting.

(B) HeLa cells were plated on 12 mm coverslips (Fisher Scientific) at 5.0×10^4 cells and allowed to attach overnight. The next day, cells were transfected with the indicated siRNAs. Following 24 hours incubation, the cells were washed twice with PBS, fixed and immunostained with anti-Bax clone 6A7 as described in Materials and Methods. Quantification was done by drawing a region of interest around each cell in the acquired images (200–250 cells). The intensity was determined by SlideBook and is expressed as the percentage of Bax immunostaining induced by Triton X-100.

8. Activation of Bax and Bax causes mitochondrial injury

Bak/Bax induced mitochondrial damage brings about an increase in the generation of reactive oxygen species (ROS) and eventual loss of mitochondrial membrane potential. As shown in Fig. 8A, B, following 24 hours of incubation, simultaneous suppression of Mcl-1 and Bcl-X_L expression provoked a reduction of mitochondrial membrane potential and stimulation of ROS production that was prevented by suppression of Bak/Bax expression. Importantly, depletion of sirt-3 also prevented the loss of mitochondrial membrane potential and stimulation of ROS production induced by suppression of Mcl-1 and Bcl-X_L to the same extent as did Bak/Bax depletion. Mitotracker-Green labels mitochondria independent of membrane potential, making it useful to determine if there are any effects of Mcl-1, Bcl-X_L or sirt-3 depletion on mitochondrial mass. As shown in Fig. 8A, there were no changes to Mito-tracker-Green labeling in any of the conditions studied, suggesting that at the time frames under scrutiny, there are no alterations in mitochondrial mass. Also, depletion of sirt-3 is shown to have no effect on expression of UQCRC1, a core component of complex III of the mitochondrial respiratory complex. Also, suppression of Mcl-1 and Bcl-X_L did not alter levels of UQCRC1 in the presence or absence of sirt-3, indicating that there is no discernible effect on mitochondrial biogenesis in the time frame under study.

Figure 8. Depletion of sirt-3 prevents Bak/Bax dependent mitochondrial injury

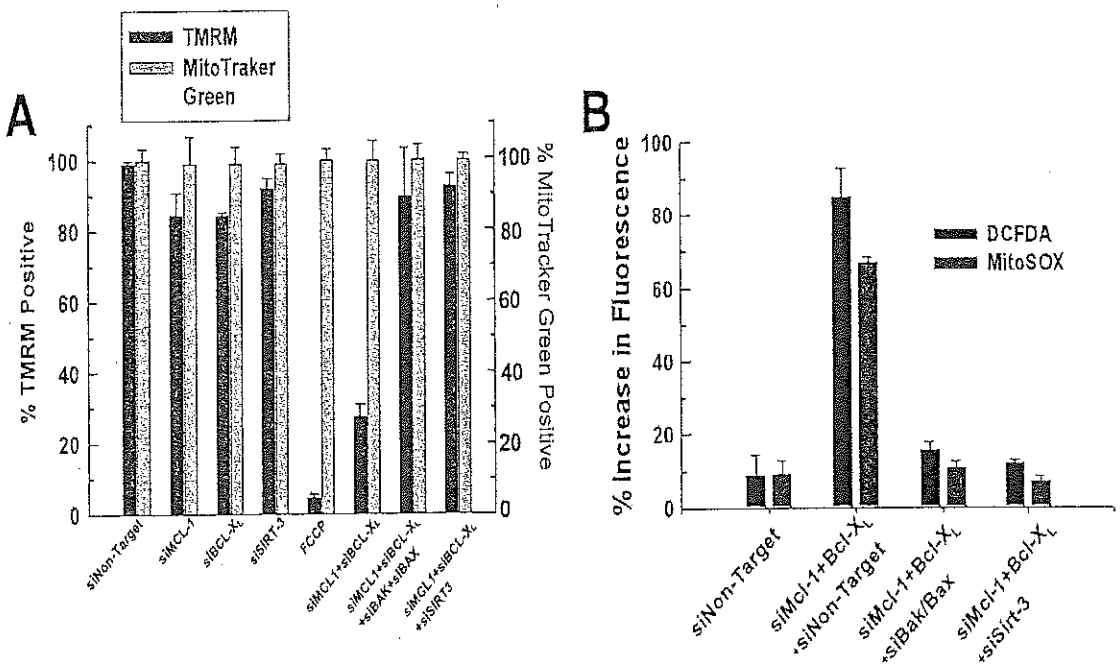

(A) HeLa cells were transfected with 50 nM of a non-targeting control siRNA or siRNAs targeting Mcl-1, Bcl-X_L, Bak, Bax, sirtuin-3; either alone or in tandem. Forty-eight hours after siRNA transfection, 200 nM TMRM and 200 nM of Mito-Tracker Green was added to each well and the cells were incubated at 37°C for 30 minutes. After incubation, floating and attached cells were collected and washed twice with ice cold PBS. The cells were suspended in ice cold PBS and analyzed immediately using flow cytometry as described in Materials and Methods. Values are the means of three independent experiments with the error bars indicating standard deviations.

(B) HeLa cells were transfected with 50 nM of a non-targeting control siRNA or siRNAs targeting Mcl-1, Bcl-X_L, Bak, Bax, or sirtuin-3, either alone or in tandem. Forty-eight hours after siRNA transfection, 200 nM of MitoSOX or 10 μM DCFDA was added to each well and the cells were incubated for 30 minutes at 37°C. After incubation, floating and attached cells were collected and washed twice with ice cold PBS. After the final wash, cells were suspended in ice cold PBS and analyzed immediately by flow cytometry

as described in Materials and Methods. Values are the means of three independent experiments with the error bars indicating standard deviations.

9. Mitochondrial injury causes caspase activation and phosphatidylserine externalization

Downstream effects of mitochondrial injury during the progression of apoptosis include caspase-3 activation and externalization of phosphatidylserine (PS) on the exterior leaflet of the plasma membrane. As shown in Fig. 9A, as assessed by cleavage of a fluorometric caspase substrate (DEVD-Nunc View 488), 36 hours following transfection suppression of Mcl-1 and Bcl-X_L brings about caspase activation that is inhibited by depletion of Bak/Bax. Importantly, depletion of sirt-3 also prevented cleavage of DEVD-NuncView 488 brought about by suppression of Mcl-1 and Bcl-X_L expression (Fig. 9A). Similarly, the endogenous caspase-3 substrate, PARP, was cleaved and degraded by suppression of Mcl-1 and Bcl-X_L expression, which in turn was prevented by a caspase-3 inhibitor or depletion of sirt-3 (Fig. 9A, inset). Externalization of PS on the exterior leaflet of the plasma membrane promotes phagocytosis and is utilized as a marker for apoptosis. As assessed by annexin V binding, suppression of Mcl-1 and Bcl-X_L induced externalization of PS on the plasma membrane, which was prevented by depletion of Bak/Bax or sirt-3 (Fig. 9B). The above results indicate that by preventing the proximal activation of Bak/Bax, depletion of sirt-3 prevents the mitochondrial injury mediated by suppression of Mcl-1 and Bcl-X_L expression and the resultant onset of downstream apoptotic events such as depolarization of the mitochondria, mitochondrial ROS generation, caspase activation, PS externalization and eventual loss of cell viability.

Figure 9. Depletion of sirt-3 prevents Bak/Bax dependent caspase activation and phosphatidylserine externalization.

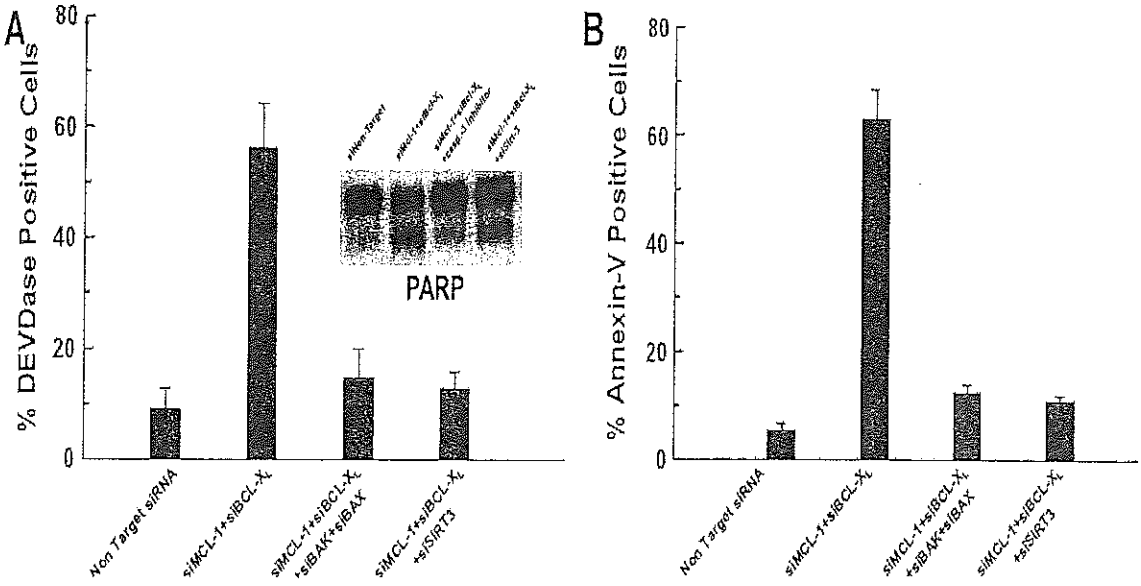

(A) HeLa cells were transfected with 50 nM of a non-targeting control siRNA or siRNAs targeting Mcl-1, Bcl-X_L, Bak, Bax, sirtuin-3; either alone or in tandem. Following 24 hours incubation, the cells were harvested. The samples were separated by SDS-PAGE and immunoblotted onto PVDF membranes to detect PARP cleavage. Alternatively, caspase activity was determined using NucView 488 Caspase-3 activity kit as described in Materials and Methods. Values are the means of three independent experiments with the error bars indicating standard deviations.

(B) HeLa cells were transfected with 50 nM of a non-targeting control siRNA or siRNAs targeting Mcl-1, Bcl-X_L, Bak, Bax, sirtuin-3; either alone or in tandem. Following 48 hours incubation, the cells were harvested. Floating and attached cells were collected and resuspended in 100 µl of binding buffer at 1.0×10^6 cells/ml. FITC-Annexin-V (5 µl) was added to determine phosphatidylserine (PS) externalization, and the cells were incubated for 15 minutes at room temperature. PS positive cells were determined by flow cytometry. Values are the means of three independent experiments with the error bars indicating standard deviations.

10. Breast cancer cell line, MDA-MB231, recapitulated the results with HeLa cell line

We next wanted to determine if the results that we obtained with HeLa cells were applicable to another cancer cell line with a high glycolytic rate. Cells of the breast cancer cell line, MDA-MB-231, also express a high level of hexokinase II (Furtado et al., 2012; Zancan et al., 2010). As shown in Fig. 10A, simultaneous suppression of Mcl-1 and Bcl-X_L in the presence of non-targeting siRNA induced an 80% and 60% increase in the number of cells staining positive for Yo-Pro or annexin V, respectively. Suppression of Bak and Bax largely suppressed the loss of cell viability induced by depletion of Mcl-1 and Bcl-X_L. Importantly, as in HeLa cells, suppression of sirt-3 expression prevented the loss of cell viability brought about by depletion of Mcl-1 and Bcl-X_L to the same degree as suppression of Bak/Bax expression. As shown in Fig. 10B, C, the loss of cell viability induced by depletion of Mcl-1 and Bcl-X_L in MDA-MB-231 cells was accompanied by depolarization of the mitochondrial membrane potential and increase of ROS formation as measured by TMRM and MitoSOX or DCF fluorescence, respectively. Both mitochondrial depolarization and ROS formation was prevented by depletion of Bak/Bax or sirt-3. Importantly, as shown in Fig. 10B, there were no changes in Mito-Tracker Green fluorescence, indicating that there are no alterations in the mitochondrial mass of the MDA-MB-231 cells under the conditions and time course under study. Accompanying the ability to preserve mitochondrial integrity, depletion of sirt-3 also prevented the activation of Bax induced by suppression of Mcl-1 and Bcl-X_L expression (Fig. 10D).

Figure 10. Sirt-3 is required for Bak/Bax dependent apoptosis in MDA-MB-231 breast cancer cells.

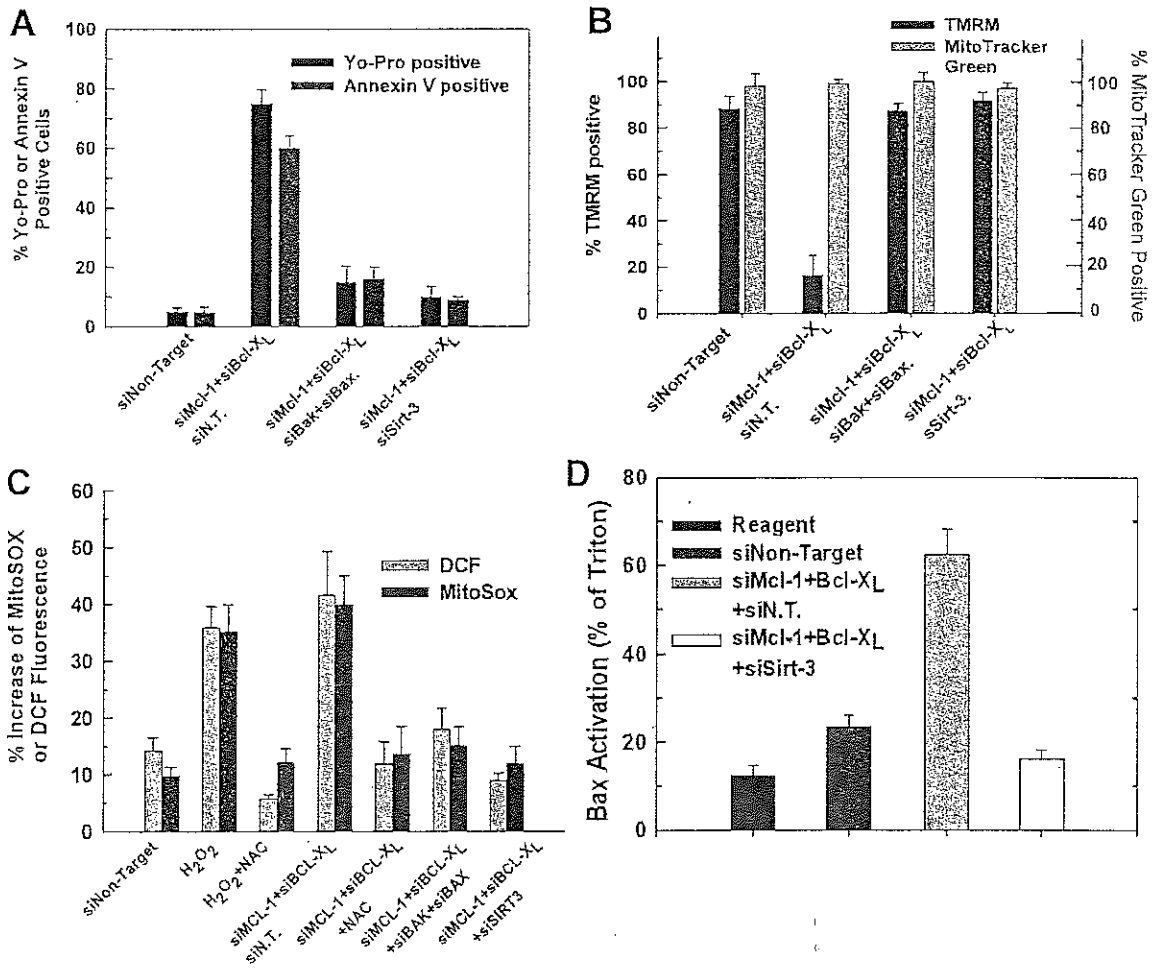

(A) MDA-MB-231 cells were transfected with 50 nM of the indicated siRNAs, either individually or in tandem. Following 48 hours, the cells were harvested and the degree of apoptosis determined by staining with Yo-Pro-1 as described in Materials and Methods. Values are the means of three independent experiments with the error bars indicating standard deviations. For annexin V staining, floating and attached cells were collected and re-suspended in 100 µl of binding buffer at 1.0×10^6 cells/ml. FITC-Annexin-V (5 µl) was added to determine phosphatidylserine (PS) externalization, and the cells were incubated for 15 minutes at room temperature. PS positive cells were determined by flow

cytometry. Values are the means of three independent experiments with the error bars indicating standard deviations.

(B) MDA-MB-231 cells were transfected with 50 nM of a non-targeting control siRNA or siRNAs targeting Mcl-1, Bcl-X_L, Bak, Bax, sirtuin-3; either alone or in tandem. Forty-eight hours after siRNA transfection, 200 nM TMRM and 200 nM of Mito-Tracker Green was added to each well and the cells were incubated at 37°C for 30 minutes. After incubation, floating and attached cells were collected and washed twice with ice cold PBS. The cells were suspended in ice cold PBS and analyzed immediately using flow cytometry as described in Materials and Methods. Values are the means of three independent experiments with the error bars indicating standard deviations.

(C) MDA-MB-231 cells were transfected with 50 nM of a non-targeting control siRNA or siRNAs targeting Mcl-1, Bcl-X_L, Bak, Bax, sirtuin-3; either alone or in tandem. Forty-eight hours after siRNA transfection, 200 nM MitoSOX or 10 μM DCFDA was added to each well and the cells were incubated for 30 minutes at 37°C. After incubation, floating and attached cells were collected and washed twice with ice cold PBS. After the final wash, cells were suspended in ice cold PBS and analyzed immediately by flow cytometry as described in Materials and Methods. Values are the means of three independent experiments with the error bars indicating standard deviations.

(D) MDA-MB-231 cells were plated on 12 mm coverslips (Fisher Scientific) at 5.0×10^4 cells and allowed to attach overnight. The next day, cells were transfected with the indicated siRNAs. Following 24 hours incubation, the cells were washed twice with PBS, fixed and immunostained with anti-Bax clone 6A7 as described in Materials and Methods. Quantification was done by drawing a region of interest around each cell in the acquired images. The intensity was determined by SlideBook and is expressed as the percentage of Bax immunostaining induced by Triton X-100. The results are mean of three independent experiments ± s.d.

11. Bax, Bak and sirt-3 knockdown prevents truncated Bid (tBid) induced mitochondrial membrane depolarization and ROS production

To more directly assess the mechanism(s) by which sirt-3 modulates mitochondrial injury, we selectively permeabilized the plasma membrane utilizing digitonin as described in Materials and Methods. As shown in Fig. 11A, over an 18-minute time course, as assessed by the retention of the potentiomeric fluorophore, tetramethyl-rhodamine methyl ester (TMRM), digitonin permeabilized cells maintain a relatively steady mitochondrial membrane potential. Upon addition of truncated Bid (t-Bid), a BH3 domain only pro-apoptotic protein, mitochondria underwent depolarization. However, when cells were depleted of Bak/Bax, mitochondria became insensitive to t-Bid induced depolarization; consistent with the notion that t-Bid induces mitochondrial injury by activating Bak/Bax, either directly or by antagonizing the inhibition on Bak/Bax exerted by Mcl-1 and Bcl-X_L. Significantly, depletion of sirt-3 rendered mitochondria refractory to t-Bid induced mitochondrial depolarization to the same extent as did depletion of Bak/Bax.

The addition of t-Bid also brought about secondary manifestations of mitochondrial injury, such as generation of ROS and release of cytochrome c. As shown in Fig. 11B, t-Bid stimulated a 95% increase in the fluorescence of MitoSOX; mitochondria localized fluorophor sensitive to ROS. Importantly, as with mitochondrial membrane potential, depletion of sirt-3 prevented the t-Bid induced stimulation of ROS to the same extent as did suppression of Bak/Bax expression. The stimulation of ROS and depolarization of mitochondria are thought to be due in part to release of cytochrome c

from the mitochondrial inter-membrane space. As shown in Fig. 11C, t-Bid induced a complete loss of mitochondrial cytochrome c, which was prevented by suppression of Bak/Bax expression (lanes 2 and 3, respectively). Markedly, depletion of sirt-3 also prevented the loss of mitochondrial cytochrome c induced by t-Bid (lane 4).

Figure 11. Bax, Bak and sirt-3 knockdown prevents truncated Bid (tBid) induced mitochondrial membrane depolarization and ROS production

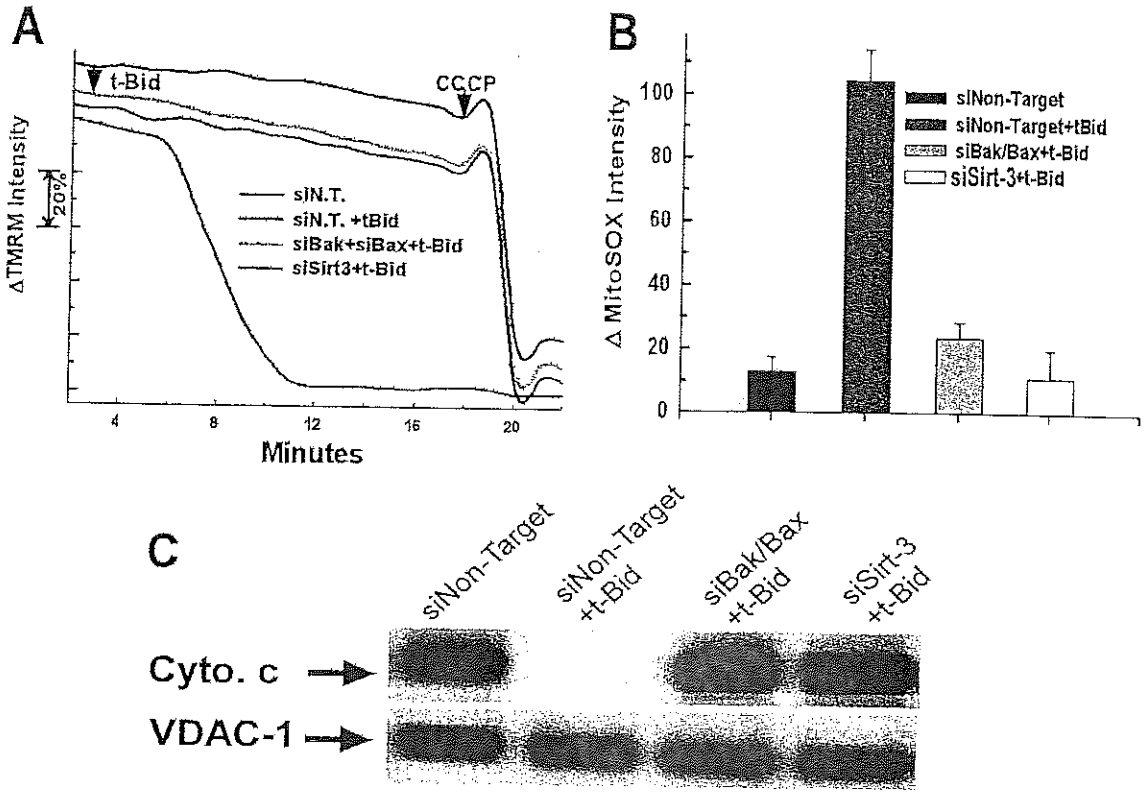

(A) HeLa cells were transfected with 50 nM of a non-targeting control siRNA or siRNA targeting Bak/Bax or sirtuin-3. Following 48 hours incubation, HeLa cells were loaded with 200 nM of TMRM for 30 minutes. The cells were then washed twice and placed in respiratory buffer. The cells were mounted on a heated stage kept at 37°C. Digitonin (2.5 μg/ml final concentration) was then added to permeabilize the plasma membrane and TMRM fluorescence was monitored over a 20 minute time course. Recombinant truncated Bid (t-Bid) was added at a concentration of 5 μM at the 2-minute time point and 5 μM of CCCP was added at the 18 minute time point. The result is the average of three independent experiments.

(B) HeLa cells were plated and then transfected with siRNAs targeting Bak/Bax or sirt-3. Following 48 hours, the cells were loaded with MitoSOX and mounted on a heated microscopy stage. Digitonin (2.5 μg/ml) was then added to permeabilize the plasma membrane. Recombinant truncated Bid (t-Bid) was added at a concentration of 5 μM.

Time-lapse microscopy was conducted over a 20 minute time course with MitoSOX fluorescence intensity assessed as described in Materials and Methods. The results are mean of three independent experiments±s.d.

(C) Following time lapse microscopy, cells from four wells for each condition were pooled and mitochondria isolated. Cytochrome c content was determined by western blotting using mouse anti-cytochrome c antibody (BD Pharmingen) at 1:1000 dilution. The results are representative of three independent experiments.

12. Hexokinase II mediates Sirt-3 control of Bak/Bax dependent mitochondrial injury

The data indicate that depletion of sirt-3 prevents t-Bid dependent mitochondrial injury that is mediated by Bak/Bax. We next wanted to determine the mechanism(s) by which sirt-3 modulates mitochondrial injury. We and others have demonstrated that hexokinase II, when bound to the mitochondria, inhibits Bak/Bax induced mitochondrial dysfunction (Majewski et al., 2004b; Pastorino et al., 2002; Vyssokikh et al., 2002). Moreover, we have demonstrated that depletion of sirt-3 increases the binding of hexokinase II to mitochondria, suggesting a possible mechanism for the protective effects of sirt-3 depletion (Shulga et al., 2010). Indeed as shown in Fig. 12A, suppression of hexokinase II expression reversed the ability of sirt-3 depletion to prevent t-Bid induced mitochondrial depolarization. Similarly, pre-treatment with clotrimazole (CTZ), an agent that detaches hexokinase II from the mitochondria, also neutralized the ability of sirt-3 depletion to prevent t-Bid induced mitochondrial depolarization. Moreover, downregulation of hexokinase II or pre-treatment with CTZ, reversed the ability of sirt-3 depletion to prevent t-Bid induced mitochondrial ROS generation and loss of mitochondrial cytochrome c (Fig. 12B, C).

Figure 12. The protective effect of sirt-3 depletion is dependent on hexokinase II binding to mitochondria.

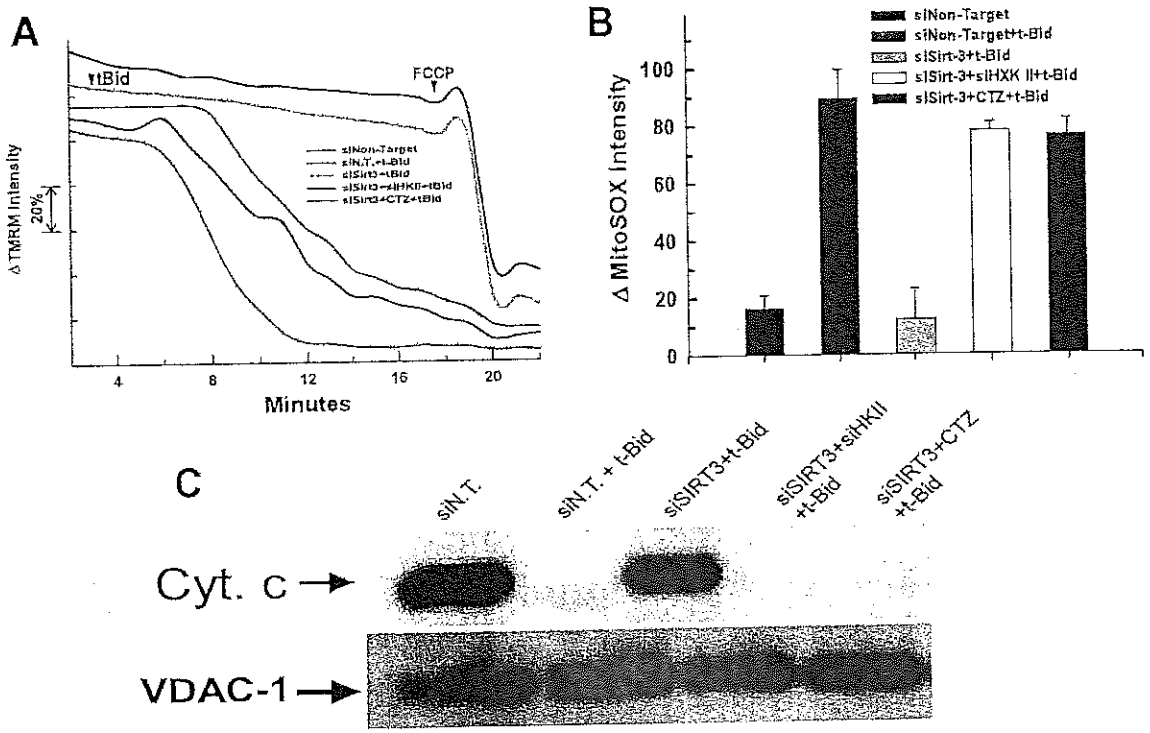

(A) HeLa cells were transfected with 50 nM of a non-targeting control siRNA, siRNA targeting sirtuin-3 or siRNA targeting sirt-3 and hexokinase II in tandem. Following 48 hours incubation, the cells were loaded with 200 nM of TMRM for 30 minutes. The cells were mounted on a heated microscopy stage kept at 37°C. The cells were then washed twice and placed in respiratory buffer. Where indicated, the cells were pre-treated with 10 μM of clotrimazole (CTZ) for 10 minutes. Digitonin (2.5 μg/ml) was then added to permeabilize the plasma membrane and TMRM fluorescence was monitored over a 20 minute time course. Recombinant truncated Bid (t-Bid) was added at a concentration of 5 μM at 2 minutes and 5 μM of CCCP was added at the 18 minute time point. The result is the average of three independent experiments.

(B) HeLa cells were transfected with 50 nM of a non-targeting control siRNA, siRNA targeting sirtuin-3 or siRNAs targeting sirt-3 and hexokinase II in tandem. Following 48 hours incubation, the cells were loaded with MitoSOX for 30 minutes and then mounted on a heated microscopy stage kept at 37°C. Cells were then washed twice and placed in

respiratory buffer. Where indicated, the cells were pre-treated with 10 μM of clotrimazole (CTZ) for 10 minutes. Digitonin at 2.5 μg/ml was then added to permeabilize the plasma membrane. Recombinant truncated Bid (t-Bid) was added at a concentration of 5 μM at 2 minutes. Time-lapse microscopy was conducted over a 20 minute time course with MitoSOX fluorescence intensity assessed as described in Materials and Methods. The results are mean of three independent experiments±s.d.

(C) Following time lapse microscopy, cells from four wells for each condition were harvested and mitochondria isolated. Cytochrome c content was detected by western blotting using mouse anti-cytochrome c antibody (BD Pharmingen) at 1:1000 dilution. The results are representative of three independent experiments.

13. Cyclophilin-D knockdown reverses protection mediated by Sirt-3 depletion

We have shown that suppression of sirt-3 expression stimulates the binding of hexokinase II to the mitochondria by increasing the acetylation and activity of cyclophilin-D (CyP-D) (Shulga et al., 2010). Therefore, suppression of CyP-D expression should reverse the protective effect of sirt-3 depletion. Indeed, Fig. 13A demonstrates that suppression of CyP-D expression reversed the protective effect exerted by sirt-3 depletion against t-Bid induced mitochondrial depolarization. Additionally, inhibition of cyclophilin-D peptidyl-prolyl cis-trans isomerase activity with cyclosporine A (CsA) also neutralized the ability of sirt-3 depletion to protect against t-Bid induced mitochondrial depolarization. Moreover, suppression of CyP-D and inhibition of CyP-D activity reversed the protective effects exerted by depletion of sirt-3 on t-Bid induced mitochondrial ROS generation (Fig. 13B) and loss of mitochondrial cytochrome c (Fig. 13C).

Figure 13. Cyclophilin-D is required for sirt-3 depletion to protect against mitochondrial injury.

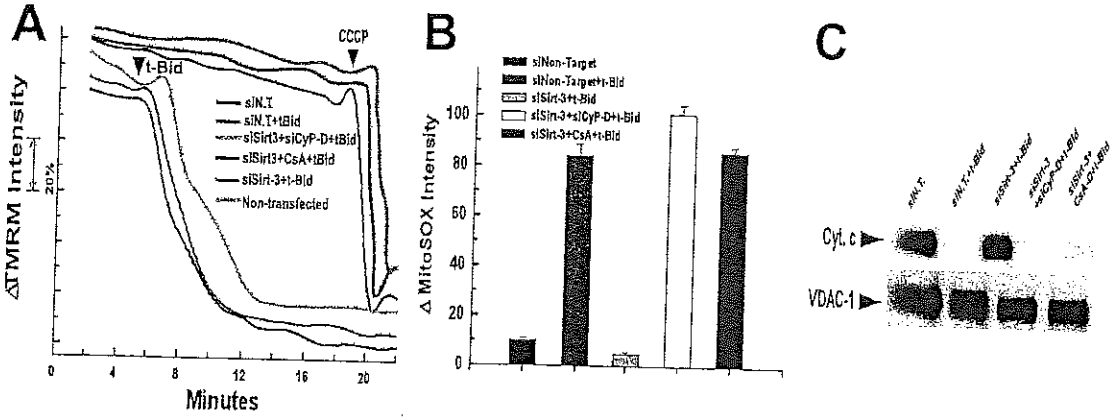

(A) HeLa cells were transfected with 50 nM of a non-targeting control siRNA, siRNA targeting sirtuin-3 or siRNAs targeting sirt-3 and CyP-D in tandem. Following 48 hours incubation, the cells were loaded with 200 nM of TMRM for 30 minutes. The cells were then mounted on a heated microscopy stage kept at 37°C. The cells were then washed twice and placed in respiratory buffer. Where indicated, the cells were pre-treated with 10 μM of cyclosporin A (CsA) for 10 minutes. Digitonin (2.5 μg/ml) was then added to permeabilize the plasma membrane. TMRM fluorescence was monitored over a 20 minute time course. Recombinant truncated Bid (t-Bid) was added at a concentration of 5 μM at 2 minutes and 5 μM of CCCP was added at the 18 minute time point. The result is the average of three independent experiments.

(B) HeLa cells were transfected with 50 nM of a non-targeting control siRNA, siRNA targeting sirtuin-3 or siRNAs targeting sirt-3 and cyclophilin-D in tandem. Following 48 hours incubation, the cells were loaded with MitoSOX for 30 minutes. The cells were then washed twice, placed in respiratory buffer and mounted on a heated microscopy stage kept at 37°C. Where indicated, the cells were pre-treated with 10 μM of CsA (CsA) for 10 minutes. Digitonin at 2.5 μg/ml was then added to permeabilize the plasma membrane. Recombinant truncated Bid (t-Bid) was added at a final concentration of 5 μM at 2 minutes. Time-lapse microscopy was conducted over a 20 minute time course with MitoSOX fluorescence intensity assessed as described in Materials and Methods. The results are mean±s.d. of three independent experiments.

(C) Following time lapse microscopy, cells from four wells per condition were harvested and mitochondria isolated. Cytochrome c content was detected by western blotting using mouse anti-cytochrome c antibody (BD Pharmingen) at 1:1000 dilution. The results are representative of three independent experiments.

14. Hexokinase II and Cyclophilin-D act upstream of Bax and Bak

Importantly, downregulation of CyP-D or inhibition of CyP-D activity with CsA failed to reverse the protective effect exerted by Bak/Bax depletion against t-Bid induced mitochondrial depolarization (Fig. 14A). Similarly, whereas the protection afforded by sirt-3 depletion against t-Bid induced mitochondrial injury is dependent on mitochondrial hexokinase II, suppression of hexokinase II expression or treatment with clotrimazole (CTZ) failed to reverse the protective effect exerted by Bak/Bax depletion against t-Bid induced mitochondrial depolarization (Fig. 14B). Likewise, the inhibition of t-Bid induced mitochondrial ROS production or loss of cytochrome c, mediated by Bak/Bax depletion, was not reversed by suppressing or inhibiting CyP-D or hexokinase II (Fig. 14C, D respectively). The dichotomy between the ability to reverse the protective effect of sirt-3 depletion versus the insensitivity of Bak/Bax depletion to reversal, indicate that the protective effect exerted by sirt-3 depletion lies upstream of Bak/Bax. To support this notion, suppression CyP-D or hexokinase II expression reversed the ability of sirt-3 depletion to prevent t-Bid induced Bak oligomerization (Fig. 14E, lanes 4 and 5, respectively).

Figure 14. Hexokinase II and Cyclophilin-D act upstream of Bax and Bak

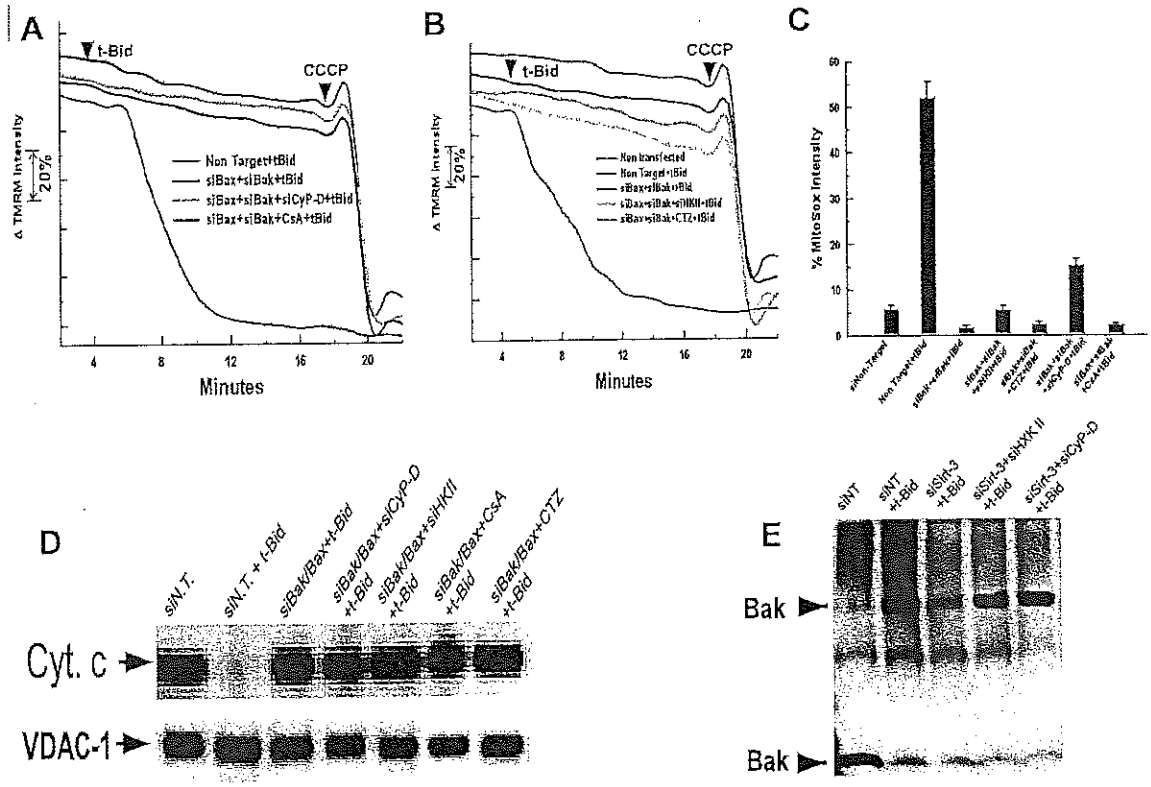

(A,B) HeLa cells were transfected with 50 nM of a non-targeting control siRNA, siRNAs targeting Bak/Bax or siRNAs targeting Bak/Bax and CyP-D or HXK II in tandem. Following 48 hours incubation, the cells were loaded with 200 nM of TMRM for 30 minutes. The cells were washed twice, placed in respiratory buffer and mounted on a heated microscopy stage kept at 37°C. Where indicated, the cells were pre-treated with 10 μM of cyclosporin A (CsA) or clotrimazole (CTZ) for 10 minutes. Digitonin (2.5 μg/ml) was then added to permeabilize the plasma membrane. TMRM fluorescence was monitored over a 20 minute time course. Recombinant truncated Bid (t-Bid) was added at a concentration of 5 μM at 2 minutes and 5 μM of CCCP was added at the 18 minute time point. The results are the average of three independent experiments.

(C) HeLa cells were transfected with 50 nM of a non-targeting control siRNA, siRNAs targeting Bak/Bax or siRNAs targeting Bak/Bax and CyP-D or HXK II in tandem.

Following 48 hours incubation, the cells were loaded with MitoSOX for 30 minutes. The cells were then washed twice, placed in respiratory buffer and mounted on a heated microscopy stage kept at 37°C. Where indicated, the cells were pre-treated with 10 μM of cyclosporin A (CsA) or clotrimazole (CTZ) for 10 minutes. Digitonin (2.5 μg/ml) was then added to permeabilize the plasma membrane. Recombinant truncated Bid (t-Bid) was added at a concentration of 5 μM at 2 minutes. Time-lapse microscopy was conducted over a 20 minute time course with MitoSOX fluorescence intensity assessed as described in Materials and Methods. The results are the mean±s.d. of three independent experiments.

(D) Following time lapse microscopy, cells from four wells for each condition were harvested and mitochondria isolated. Cytochrome c content was determined by western blotting using mouse anti-cytochrome c antibody (BD Pharmingen) at 1:1000 dilution. The results are representative of three independent experiments.

(E) HeLa cells were transfected with 50 nM of the indicated siRNAs, either individually or in tandem. Following 48 hours incubation, the cells were permeabilized with digitonin (2.5 μg/ml). Recombinant truncated Bid (t-Bid) was added at a concentration of 5 μM at 18 minutes. The cells were then harvested from four wells per condition and the mitochondria fraction isolated. The isolated mitochondria were incubated with 0.1 mM of the cross-linking reagent BMH for 30 minutes. The samples were then run out on 12% SDS-PAGE gels and Bak oligomerization was assessed by western blotting. The results are representative of three independent experiments.

15. Sirt-3 modulates sensitivity to cisplatin induced cytotoxicity

We have demonstrated that cisplatin induces Bid dependent cytotoxicity, which is potentiated by detachment of hexokinase II from the mitochondria (Shulga et al., 2009). Therefore we wanted to determine if sirtuin-3 can modulate sensitivity to cisplatin induced cytotoxicity. HeLa cells were treated with 30 μM of cisplatin over a 48 hour time course. As shown in Fig. 15A, lane 2, at 24 hours, treatment with cisplatin induced Bak oligomerization that was not prevented by transfection with non-targeting siRNA. However, cisplatin induced Bak oligomerization was prevented by siRNAs targeting sirt-3 or Bid (lanes 3 and 4, respectively). Fig. 15B demonstrates that treatment with 30 μM of cisplatin brought about a 36% loss of cell viability at 24 hours and a 74% loss of cell viability at 48 hours. As expected, suppressing Bid expression reduced the degree of cytotoxicity induced by cisplatin, as did suppression of Bak/Bax expression. Significantly, depletion of sirt-3 also reduced cytotoxicity induced by cisplatin, with only a 20% loss of cell viability in cells treated with cisplatin over 48 hours (Fig. 15B).

Figure 15. Sirt-3 depletion protects against cisplatin induced cytotoxicity by regulating the binding of hexokinase II to the mitochondria.

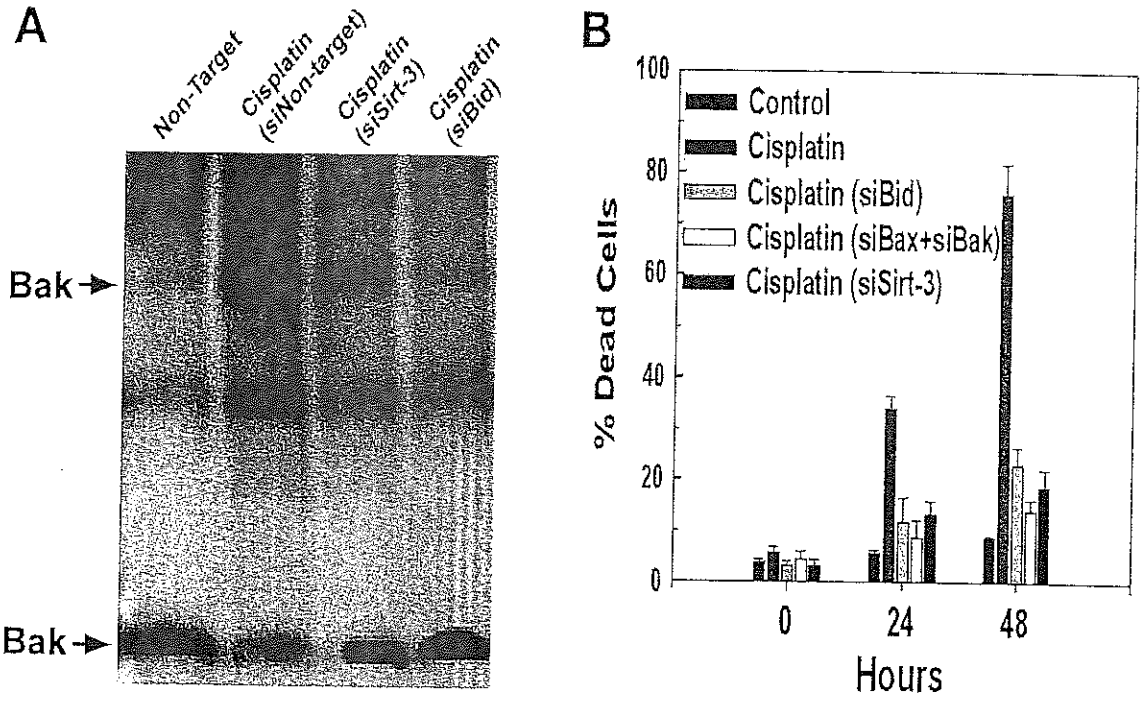

(A) HeLa cells were transfected with 50 nM of the indicated siRNAs. Following 24 hours incubation, the cells were treated with 30 μM of cisplatin. Following 24 hours exposure to cisplatin, the cells from four wells per condition were harvested and the mitochondrial fraction isolated. The isolated mitochondria were incubated with 0.1 mM of the cross-linking reagent BMH for 30 minutes. The samples were then run out on 12% SDS-PAGE gels and Bak oligomerization was assessed by western blotting. The result is representative of three independent experiments.

(B) HeLa cells were transfected with 50 nM of the indicated siRNAs. Following 24 hours incubation, the cells were treated with 30 μM of cisplatin. At the time points indicated, the cells were harvested and viability determined utilizing Yo-Pro-1 as described in Materials and Methods. Values are the mean of three independent experiments with the error bars indicating standard deviations.

16. Knock down of HKII or CyP-D reverses Sirt-3 mediated protection when treated with cisplatin

If sirt-3 depletion protects against cisplatin induced cytotoxicity by enhancing the binding of hexokinase II to the mitochondria, then suppression of hexokinase II or cyclophilin-D expression should reverse the protective effect of sirt-3 depletion. As shown in Fig. 16A, 24 hour treatment with 30 μM of cisplatin brought about Bak oligomerization that was prevented by sirt-3 depletion (lane 2 versus lane 3). However, suppression of hexokinase II or cyclophilin-D expression reversed the ability of sirt-3 depletion to prevent cisplatin induced Bak oligomerization (Fig. 16A, lanes 4 and 5, respectively). Moreover, as demonstrated in Fig. 16B, right and left graphs respectively, suppression of hexokinase II or cyclophilin-D expression reversed the ability of sirt-3 depletion to prevent cisplatin induced cytotoxicity. Similarly, detachment of hexokinase II from the mitochondria with clotrimazole or inhibition of cyclophilin-D activity with cyclosporine A (CsA) also reversed the protective effect of sirt-3 depletion against cisplatin induced cytotoxicity. Importantly, suppression of CyP-D or hexokinase II or their activity failed to reverse the protective effect exerted by suppressing Bid expression.

Figure 16. Knock down of HKII or CyP-D reverses Sirt-3 mediated protection when treated with cisplatin

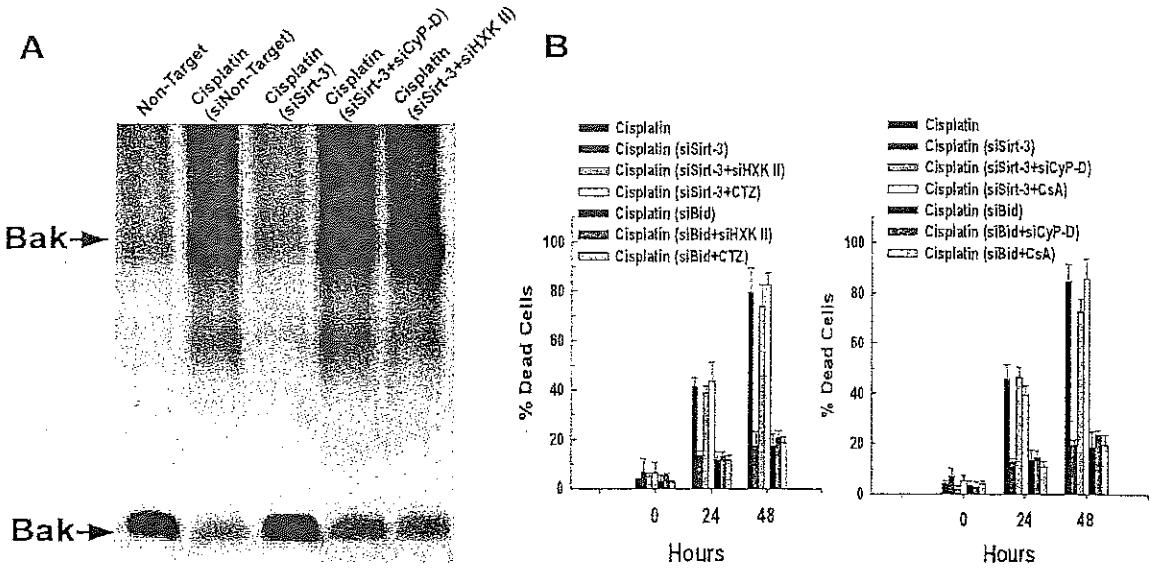

(A) HeLa cells were transfected with 50 nM of the indicated siRNAs. Following 24 hours incubation, the cells were treated with 30 μM of cisplatin. After 24 hours exposure to cisplatin, the cells from four wells for each condition were harvested and the mitochondrial fraction isolated. The isolated mitochondria were incubated with 0.1 mM of the cross-linking reagent BMH for 30 minutes. The samples were then run out on 12% SDS-PAGE gels and Bak oligomerization was assessed by western blotting. The results are representative of three independent experiments.

(B) HeLa cells were transfected with 50 nM of siRNAs targeting sirt-3 and Bid, either separately or in tandem with siRNAs targeting HXK II or CyP-D. Following 24 hours incubation, the cells were treated with 30 μM of cisplatin in the absence or presence of 10 μM of CsA or 10 μM of CTZ. At the time points indicated, the cells were harvested and viability determined utilizing Yo-Pro-1 as described in Materials and Methods. Values are the mean of three independent experiments with the error bars indicating standard deviations.

17. Osteosarcoma cell line U2OS, display a dependence on sirt-3 expression during t-Bid induced mitochondrial injury.

As shown in Fig. 17A, the addition of t-Bid to permeabilized U2OS cells transfected with non-targeting siRNA brought about complete depolarization of the mitochondria over an 18 minute time course. The t-Bid induced depolarization was dependent on Bak/Bax expression, and was prevented by depletion of sirt-3. The depolarization induced by the addition of t-Bid was preceded by stimulation in the production of ROS. Fig. 17B shows a sharp increase of MitoSOX fluorescence induced by t-Bid that was largely prevented by depletion of sirt-3 or Bak/Bax. Fig. 17C demonstrates that the ability of sirt-3 depletion to prevent t-Bid induced mitochondrial depolarization is dependent on hexokinase II. Suppression of hexokinase II expression reverses the protective effect of sirt-3 depletion against t-Bid induced depolarization as does detachment of hexokinase II from the mitochondria with clotrimazole. The protective effect of sirt-3 depletion was also dependent on the activity of cyclophilin-D, as suppression of cyclophilin-D expression or treatment with CsA restored the ability of t-Bid to bring about mitochondrial depolarization (Fig. 17D). Importantly, the ability of Bak/Bax depletion to prevent t-Bid induced mitochondrial depolarization was independent of hexokinase II or cyclophilin-D expression (Fig. 17E). Depletion of sirt-3 also rendered the U2OS cells resistant to cisplatin induced cytotoxicity. As shown in Fig. 17F, cisplatin at a dose of 30 μM, induced a progressive increase in the number of dead cells over a 48 hour time course, reaching an 80% loss of cell viability after 48 hours of exposure. Importantly, depletion of sirt-3 greatly ameliorated the cytotoxicity brought about by cisplatin (Fig. 17F). Moreover, the ability of sirt-3 depletion to protect against

cisplatin induced cytotoxicity is dependent on hexokinase II and cyclophilin-D expression or activity. Suppression of hexokinase II or cyclophilin-D expression or treatment with clotrimazole or CsA, reversed the protective effect of sirt-3 depletion against cisplatin induced cytotoxicity, but did not reverse the protective effect of depleting Bid expression.

Figure 17. Sirt-3 is required for Bak/Bax dependent apoptosis in U2OS osteosarcoma cells.

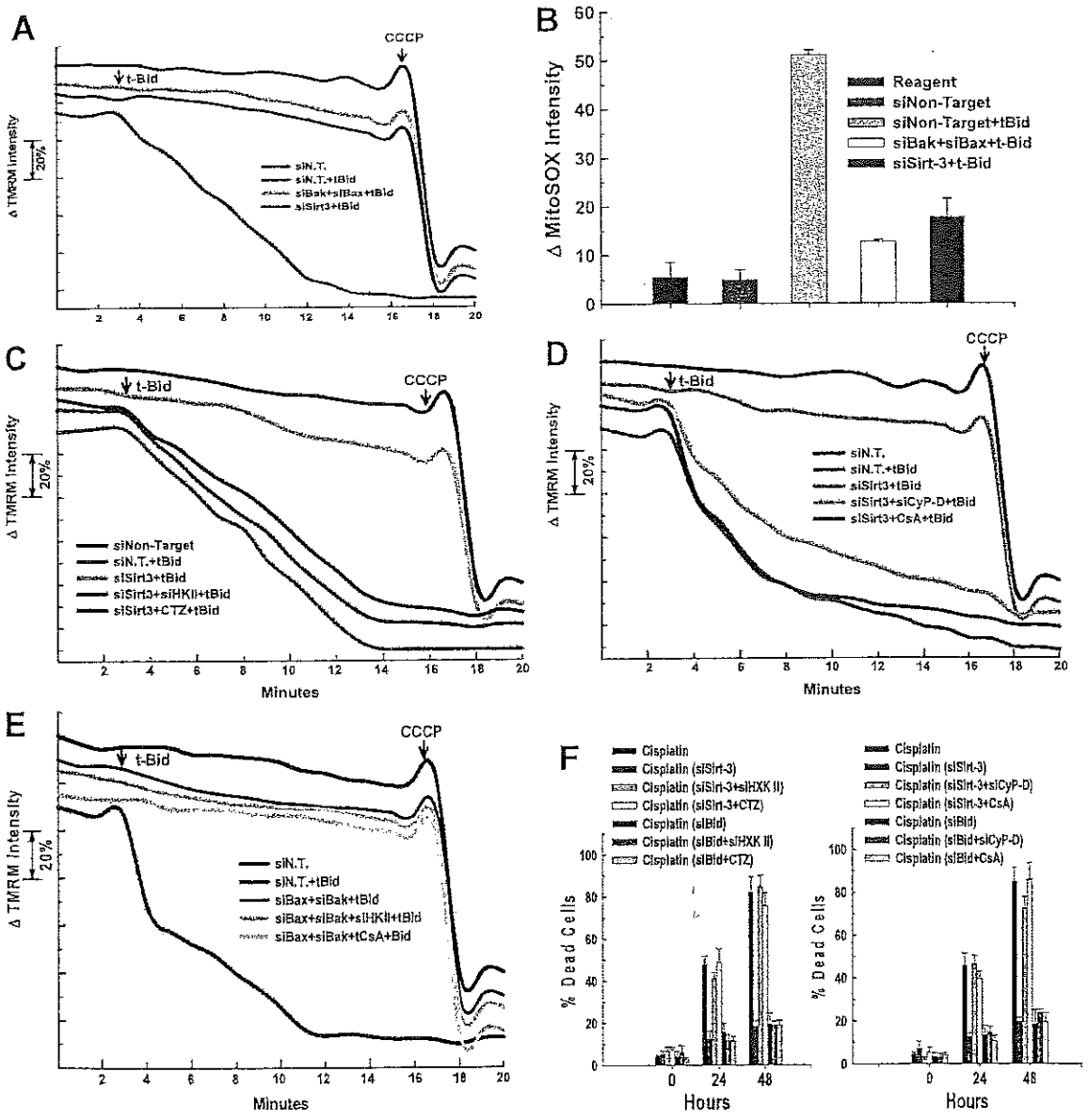

(A) U2OS cells were transfected with 50 nM of a non-targeting control siRNA or siRNA targeting Bak/Bax or sirtuin-3. Following 48 hours incubation, U2OS cells were loaded with 200 nM of TMRM for 30 minutes. The cells were then washed twice and placed in respiratory buffer. The cells were mounted on a heated stage kept at 37°C. Digitonin (2.5 μg/ml final concentration) was then added to permeabilize the plasma membrane and

TMRM fluorescence was monitored over a 20 minute time course. Recombinant truncated Bid (t-Bid) was added at a concentration of 5 μM at the 2 minute time point and 5 μM of CCCP was added at the 18 minute time point. The result is the average of three independent experiments.

(B) U2OS cells were plated and then transfected with siRNAs targeting Bak/Bax or sirt-3. Following 48 hours, the cells were loaded with MitoSOX and mounted on a heated microscopy stage. Digitonin (2.5 μg/ml) was then added to permeabilize the plasma membrane. Recombinant truncated Bid (t-Bid) was added at a concentration of 5 μM. Time-lapse microscopy was conducted over a 20 minute time course with MitoSOX fluorescence intensity assessed as described in Materials and Methods. The results are mean of three independent experiments±s.d.

(C) U2OS cells were transfected with 50 nM of a non-targeting control siRNA, siRNA targeting sirtuin-3 or siRNA targeting sirt-3 and hexokinase II in tandem. Following 48 hours incubation, the cells were loaded with 200 nM of TMRM for 30 minutes. The cells were mounted on a heated microscopy stage kept at 37°C. The cells were then washed twice and placed in respiratory buffer. Where indicated, the cells were pre-treated with 10 μM of clotrimazole (CTZ) for 10 minutes. Digitonin (2.5 μg/ml) was then added to permeabilize the plasma membrane and TMRM fluorescence was monitored over a 20 minute time course. Recombinant truncated Bid (t-Bid) was added at a concentration of 5 μM at 2 minutes and 5 μM of CCCP was added at the 18 minute time point. The result is the average of three independent experiments.

(D) U2OS cells were transfected with 50 nM of a non-targeting control siRNA, siRNA targeting sirtuin-3 or siRNAs targeting sirt-3 and CyP-D in tandem. Following 48 hours incubation, the cells were loaded with 200 nM of TMRM for 30 minutes. The cells were then mounted on a heated microscopy stage kept at 37°C. The cells were then washed twice and placed in respiratory buffer. Where indicated, the cells were pre-treated with 10 μM of cyclosporine A (CsA) for 10 minutes. Digitonin (2.5 μg/ml) was then added to permeabilize the plasma membrane. TMRM fluorescence was monitored over a 20 minute time course. Recombinant truncated Bid (t-Bid) was added at a concentration of 5 μM at 2 minutes and 5 μM of CCCP was added at the 18 minute time point. The result is the average of three independent experiments.

(E) U2OS cells were transfected with 50 nM of a non-targeting control siRNA, siRNAs targeting Bak/Bax or siRNAs targeting Bak/Bax or HXK II in tandem. Following 48 hours incubation, the cells were loaded with 200 nM TMRM for 30 minutes. The cells were then washed twice, placed in respiratory buffer and mounted on a heated microscopy stage kept at 37°C. Where indicated, the cells were pre-treated with 10 μM of cyclosporine A (CsA) for 10 minutes. Digitonin (2.5 μg/ml) was then added to permeabilize the plasma membrane. Recombinant truncated Bid (t-Bid) was added at a concentration of 5 μM at 2 minutes. Time-lapse microscopy was conducted over a 20 minute time course with TMRM fluorescence intensity assessed as described in Materials and Methods. The result is the average of three independent experiments.

(F) U2OS cells were transfected with 50 nM of siRNAs targeting sirt-3 and Bid, either separately or in tandem with siRNAs targeting HXK II or CyP-D. Following 24 hours incubation, the cells were treated with 30 μM of cisplatin in the absence or presence of 10 μM of CsA or 10 μM of CTZ. At the time points indicated, the cells were harvested and viability determined utilizing Yo-Pro-1 as described in the Materials and Methods. Values are the mean of three independent experiments with the error bars indicating standard deviations.

18. Increased expression of Sirt-3 enhances sensitivity to cell death

We next wanted to determine if increasing the expression of sirt-3 enhances sensitivity to mitochondrial injury. Galactose cannot be readily utilized for glycolysis. We have shown that the substitution of galactose for glucose in the culture media of transformed cells increases the expression of sirt-3, bringing about detachment of hexokinase II from the mitochondria (Shulga et al., 2010). As shown in Fig. 18A, a fivefold lower dose of t-Bid (1 μM) did not induce mitochondrial depolarization in cells kept in glucose based media. However, the sub-threshold dose of t-Bid induced rapid and complete mitochondrial depolarization in cells incubated in galactose based media. Further, suppression of sirt-3 expression prevented t-Bid induced mitochondrial depolarization in galactose based media, even at the fivefold higher concentration of t-Bid (5 μM) which brings about mitochondrial depolarization in cells incubated in glucose based media. Incubation in galactose based media also sensitized to cisplatin induced cytotoxicity. As show in Fig. 18B, treatment with half the dose of cisplatin (15 μM) utilized in glucose based media induced an over 80% loss of cell viability following only 16 hours of exposure. Importantly, the galactose induced potentiation of cisplatin induced cell killing was prevented by depletion of sirt-3 (Fig. 18B). Moreover, the protection afforded by sirt-3 depletion was dependent on the expression of hexokinase II and cyclophilin-D activity, with suppression of hexokinase II expression or treatment with CsA reversing the protective effect of sirt-3 depletion (Fig. 18B). Importantly, neither CsA nor suppression of hexokinase II reversed the protective effect of Bid depletion against cisplatin induced cytotoxicity in galactose based media. We next attempted to determine if increased expression of sirt-3 in cells incubated in glucose had any effect on

cell viability. Significantly, overexpression of sirt-3 in cells incubated in medium containing glucose brought about Bak oligomerization and loss of cell viability (Fig. 18C, D, respectively). However, overexpression of an inactive sirt-3 mutant, sirt-3 (H248Y) did not bring about Bak oligomerization and had little effect on cell viability.

Figure 18. Increased sirt-3 expression sensitizes cells to cisplatin induced cytotoxicity.

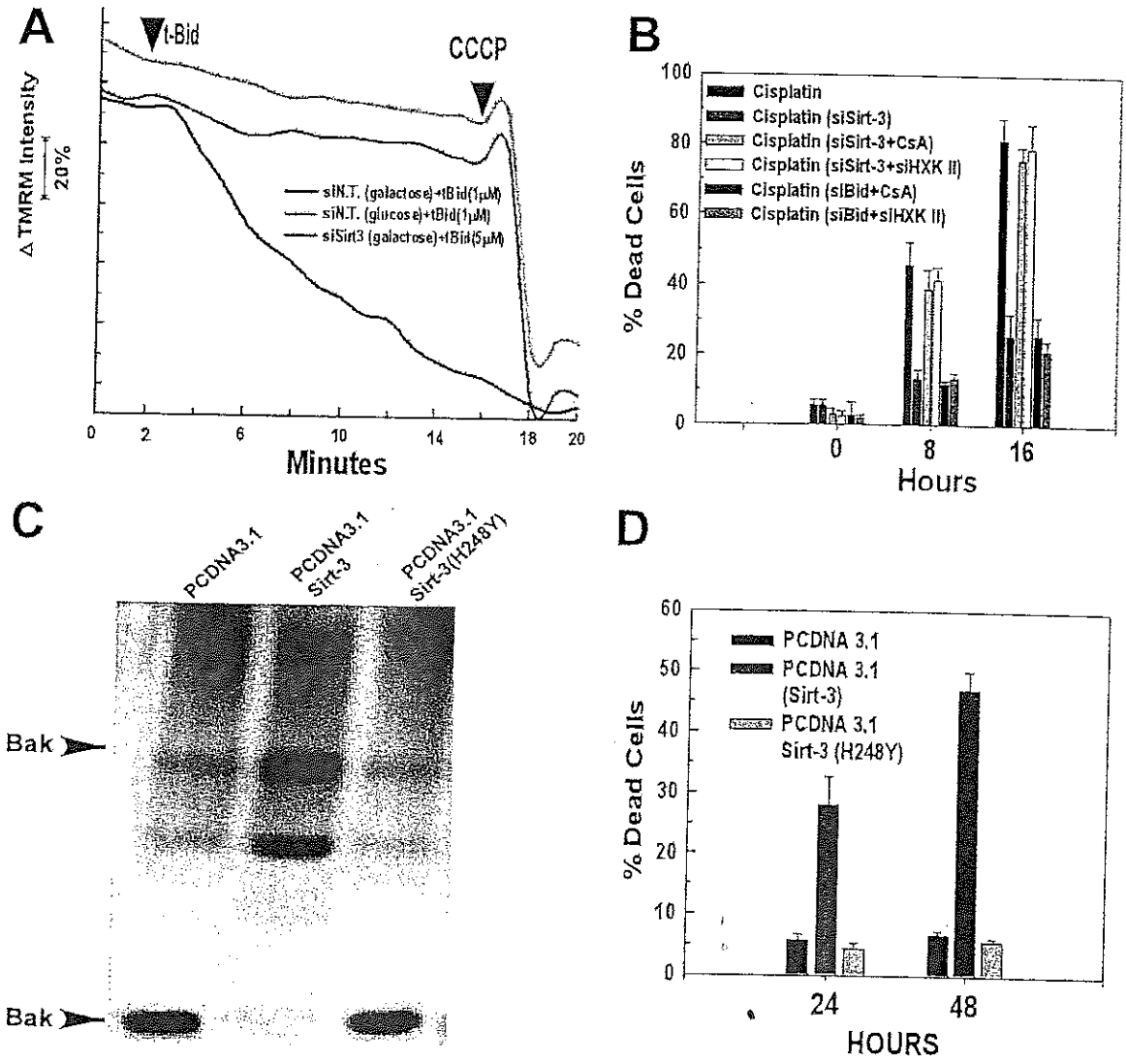

(A) HeLa cells were incubated in DMEM containing glucose (4.5 g/l) or transferred to DMEM containing galactose at 4.5 g/l. Following 24 hours incubation, HeLa cells were transfected with 50 nM of non-targeting siRNA or siRNA targeting sirt-3. After 48 hours incubation, the cells were loaded with 200 nM of TMRM for 30 minutes. The cells were washed twice, placed in respiratory buffer and mounted on a heated microscopy stage kept at 37°C. Digitonin (2.5 μg/ml) was then added to permeabilize the plasma

membrane and TMRM fluorescence was monitored over a 20 minute time course. Recombinant truncated Bid (t-Bid) was added at a concentration of 5 μM at 2 minutes and 5 μM of CCCP was added at the 18 minute time point. The result is the average of three independent experiments.

(B) HeLa cells were transferred to DMEM containing galactose at 4.5 g/l. Following 24 hours incubation, HeLa cells were transfected with 50 nM of siRNA targeting sirt-3 or Bid, either separately or in tandem with siRNA against HXK II. The cells were incubated for another 24 hours. Where indicated, the cells were pre-treated for 30 minutes with 10 μM of CsA. The cells were then treated with 15 μM of cisplatin and cell viability determined at the time points indicated. Values are the means of three independent experiments with the error bars indicating standard deviations.

(C) U2OS cells were transfected with 250 nM of the indicated plasmids. Following 24 hours incubation, the cells were harvested and the mitochondrial fraction isolated from four wells for each condition. The isolated mitochondria were incubated with 0.1 mM of the cross-linking reagent BMH for 30 minutes. The samples were then run out on 12% SDS-PAGE gels and Bak oligomerization was assessed by western blotting.

(D) U2OS cells were co-transfected with 250 nM of the indicated plasmids and 250 nM of EGFP. Following 48 hours, the cells were harvested and the number of EGFP positive cells stained with Yo-Pro-1 determined as described in Materials and Methods. Values are the means of three independent experiments with the error bars indicating standard deviations.

Discussion:

The results of the present study indicate that sirtuin-3 exerts a cyclophilin-D dependent tumor suppressor effect by regulating the binding of hexokinase II to the mitochondria, which in turn controls the ability of Bak/Bax to bring about mitochondrial injury and loss of cell viability. Suppression of sirt-3 prevented all of the manifestations of Bak/Bax dependent mitochondrial injury and apoptosis induction; including mitochondrial depolarization, release of cytochrome c, stimulation of ROS production, caspase-3 activation, PS externalization and activation of Bak and Bax. Moreover depletion of sirtuin-3 protected against Bak/Bax dependent mitochondrial injury and cell death in three models and three different cell types; downregulation of Mcl-1 and Bcl-X_L expression in HeLa and MDA-MB-231 cells and exposure of mitochondria to t-Bid and treatment with cisplatin in HeLa and U2OS cells. Importantly, the ability of sirt-3 depletion to protect against mitochondrial injury and subsequent cell death was dependent on hexokinase II and cyclophilin-D. Suppression of hexokinase II expression or forced detachment of hexokinase II from the mitochondria with clotrimazole reversed the protective effect of sirt-3 depletion. Similarly, suppression of cyclophilin-D expression or inhibition of cyclophilin-D cis-trans isomerase activity with CsA negated the protective effect of sirt-3 depletion. Importantly, suppression of Bak/Bax expression protected under all conditions and was not reversible by suppression or inhibition of hexokinase II or cyclophilin-D, indicating that sirt-3 depletion exerts a protective effect up-stream of Bak/Bax.

Sirtuin-3 has emerged as a central regulator of mitochondrial metabolism. The acetylation-deacetylation cycle impacts on the stability and activity of a multitude of mitochondrial components that directly or indirectly effect cell survival. Paradoxically, sirt-3 has been demonstrated to protect against loss of cell viability while also being identified as a tumor suppressor, whose absence enhances cellular transformation and the ability of transformed cells to survive. The protective effects of sirt-3 against cellular stress include a decrease in ROS levels, mediated by sirt-3 stimulating anti-oxidant capacity and diminishing ROS generation from the mitochondrial respiratory chain. Indeed, it has been shown that sirt-3 mediates a reduction of oxidative damage during age-related hearing loss in part by deacetylating and activating IDH-2, which increases the levels of reduced glutathione (Someya et al., 2010; Yu et al., 2012). Sirt-3 also activates mitochondrial manganese superoxide dismutase, another key element of the mitochondrial ROS detoxification pathway (Tao et al., 2010). Importantly, sirt-3 has been demonstrated to exert a protective effect against hypoxia and staurosporine induced cell death by inhibiting the mitochondrial permeability transition and dampening intracellular acidification (Pellegrini et al., 2012; Zamzami et al., 1997). Carbonic anhydrase helps to regulate intracellular pH by catalyzing the conversion of carbon dioxide to bicarbonate. In particular, carbonic anydrase VB, localized to the mitochondria, requires sirt-3 expression to maintain activity.

The mitochondrial permeability transition is a central event in the onset of necrotic cell death (Baines et al., 2005; Halestrap et al., 2004; Zamzami et al., 1997). The constituents of the permeability transition pore (PTP) are ill defined, but cyclophilin-D is a key regulator of PTP sensitivity. We have shown that sirt-3 deacetylates and inactivates

the peptidyl-prolyl cis-trans isomerase activity of cyclophilin-D, thereby dampening PTP induction and preventing TNF mediated necrotic cell death in hepatocytes (Shulga and Pastorino, 2010). All of these processes regulated by sirt-3 converge to make the mitochondria and cell more resilient against necrotic induced damage. However sirt-3 also acts as a tumor suppressor, whose loss increases the chances of cellular transformation and the ability of cancer cells to survive.

Loss of sirt-3 is thought to promote cellular transformation by stimulating ROS generation. The increased ROS contributes to cellular transformation by promoting genomic instability, with sirt-$3^{-/-}$ mouse embryonic fibroblasts displaying a transformation-permissive phenotype (Haigis et al., 2012a). Moreover, once transformed, a cancer cell must survive in a hostile environment. By increasing the basal level of ROS, sirt-3 depletion enhances the stability of hypoxia factor 1α (HIF-1α) (Bell et al., 2011; Schumacker, 2011). The increased stability of HIF-1α contributes to the enhanced rate of glycolysis exhibited by many cancers even in the presence of adequate oxygen, a phenomena known as the Warburg effect (Pedersen, 2007). Aside from producing ATP under hypoxic conditions, the stimulation of glycolysis maybe more critical for generating glucose-6-phosphate (G-6-P) that is a ready conduit to a variety of biosynthetic pathways required for cellular proliferation, such as lipid synthesis and shunting to the pentose phosphate pathway for the generation of NADPH.

The first and rate controlling enzymes of glycolysis are hexokinase I or II, which catalyzes the conversion of glucose to glucose-6-phosphate utilizing ATP. Hexokinase II is highly expressed in cancer cells, in part due to transcriptional activation of the

hexokinase II gene by HIF-1α (Gwak et al., 2005; Marín-Hernández et al., 2009). Moreover, in cancer cells, hexokinase I or II activity is accelerated by their ncreased binding to the mitochondria (Azoulay-Zohar et al., 2004; Pastorino and Hoek, 2008). Hexokinase I or II binds to the mitochondria via an interaction with the voltage dependent anion carrier (VDAC), embedded in the mitochondrial outer membrane (Shoshan-Barmatz et al., 2009). In this position, hexokinase I or II gains preferential access to ATP generated by oxidative phosphorylation, thereby accelerating G-6-P production and utilization. Indeed, the binding of hexokinase II to the mitochondria and its ability to funnel ATP produced in the mitochondria to form G-6-P is a primary mechanism driving the phenomena of aerobic glycolysis.

In addition to promoting aerobic production of G-6-P, the binding of hexokinase I or II to mitochondria interferes with Bak/Bax dependent mitochondrial injury (Gall et al., 2011; Majewski et al., 2004a; Majewski et al., 2004b; Pastorino et al., 2002; Shulga et al., 2009; Tajeddine et al., 2008; Vyssokikh et al., 2002). The mechanism by which mitochondrial bound hexokinase I or II interferes with Bak/Bax induced mitochondrial damage is not fully clear. However, a number of reports indicate that Bak/Bax interacts with or are modulated by VDAC, thereby supporting the notion that hexokinase I or II prevents Bak/Bax activation by interfering with their ability to interact with VDAC (Abu-Hamad et al., 2008; Adachi et al., 2004; Cheng et al., 2003; Lazarou et al., 2010; Roy et al., 2009; Tajeddine et al., 2008). The binding of hexokinase II to mitochondria is mediated in part by cyclophilin-D (Machida et al., 2006; Shulga et al., 2010). Cyclophilin-D has been demonstrated to exert an anti-apoptotic effect in a variety of contexts (Eliseev et al., 2009; Li et al., 2004; Schubert and Grimm, 2004). Cyclophilin-D

expression and activity were found to prevent Bax dependent apoptosis, which in turn was reversed by detachment of hexokinase II from the mitochondria (Machida et al., 2006). This is in contrast with cyclophilin-D promoting opening of the PTP and onset of necrotic cell death. Indeed, it has been shown that cyclophilin-D can exert opposite effects on apoptosis versus necrosis. These observations are in keeping with the ability of cyclophilin-D ablation to protect against necrotic cell death but not apoptosis. Indeed, it has been demonstrated that a developmental shift occurs with regards to the role of cyclophilin-D in neuronal survival (Wang et al., 2009). In the immature brain, cyclophilin-D exerts a protective effect, whereas in the adult brain, cyclophilin-D promotes loss of neuronal viability. Intriguingly, hexokinase II is expressed at much higher concentrations in the developing brain than in the adult brain, perhaps accounting in this instance for the dichotomy of cyclophilin-D effects on cell viability.

The regulation exerted on cyclophilin-D by sirtuin-3 may help to explain some of the paradoxical effects of both on necrosis versus apoptosis. We have shown that sirtuin-3 deacetylates and inactivates cyclophilin-D (Shulga et al., 2010). By contrast when sirt-3 is depleted, cyclophilin-D becomes acetylated and exhibits increased activity, which in turn promotes increased binding of hexokinase II to the mitochondria (Shulga et al., 2010). Therefore, when sirtuin-3 is expressed and active, it prevents onset of permeability transition pore opening and necrosis by dampening cyclophilin-D activity. Sirt-3 activity also inhibits PTP opening by lowering ROS levels through stimulating the anti-oxidant activity of MnSOD and IDH2. By contrast, when sirt-3 is downregulated, cyclophilin-D becomes more active, increasing the probability of PTP opening and vulnerability to necrosis. However, in a transformed cell, depletion of sirt-3 leads to HIF-1α activation

that stimulates expression of hexokinase II. Moreover, the increased acetylation of cyclophilin-D by sirt-3 depletion stimulates cyclophilin-D peptidyl-prolyl cis-trans isomerase activity, which promotes hexokinase II binding to the mitochondria where it prevents Bak/Bax dependent mitochondrial injury and apoptosis. Therefore, sirt-3 depletion has the twofold effect of increasing hexokinase II expression and the binding of hexokinase II to the mitochondria. These effects of sirt-3 depletion promote the proliferative capacity of transformed cells and their ability to survive austere conditions, thus placing sirt-3 in a key position to regulate sensitivity or resistance to chemotherapeutic agents (Fig. 19).

Figure 19. Sirtuin 3 exerts opposing effects on apoptosis and necrosis by mediating localization and activity of cyclophilin-D and hexokinase II.

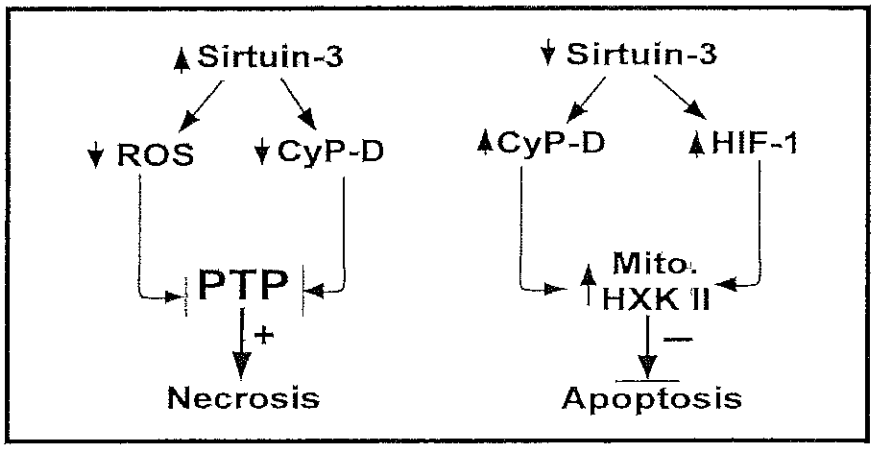

Sirtuin 4 modulates sensitivity to induction of permeability transition pore

Rationale

Opening of the mitochondrial permeability transition pore (PTP) is a critical juncture in the evolution of mitochondrial injury and onset of necrotic cell death incited by a number of conditions, one prominently being oxidative stress caused by ischemia/reperfusion(Di Lisa et al., 2001; Halestrap et al., 1997; Sharov et al., 2007). Despite significant efforts, the constituents of the PTP remain remarkably elusive. However, progress has been made in identifying endogenous regulators of PTP sensitivity, the most critical being cyclophilin-D (Baines et al., 2005; Nakagawa et al., 2005). Exogenous factors such as oxidative stress and calcium overload were identified early on as being capable of increasing sensitivity to PTP opening (Bernardi, 1992; Bernardi et al., 1992; Szabó et al., 1992). In particular, the thiol reactive agent, phenylarsine oxide (PAO), served as a useful tool to study the effects of oxidative modification of mitochondrial constituents on PTP sensitivity (Korge et al., 2001; Lenartowicz et al., 1991). Induction of PTP opening by PAO is dependent on cyclophilin-D and is sensitive to inhibition of cyclophilin-D peptidyl-prolyl cis-trans isomerase activity by agents such as cyclosporine A.

Recently, mitochondrial sirtuins have emerged as critical regulators of mitochondrial metabolism, controlling metabolic processes such as mitochondrial fatty acid oxidation and urea synthesis (Ahn et al., 2008; Nakagawa et al., 2009). We have shown that sirtuin-3 mediates the deacetylation of cyclophilin-D, and in so doing inhibits its peptidyl-prolyl cis-trans isomerase activity (Shulga et al., 2010). Inhibition or down-regulation of sirtuin-3 increases cyclophilin-D acetylation and activity, which in turn sensitizes mitochondria to PTP opening. Sirtuin-4, also localized to the mitochondria,

lacks deacetylase activity, but possesses ADP-ribosyltransferase activity (Ahuja et al., 2007; Haigis et al., 2006).

The aims of this study were to determine:

1. If Sirt4 has any role in induction of mitochondrial permeability transition (mPT)?
2. If GDH-1, which is negatively regulated by Sirt4 has any role in induction of mPT?
3. Could Sirt4 expression affect cytotoxicity induced by treatment of TNF and doxorubicin, drugs known to induce cell death by induction of mPT?

20. Determination of mitochondrial permeability transition in permeabilized cells

As shown in Fig. 20A, trace #1, as measured by TMRM fluorescence, HeLa cells permeabilized with digitonin maintained a relatively stable mitochondrial membrane potential. Significantly, addition of the mitochondrial un-coupler, CCCP, at 18 minutes caused a rapid decline of TMRM fluorescence, indicating depolarization of the mitochondria. Addition of calcium (Ca^{2+}) to give a final free calcium concentration of 250 μM also provoked mitochondrial depolarization (Fig. 20A, trace #4). Significantly, the depolarization brought about by Ca^{2+} was due to sustained opening of the permeability transition pore (PTP). Cyclophilin-D is a critical mediator of PTP sensitivity, with cyclosporine A (CsA) inhibiting the peptidyl-prolyl cis-trans isomerase activity of cyclophilin-D and lessening sensitivity to PTP induction. A five minute pretreatment with 10 μM of CsA completely prevented the calcium induced mitochondrial depolarization, but had no effect on loss of TMRM fluorescence upon subsequent addition of CCCP (Fig. 20A, trace #2). Significantly, inhibition of the calcium uniporter with ruthenium-red, which inhibits mitochondrial calcium uptake, also prevented induction of the PTP brought about by calcium (Fig. 20A, trace #3).

Phenylarsine oxide (PAO) induces PTP opening independently of an increase of Ca^{2+} by an oxidative dependent cross-linking of PTP components. As shown in Fig. 20B, trace #4, addition of 5 μM PAO induced rapid mitochondrial depolarization, which was prevented by pre-treatment with CsA (Fig. 20B, trace #2). As would be expected, ruthenium-red had no effect on the ability of PAO to induce the PTP, since in this instance, PTP induction is calcium independent (Fig. 20B, trace #3). These results

confirm that the permeabilized cell system recapitulates the behavior of isolated mitochondria with regards to agents capable of inducing and inhibiting the PTP.

Figure 20.Measurement and control of PTP induction in permeabilized cells.

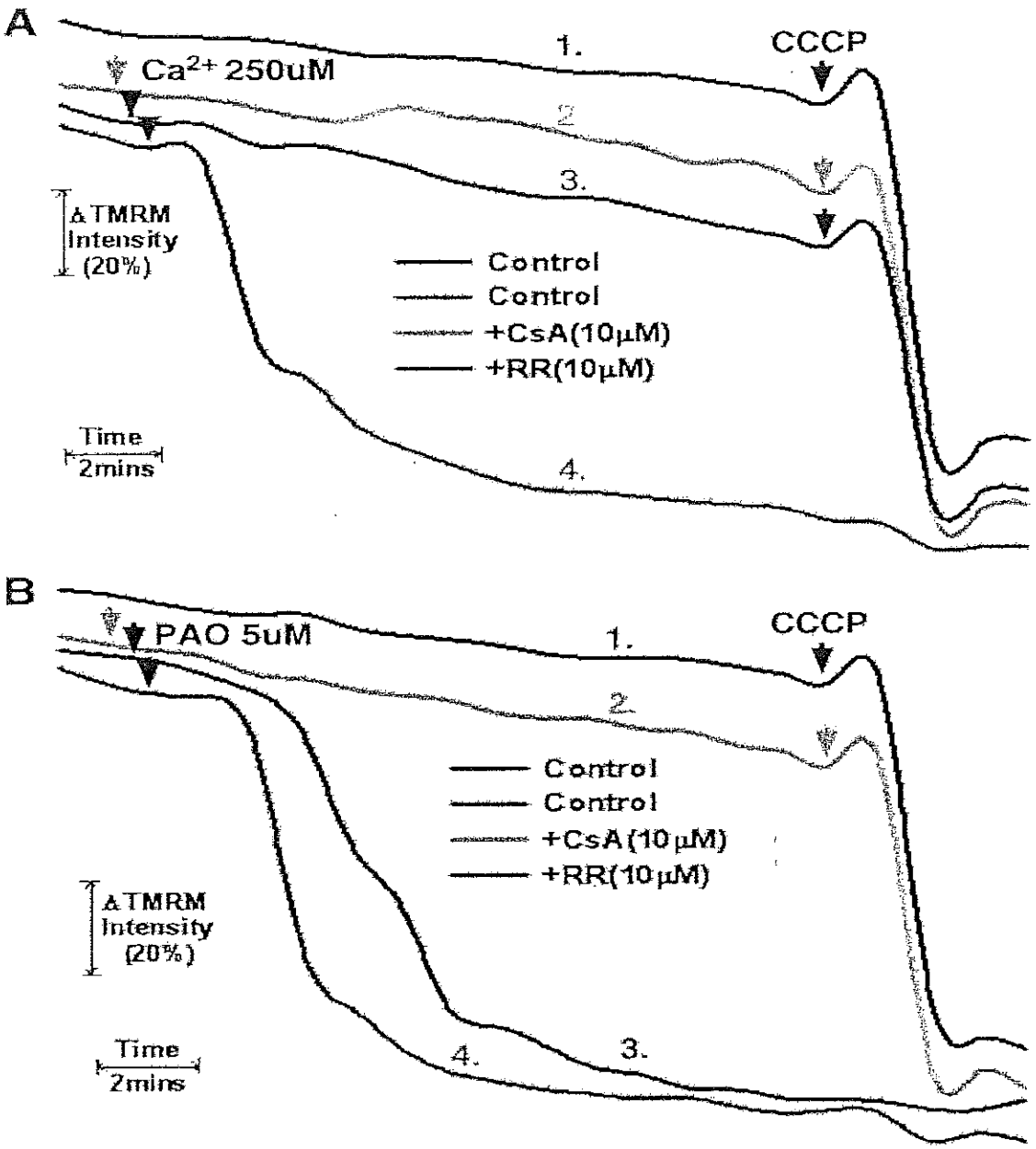

(A) and (B). HeLa cells were loaded with 200 nM TMRM in DMEM for 30 minutes. The cells were then washed twice with PBS and incubated further for 5 minutes in respiratory buffer containing 20 nM of TMRM. Digitonin at 2.5 μg/ml was then added to permeabilize the plasma membrane and the cells were mounted on a heated stage kept at 37 °C. Where indicated, cells were pretreated with 10 μM of cyclosporine A or ruthenium

red for 5 minutes. Phenylarsine oxide (PAO) or Ca^{2+} was added at final concentrations of 5 μM and 250 μM, respectively. TMRM fluorescence was monitored over a 20 minute time course. 5 μM of CCCP was added at the 18 minute time point. The result is the average of three independent experiments.

21. Suppression of sirtuin-4 prevents Ca^{2+} and PAO induction of the Permeability Transition Pore

HeLa cells were transfected with siRNAs targeting sirtuin-4, sirtuin-3, glutamate dehydrogenase I (GDH-1) or CyP-D (cyclophilin-D). As shown in Fig. 21A, the siRNAs selectively suppressed the expression of their targets while having minimal off-target effects. The siRNA targeting sirt-4 suppressed its expression by $85\% \pm 6\%$ by densitometry analysis. Particularly important is that the siRNA targeting sirt-4 had no effect on the expression of cyclophilin-D. Similarly, GDH-1 and CyP-D suppressed the expression of their respective targets by $89\% \pm 7\%$and $79\% \pm 5\%$, respectively. As shown in Fig. 21B and C (trace #1), depletion of cyclophilin-D (CyP-D) prevented PTP induction by both Ca^{2+} and PAO, respectively. Remarkably, as shown in Fig. 21B, trace #2, cells in which sirt-4 was depleted exhibited robust resistance to PTP induction brought about by the addition of Ca^{2+}. Similarly, depletion of sirtuin-4 rendered mitochondria resistant to PTP induction by PAO to the same degree as CyP-D knock-down (Fig. 21C, trace #2). Importantly, suppression of sirt-3 or sirt-5, both localized to the mitochondria, did not prevent PTP induction by either Ca^{2+} or PAO (Fig. 21B and C, traces #3 and #4, respectively).

Figure 21.Sirt-4 controls sensitivity to PTP induction by Ca^{2+} and Phenylarsine Oxide (PAO)

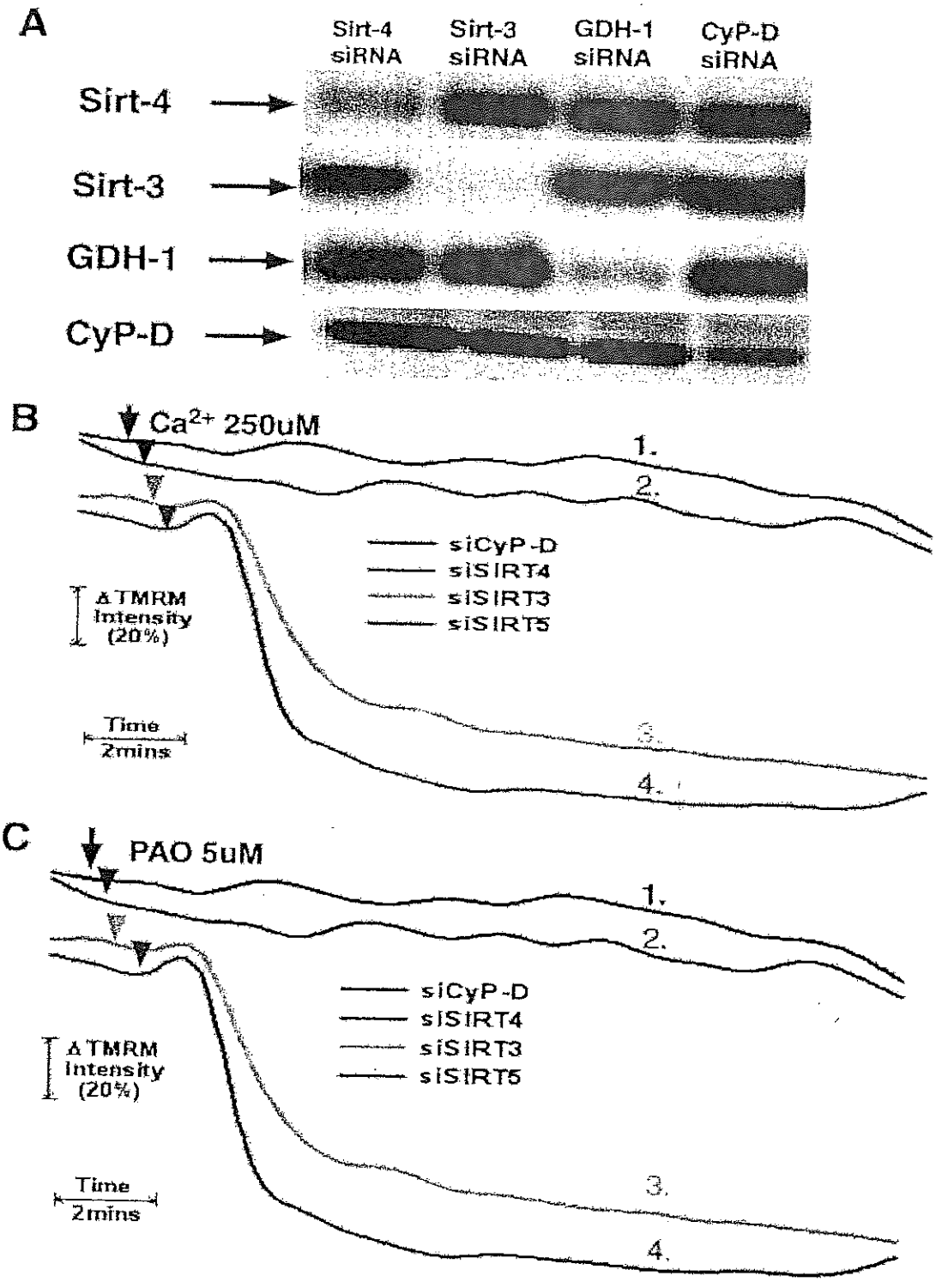

(A). HeLa cells were plated and then transfected with siRNAs targeting sirt-4, sirt-3, sirt-5, cyclophilin-D or a non-targeting control. Following 48 hours, the cells were harvested. Mitochondrial extracts were prepared and separated on 12% SDS-PAGE gels followed by blotting to PVDF membranes. The western blots were developed with antibodies against sirt-4, CyP-D, GDH-1, sirt-3 or sirt-5. The results are representative of three independent experiments.

(B) and (C). HeLa cells were plated and then transfected with siRNAs targeting sirt-4, sirt-3, sirt-5 or cyclophilin-D. Following 48 hours, the cells were loaded with 200 nM TMRM in DMEM for 30 minutes. The cells were then washed twice with PBS and incubated further for 5 minutes in respiratory buffer containing 20 nM of TMRM. Digitonin at 2.5 μg/ml was then added to permeabilize the plasma membrane and the cells were mounted on a heated stage kept at 37 °C. the cells were loaded with TMRM and mounted on a heated microscopy stage. Following permeabilization with digitonin, Ca^{2+} or PAO were added at final concentrations of 250 μM and 5 μM, respectively. Time-lapse microscopy was conducted over a 20 minute time course with TMRM fluorescence intensity assessed as described in Materials and methods. The result is the average of three independent experiments.

22. Permeability transition induced reactive oxygen species (ROS) is prevented by sirtuin-4 depletion

Induction of the PTP is frequently accompanied by an increased generation of reactive oxygen species (ROS) by mitochondria. The fluorescent probe, MitoSOX, localizes to the mitochondria and exhibits increased fluorescence upon stimulation of mitochondrial superoxide anion production. As shown in Fig. 22A, addition of 1 mM of H_2O_2 brought about a 57% increase of MitoSOX fluorescence over a twenty minute time course, indicating the ability of MitoSOX to detect ROS in the permeabilized cell system. Importantly, induction of the PTP by Ca^{2+} or PAO was accompanied by generation of ROS. Exposure to 250 μM of Ca^{2+} or 5 μM of PAO induced a 43–46% stimulation of ROS generation in cells transfected with non-targeting siRNA (Fig. 22A and B, respectively). The generation of ROS by Ca^{2+} or PAO was due to PTP induction, as both were prevented by either suppressing cyclophilin-D expression or pretreatment with CsA (Fig. 22A and B). Importantly, as with mitochondrial depolarization, depletion of sirt-4 prevented ROS production induced by both Ca^{2+} and PAO to the same degree as depletion of cyclophilin-D or pre-treatment with CsA (Fig. 22A and B).

Mitochondria produce superoxide anion, which is converted to H_2O_2 by mitochondrial superoxide anion dismutase. Utilizing the Amplex-Red assay, we determined the rate of H_2O_2 production. As shown in Fig. 22C, the addition of 250 μM of Ca^{2+} or 5 μM of PAO to permeabilized Hela cells resulted in an over 5 fold increase in the rate of H_2O_2 production. Importantly, suppression of CyP-D expression inhibited

H_2O_2 production brought about by Ca^{2+} or PAO as did depletion of sirt-4, suggesting that both prevent H_2O_2 production by inhibiting onset of the PTP.

Figure 22. Down-regulation of sirt-4 prevents PTP dependent ROS production.

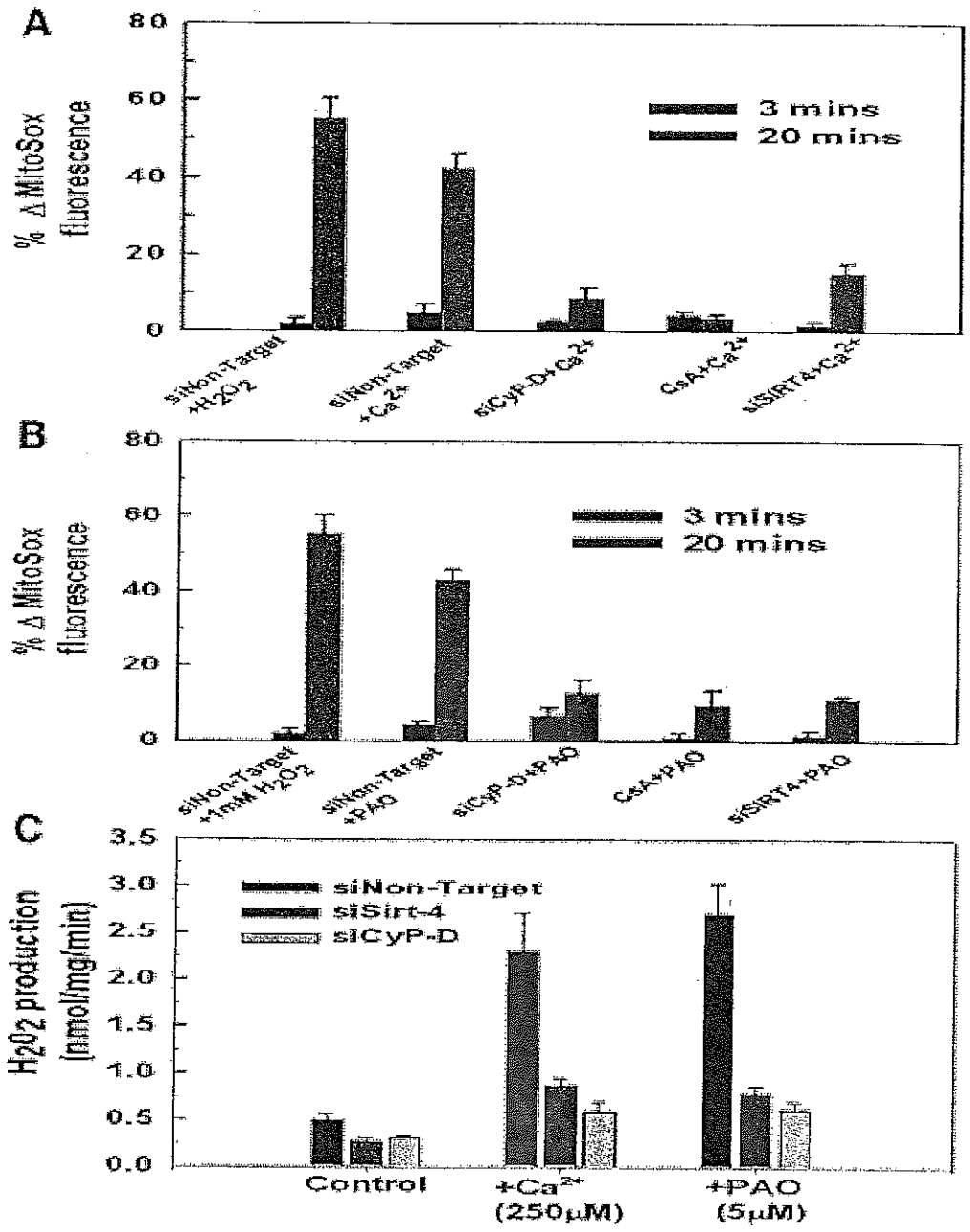

(A) and (B). HeLa cells were plated and then transfected with siRNAs targeting sirt-4, cyclophilin-D or a non-targeting control. Following 48 hours the HeLa cells were loaded with 200 nM MitoSOX in DMEM for 30 minutes. The cells were then washed twice with PBS and incubated further for 5 minutes in respiratory buffer containing 20 nM of

MitoSOX. Digitonin at 2.5 μg/ml was then added to permeabilize the plasma membrane and the cells were mounted on a heated stage kept at 37 °C. Where indicated, cells were pretreated with 10 μM of cyclosporin A for 5 minutes. Ca^{2+} and PAO were added at final concentrations of 250 μM and 5 μM, respectively. Time-lapse microscopy was conducted over a 20 minute time course with MitoSox fluorescence intensity assessed as described in Materials and methods. The results are the mean of three independent experiments ± the standard deviation.

(C). HeLa cells were plated and then transfected with siRNAs targeting sirt-4 or CyP-D. Following 48 hours, the cells were placed in respiratory buffer and permeabilized with digitonin (2.5 μg/ml). Amplex-red reagent was added at 5 μM along with 10 U/ml of horseradish peroxidase. Following addition of Ca^{2+} or PAO, fluorescence intensity was measured using a Synergy HT microplate reader with an excitation of 570 nm and emission at 585 nm at 37 °C at 1 minute intervals. The results are the mean of three independent experiments ± the standard deviation.

23. Modulation of the PTP by sirt-4 is dependent on glutamate dehydrogenase-1

Sirt-4 ADP ribosylates and inactivates glutamate dehydrogenase-1 (GDH-1); therefore the protective effect of depleting sirt-4 against PTP induction maybe due to activation of GDH-1. If this is the case, then suppression of GDH-1 expression should restore PTP sensitivity when sirt-4 levels are depleted. Therefore HeLa cells were concomitantly transfected with siRNAs targeting sirt-4 and GDH-1. As show in Fig. 23A and B, traces #2, depletion of GDH-1 reversed the protective effect exerted by suppressing sirt-4 expression on PTP induction brought about by either Ca^{2+} or PAO, respectively. Importantly, depletion of GDH-1 did not reverse the inhibition of PTP induction mediated by suppression of CyP-D, indicating that GDH-1 acts specifically in a sirt-4 dependent pathway to modulate PTP sensitivity (Fig. 23A and B, traces #1).

Figure 23. Glutamate dehydrogenase-1 expression is necessary for sirt-4 depletion to protect against the PTP.

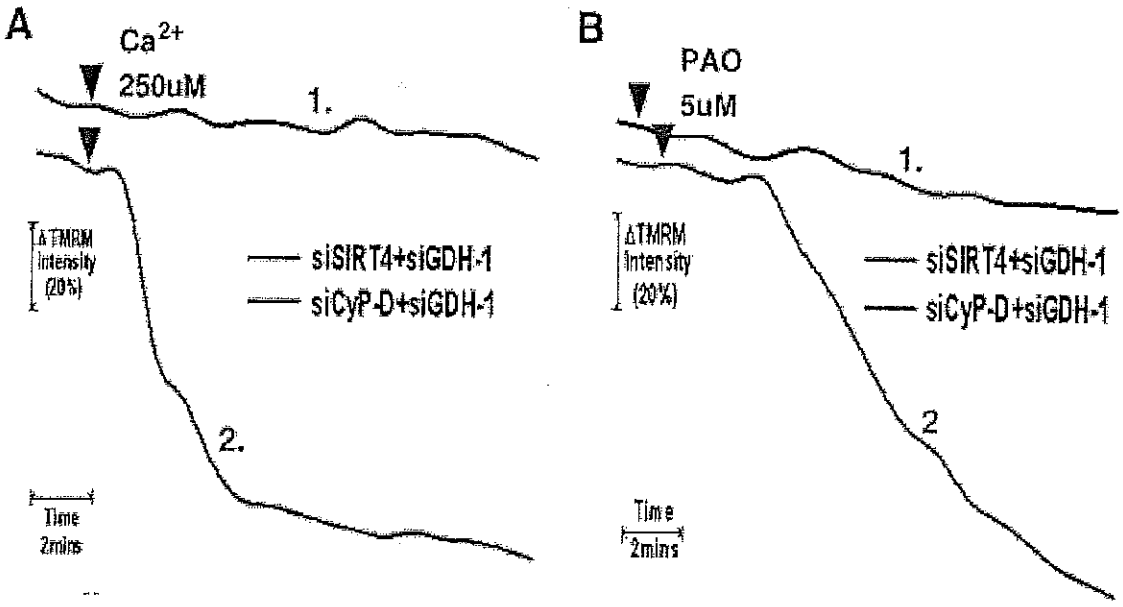

(A) and (B). HeLa cells were plated and then transfected with an siRNA targeting GDH-1 simultaneously with siRNAs targeting sirt-4 or cyclophilin-D. Following 48 hours, HeLa cells were loaded with 200 nM TMRM in DMEM for 30 minutes. The cells were then washed twice with PBS and incubated further for 5 minutes in respiratory buffer containing 20 nM of TMRM. Digitonin at 2.5 μg/ml was then added to permeabilize the plasma membrane and the cells were mounted on a heated stage kept at 37 °C. Following permeabilization with digitonin, Ca^{2+} and PAO were added at final concentrations of 250 μM and 5 μM, respectively. Time-lapse microscopy was conducted over a 20 minute time course with TMRM fluorescence intensity assessed as described in Materials and methods. The result is the average of three independent experiments.

24. Inhibition of ROS production by sirtuin-4 knockdown is reversed by simultaneous depletion of sirtuin-4 and glutamate dehydrogenase-1

Additionally, the prevention of ROS production by down-regulation of sirt-4 was also dependent on GDH-1 expression. As shown in Fig. 24A and B, depletion of GDH-1 prevented down-regulation of sirt-4 from inhibiting Ca^{2+} or PAO induced ROS generation, with the addition of Ca^{2+} or PAO triggering a 45%–58% increase in ROS production in cells where sirt-4 and GDH-1 were concomitantly down-regulated, respectively. By contrast, depletion of GDH-1 expression did not reverse the ability of CyP-D suppression to prevent Ca^{2+} or PAO induced ROS production, with only a 10–12% stimulation of ROS production when CyP-D and GDH-1 were concomitantly down-regulated, indicating that unlike sirt-4, CyP-D modulation of PTP induced ROS production is not dependent on GDH-1 expression (Fig. 24A and B). Similarly, the ability of sirt-4 depletion to prevent an increased rate of H_2O_2 production was dependent on the expression of GDH-1. As shown in Fig. 24C, suppression of GDH-1 expression reversed the protective effect of sirt-4 depletion against Ca^{2+} and PAO stimulation of H_2O_2 production. By contrast, the ability of CyP-D depletion to prevent onset of H_2O_2 production by Ca^{2+} or PAO was not dependent on GDH-1.

Figure 24. Sirtuin-4 mediated inhibition of ROS production is reversed by concomitant knock down of Sirt-4 and GDH-1

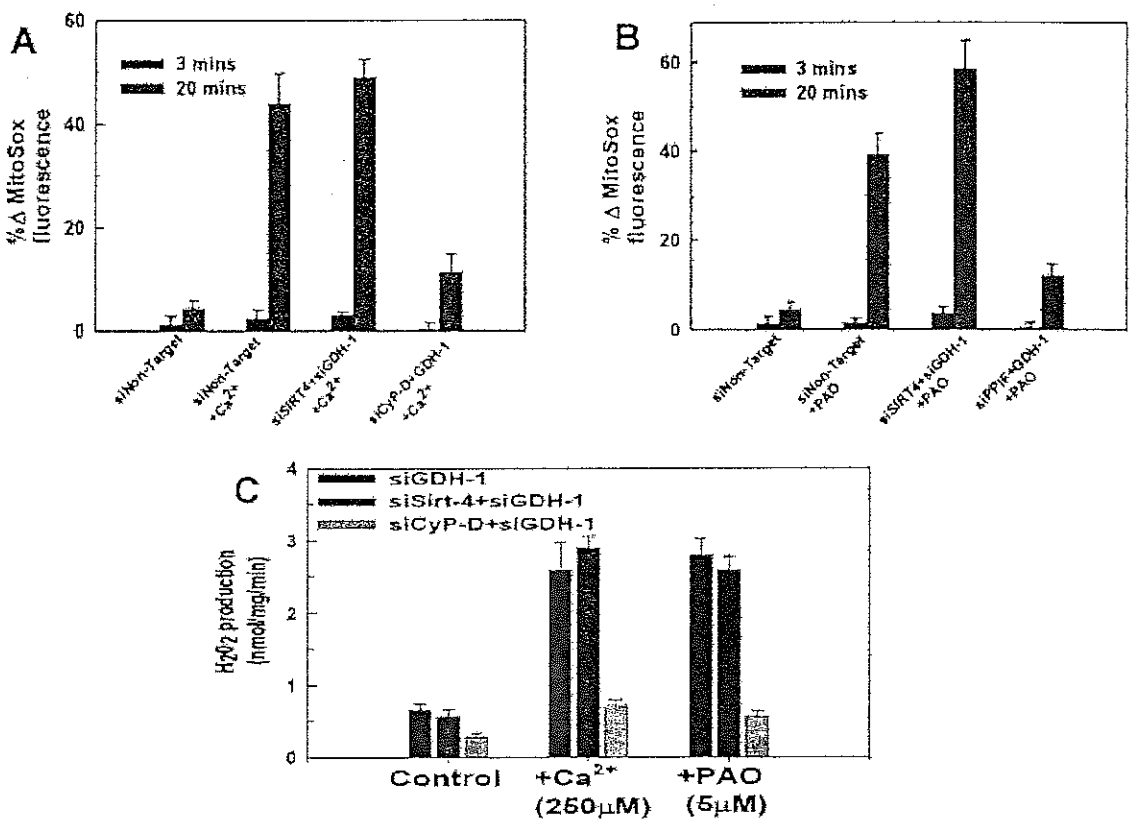

(A) and (B). HeLa cells were plated and then transfected with a siRNA targeting GDH-1 simultaneously with siRNAs targeting sirt-4 or cyclophilin-D. Following 48 hours, the cells were loaded with 200 nM of MitoSOX in DMEM for 30 minutes. The cells were then washed twice with PBS and incubated further for 5 minutes in respiratory buffer containing 20 nM of MitoSOX. Digitonin at 2.5 μg/ml was then added to permeabilize the plasma membrane and the cells were mounted on a heated stage kept at 37 °C. Following permeabilization with digitonin, Ca^{2+} and PAO were added at final concentrations of 250 μM and 5 μM, respectively. Time-lapse microscopy was conducted over a 20 minute time course with MitoSOX fluorescence intensity assessed as described in Materials and methods. The results are the mean of three independent experiments ± the standard deviation.

(C). HeLa cells were plated and then transfected with siRNAs targeting sirt-4, CyP-D individually or in tandem with siRNA targeting GDH-1. Following 48 hours, the cells

were placed in respiratory buffer and permeabilized with digitonin (2.5 μg/ml). Amplex-red reagent was added at 5 μM along with 10 U/ml of horseradish peroxidase. Following addition of Ca^{2+} or PAO, fluorescence intensity was measured using Synergy HT microplate reader with an excitation of 570 nm and emission at 585 nm at 37 °C at 1 minute intervals. The results are the mean of three independent experiments ± the standard deviation.

25. Glutamate dehydrogenase-1 down regulation potentiates Permeability Transition Pore induction

In addition to reversing the protective effect against PTP induction exerted by sirt-4 depletion, suppression of GDH-1 potentiated PTP induction triggered by sub-threshold doses of Ca^{2+} and PAO. As shown in Fig. 25A, trace #1, in cells transfected with a non-targeting siRNA, a 50 μM dose of Ca^{2+} induced the PTP to a much lesser extent than a 250 μM dose, exhibiting a longer lag phase to PTP induction and incomplete depolarization over a twenty minute time course, indicating that a large proportion of the mitochondria were resistant to PTP induction by this low dose of Ca^{2+}. By contrast, when GDH-1 levels were depleted, 50 μM of Ca^{2+} induced rapid and complete PTP induction, comparable in rapidity and extent to that induced by a 250 μM dose of Ca^{2+} in control cells (Fig. 25A, trace #2). Similarly, a sub-threshold dose of PAO (1 μM) that induced incomplete depolarization in cells transfected with non-target siRNA (Fig. 25B, trace #1), induced rapid and complete loss of membrane potential in cells where GDH-1 levels are depleted (Fig. 25B, trace #2).

Figure 25. Glutamate dehydrogenase regulates PTP sensitivity.

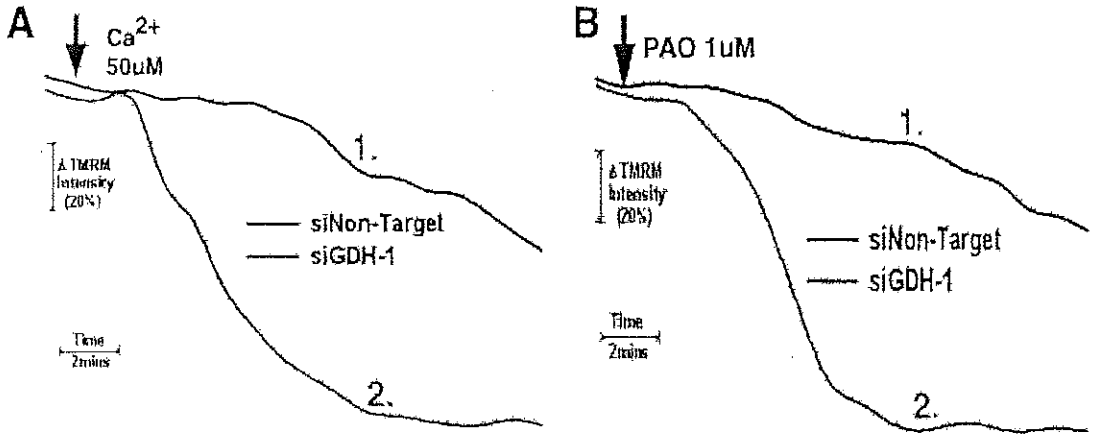

(A) and (B). HeLa cells were plated and then transfected with siRNAs targeting GDH-1 or a non-targeting control. Following 48 hours, HeLa cells were loaded with 200 nM TMRM in DMEM for 30 minutes. The cells were then washed twice with PBS and incubated further for 5 minutes in respiratory buffer containing 20 nM of TMRM. Digitonin at 2.5 μg/ml was then added to permeabilize the plasma membrane and the cells were mounted on a heated stage kept at 37 °C. Following permeabilization with digitonin, Ca^{2+} or PAO were added at final concentrations of 50 μM and 1 μM, respectively. Time-lapse microscopy was conducted over a 20 minute time course with TMRM fluorescence intensity assessed as described in Materials and methods. The result is the average of three independent experiments.

26. Stimulation of glutamate dehydrogenase-1 activity prevents PTP induction

Leucine is an allosteric stimulator of GDH-1 (Li et al., 2012; Tomita et al., 2011). As show in Fig. 26A, trace #2, in cells transfected with non-targeting siRNA, treatment with 250 μM Ca^{2+} induced rapid mitochondrial depolarization. By contrast, cells pretreated for 5 minutes with 1 mM of leucine were refractory to PTP induction brought about by the addition of 250 μM calcium (Fig. 26A, trace #1). Moreover, the ability of leucine to prevent PTP induction was dependent on expression of GDH-1. As shown in Fig. 26A, trace #3, depletion of GDH-1 neutralized the ability of leucine to prevent PTP induction by calcium, indicating that prevention of the PTP by leucine is dependent on GDH-1 expression. Similarly, exposure of cells transfected with non-targeting siRNA to 5 μM of PAO brought about rapid mitochondrial depolarization that was prevented by pretreatment with 1 mM of leucine (Fig. 26B, traces #2 and #1, respectively). However as with Ca^{2+}, the ability of leucine to prevent induction of the PTP by PAO was dependent on GDH-1, with depletion of GDH-1 reversing the protective effect of leucine (Fig. 26B, trace #3). These data indicate that GDH-1 increases the threshold for PTP induction and that when the negative regulation exerted on GDH-1 by sirt-4 is removed, PTP induction is blunted.

Figure 26. Stimulation of GDH-1 by Leucine prevents PTP induction

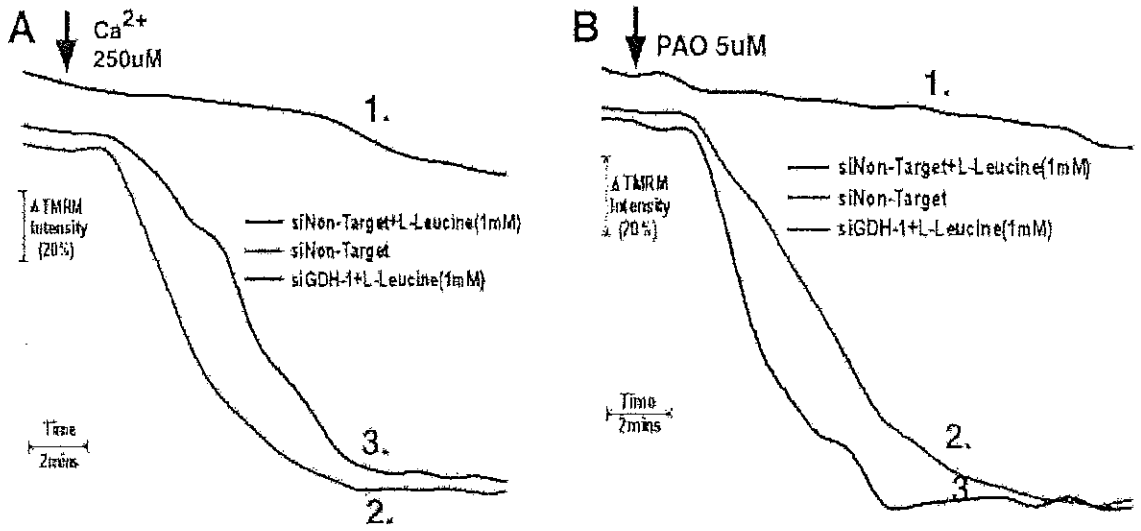

(A) and (B). HeLa cells were plated and then transfected with siRNAs targeting GDH-1 or a non-targeting control. Following 48 hours, HeLa cells were loaded with 200 nM TMRM in DMEM for 30 minutes. The cells were then washed twice with PBS and incubated further for 5 minutes in respiratory buffer containing 20 nM of TMRM. Digitonin at 2.5 μg/ml was then added to permeabilize the plasma membrane and the cells were mounted on a heated stage kept at 37 °C. Following permeabilization with digitonin, leucine at a final concentration of 1 mM was added. Following 5 minutes of pre-incubation with 1 mM leucine, Ca^{2+} or PAO were added at final concentrations of 250 μM and 5 μM, respectively. Time-lapse microscopy was conducted over a 20 minute time course with TMRM fluorescence intensity assessed as described in Materials and methods. The results are the mean of three independent experiments ± the standard deviation.

27. Plate reader assays confirmed fluorescence microscopy results

In order to verify the results obtained utilizing fluorescence microscopy, a plate reader assay was employed to determine the ability of digitonin permeabilized cells to retain TMRM upon a challenge with Ca^{2+} or PAO. As shown in Fig. 27A, in agreement with the results obtained with fluorescence microscopy, the addition of 250 μM of Ca^{2+} to digitonin permeabilized cells transfected with non-targeting siRNA resulted in a 93% loss of TMRM fluorescence. By contrast, cells pre-treated with CsA or depleted of CyP-D were resistant to calcium induced loss of TMRM fluorescence, exhibiting only a 10%–15% loss of TMRM fluorescence, indicating that the mitochondrial depolarization is due to opening of the PTP. Similarly, the addition of 5 μM of PAO brought about a 95% loss of TMRM fluorescence that was prevented by pre-treatment with CsA or depletion of CyP-D. Importantly, depletion of sirt-4 also prevented Ca^{2+} and PAO induction of the PTP (Fig. 27A). In contrast to CsA or suppression of CyP-D expression, depletion of sirt-4 required the expression of GDH-1 to prevent PTP induction by Ca^{2+} or PAO (Fig. 27B). Suppression of GDH-1 expression reversed the protective effect exerted by depletion of sirt-4 against Ca^{2+} and PAO induced loss of TMRM fluorescence (green bar). Importantly, activation of GDH-1 by leucine also prevented induction of the PTP by Ca^{2+} and PAO, which was reversed by depletion of GDH-1 (Fig. 27B, yellow and blue bars, respectively). However, depletion of GDH-1 did not reverse the protective effect exerted by pre-treatment with CsA or suppression of CyP-D expression on Ca^{2+} or PAO induction of the PTP, indicating that sirt-4 prevents the PTP via a GDH-1 dependent mechanism distinct from that mediated by inhibition of cyclophilin-D (Fig. 27B).

Figure 27. Plate reader assays confirmed fluorescence microscope results

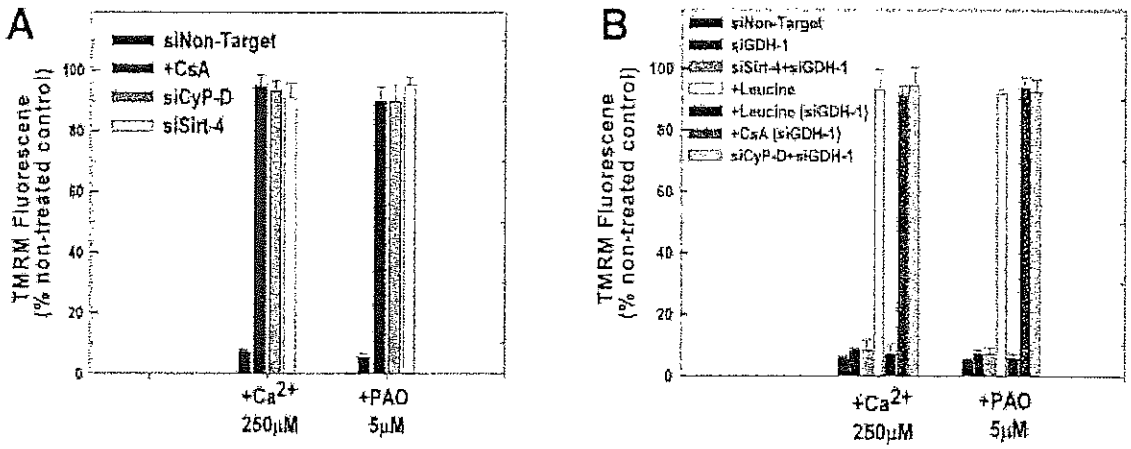

(A) and (B). HeLa cells were plated at 50,000 cells/well in 24 well plates and transfected with the indicated siRNA. After 48 hours, the cells were loaded with 200 nM TMRM in DMEM for 30 minutes. The cells were incubated further for 5 minutes in respiratory buffer containing 2.5 µg/ml digitonin and 20 nM of TMRM. Fluorescence intensity was measured using a Synergy HT microplate reader with an excitation of 550 nm and emission at 573 nm at 37 °C at 1 minute intervals. After 4 minutes, either phenylarsine oxide or Ca^{2+} was added at the indicated concentrations, with fluorescence measured over 20 minutes. The results are presented as % of TMRM retained in non-treated cells transfected with non target siRNA at the 20 minute time point. The results are the mean of three independent experiments ± the standard deviation.

28. Sirt-4 increases mitochondrial calcium retention capacity

Desensitization to PTP opening increases the ability of mitochondria to take up calcium, thereby lessening cellular injury when calcium homeostasis is perturbed. Control, non-treated HeLa cells displayed a calcium retention capacity of 250 nmole of Ca^{2+}/mg mitochondrial protein. As shown in Fig. 28, as expected, treatment with CsA or suppression of CyP-D expression increased the ability of mitochondria to retain calcium by 87% and 93%, respectively. Importantly, depletion of sirt-4 enhanced calcium retention to the same degree, increasing capacity by 94%. Intriguingly, suppression of GDH-1 decreased calcium retention capacity to below control levels, in agreement with the notion that loss of GDH-1 expression potentiates induction of the PTP. Moreover, the ability of sirt-4 to increase calcium retention capacity is dependent on GDH-1 expression. Suppression of GDH-1 reversed the ability of sirt-4 depletion to enhance calcium retention capacity, depressing calcium retention capacity to levels below that of control. Similarly, stimulation of GDH-1 activity with leucine increased calcium retention capacity that in turn was reversed by depletion of GDH-1. By contrast, the ability of CsA to increase calcium retention capacity was not dependent on GDH-1 expression (Fig. 28).

Figure 28. Depletion of Sirt-4 enhances mitochondrial calcium retention capacity.

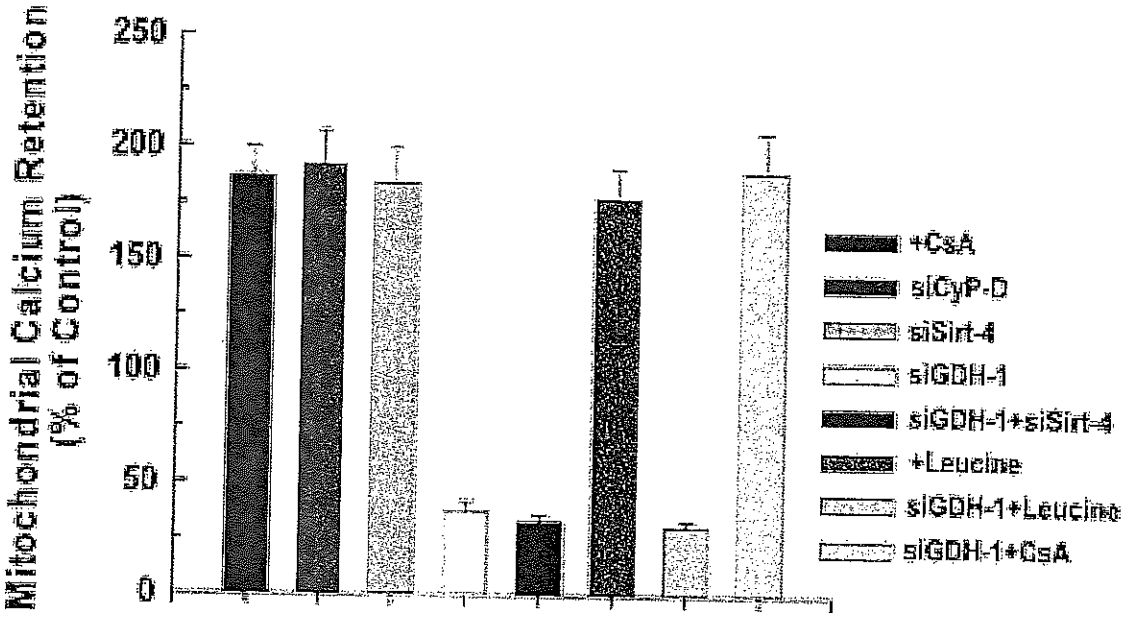

HeLa cells were plated at 50,000 cells per well in 24 well plates and transfected with the indicated siRNA. After 48 hours, the cells were incubated for 5 minutes in respiratory buffer containing 2.5 μg/ml digitonin and 1 μM of the Ca^{2+} indicator, Calcium Green-5N (excitation 505 nm; emission: 535 nm; Molecular Probes). Calcium was added in pulses of 10 μM and uptake measured as a decrease of Calcium Green-5N fluorescence. The results are the mean of three independent experiments ± the standard deviation.

29. Role of mitochondrial glutathione in sirt-4 protection

A stimulation of GDH-1 activity can increase synthesis of NADPH, which in turn can be utilized in the production of reduced glutathione (GSH). Glutathione is an antioxidant, suggesting the possibility that depletion of sirt-4 protects against the PTP by promoting the production of GSH. Control cells or cells transfected with non-targeting siRNA displayed mitochondrial GDH-1 activity of 1.86 μmol/min/mg protein). As shown in Fig. 29A, depletion of sirt-4 stimulated mitochondrial GDH-1 activity to 74% above that seen in untreated control cells. Similarly, as expected the addition of leucine also stimulated GDH-1 activity to 79% above control levels. Importantly, stimulation of GDH-1 activity with leucine or by suppression of sirt-4 expression, were both prevented by transfection with siRNA targeting GDH-1. However, despite activating GDH-1, neither depletion of sirt-4 nor the addition of leucine caused an elevation of mitochondrial GSH levels. The concentration of glutathione in mitochondria isolated from control non-treated cells was 6 nmole/mg mitochondrial proteins. The concentration of GSSG was 0.3 nmole/mg mitochondrial proteins. As shown in Fig. 29B, depletion of sirt-4 or stimulation with leucine did not bring about any appreciable change in the mitochondrial reduced or oxidized glutathione concentration. Surprisingly, depletion of GDH-1 did not provoke a decline of mitochondrial GSH. However, the addition of Ca^{2+} did promote a depletion of mitochondrial GSH and increase of GSSG. However, this is most likely due to opening of the PTP and subsequent loss of GSH, as the Ca^{2+} induced depletion of GSH is prevented by suppression of CyP-D expression or treatment with CsA. Similarly, suppression of sirt-4 expression also prevented the Ca^{2+} induced loss of mitochondrial GSH and increase of GSSG, as did stimulation of GDH-1 activity with

leucine. Importantly stimulation of GDH-1 activity by depletion of sirt-4 or addition of leucine did not increase or decrease the GSH/GSSG ratio (Fig. 29C). Together, these data suggest that stimulation of GDH-1 does not cause an absolute increase of mitochondrial GSH levels and the ability of GDH-1 stimulation to prevent onset of the PTP cannot be accounted for solely by modulation of mitochondrial GSH levels.

Figure 29. GDH-1 activity and mitochondrial GSH.

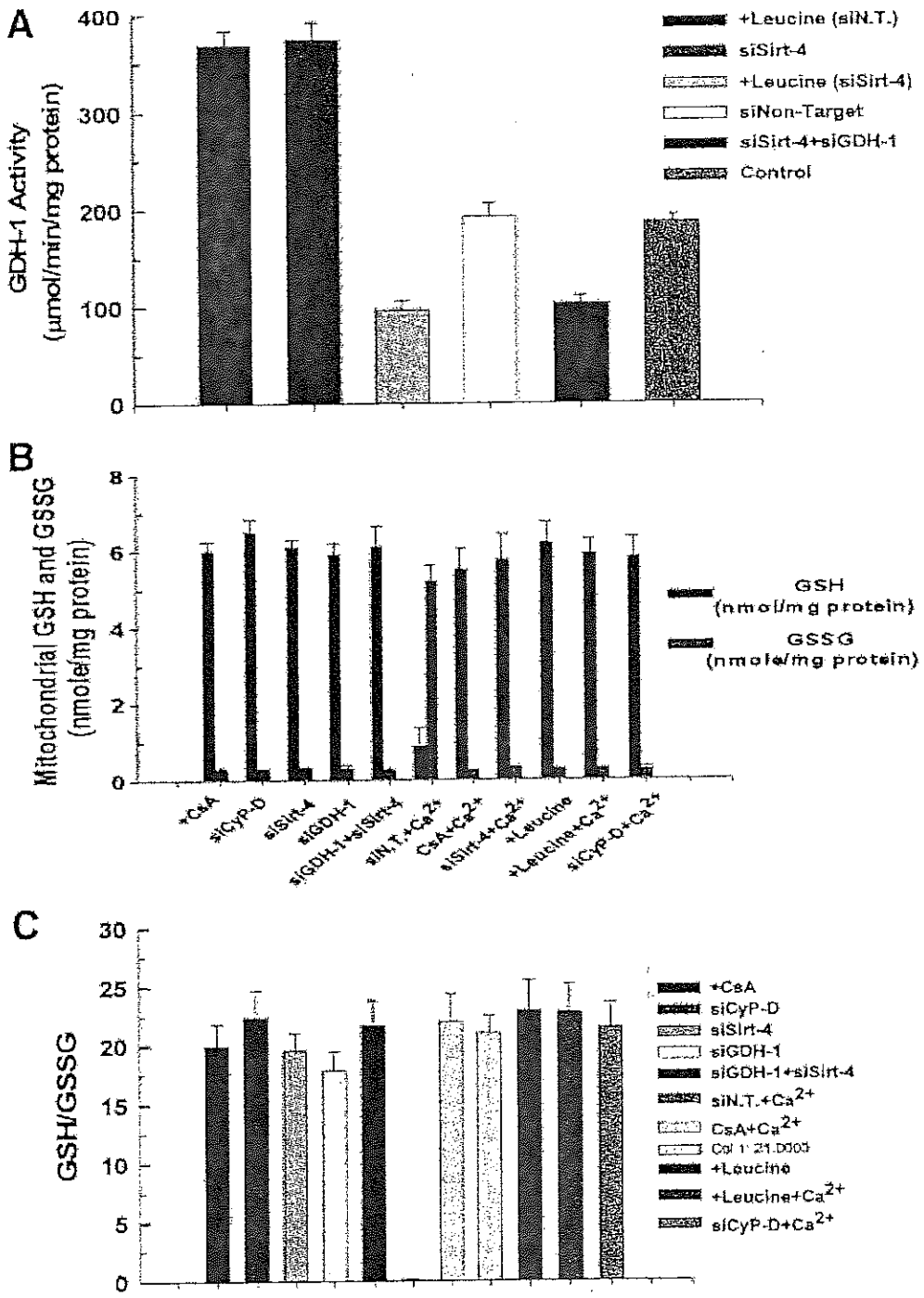

(A). HeLa cells were plated at 50,000 cells/well in 24 well plates and transfected with the indicated siRNA. Forty eight hours after transfection, cells from 4 wells were harvested by trypsinization and washed twice with ice cold PBS. Mitochondria were isolated and lysates prepared. Optical density at 450 nm was measured with Synergy HT

microplate reader (BioTek, Winooski, VT) at 37 °C at 3 minute intervals for 1 hour. The results are expressed in percentage increase or decrease in activity compared to non-treated cells transfected with non-targeting control siRNA. The results are the mean of three independent experiments ± the standard deviation.

(B). HeLa cells were plated at 50,000 cells/well in 24 well plates and transfected with the indicated siRNA. Forty eight hours after transfection, cells from 4 wells were harvested by trypsinization and washed twice with ice cold PBS. Mitochondria were isolated and lysates prepared. The supernatant was used to determine the GSH content. Fluorescence was measured at excitation of 308 nm and emission of 460 nm using a Synergy HT microplate reader. The results are presented as percentage of GSH content compared to non-treated and non-target transfected cells. The results are the mean of three independent experiments ± the standard deviation.

(C). The GSH/GSSG ratio was calculated from the measured concentrations of GSH and GSSG.

30. Sirt-4 mediates PTP dependent cytotoxicity

Our lab and others have previously demonstrated that TNF induced necroptosis is dependent on PTP induction (Bradham et al., 1998; García-Ruiz et al., 2002; Pastorino et al., 1996). As shown in Fig. 30A, in L929 fibrosarcoma cells, TNF in the presence of the pan-caspase inhibitor, ZVAD-FMK, induces a massive loss of cell viability, with only 8% of cells transfected with non-target siRNA remaining viable after 24 hours of exposure (black bar). Suppression of CyP-D expression blunted TNF + ZVAD induced cytotoxicity, with 68% of the cells still viable after 24 hours of exposure, demonstrating that in this instance, TNF induced cytotoxicity is PTP dependent (Fig. 30A, red bar). Markedly, suppression of sirt-4 expression also prevented TNF + ZVAD induced cytotoxicity, with 70% of the cells still viable after 24 hours of exposure (Fig. 30A, green bar). By contrast, suppression of sirt-3 or sirt-5 exhibited no ability to prevent TNF + ZVAD induced cell killing (results not shown). Importantly, the ability of sirt-4 down-regulation to inhibit TNF + ZVAD induced cytotoxicity was dependent on GDH-1 expression. As show in Fig. 30A, depletion of GDH-1 reversed the protective effect afforded by sirt-4 down-regulation against TNF + ZVAD induced cytotoxicity, with less than 10% of the cells remaining viable after 24 hours of exposure (yellow bar). Importantly, as with PTP induction in mitochondria, depletion of GDH-1 had no effect on the ability of CyP-D suppression to protect against TNF + ZVAD induced cytotoxicity, with 67% of the cells still viable after 24 hours of exposure (Fig. 30A, blue bar). Doxorubicin induced cytotoxicity is also dependent on PTP induction (Montaigne et al., 2011; Zhou et al., 2001) and (Cardoso et al., 2008). As shown in Fig. 30B, doxorubicin at a dose of 50 μM left only 14% of HeLa cells transfected with non-targeting siRNA viable

following 18 hours of treatment (black bar). By contrast, suppression of CyP-D or sirt-4 largely prevented doxorubicin induced cytotoxicity, with greater than 70% of the cells still viable following 18 hours of treatment. (Fig. 30B, red and green bars, respectively). Moreover, as with TNF + ZVAD, the protection afforded against doxorubicin induced cytotoxicity brought about by suppressing sirt-4 expression was dependent on GDH-1. As shown in Fig. 30B, depletion of GDH-1 reversed the protective effect of sirt-4 suppression, with only 14% of the cells remaining viable after 18 hours of doxorubicin treatment (yellow bar). By contrast, depletion of GDH-1 did not reverse the protective effect exerted by knock-down of CyP-D, with cell viability maintained at 75% following 18 hours of treatment with doxorubicin (Fig. 30B, blue bar), indicating that the protective effect exerted by down-regulating sirt-4 is dependent on GDH-1, whereas the protection afford by CyP-D suppression is not.

Figure 30. Down-regulation of sirt-4 prevents TNF and doxorubicin cytotoxicity.

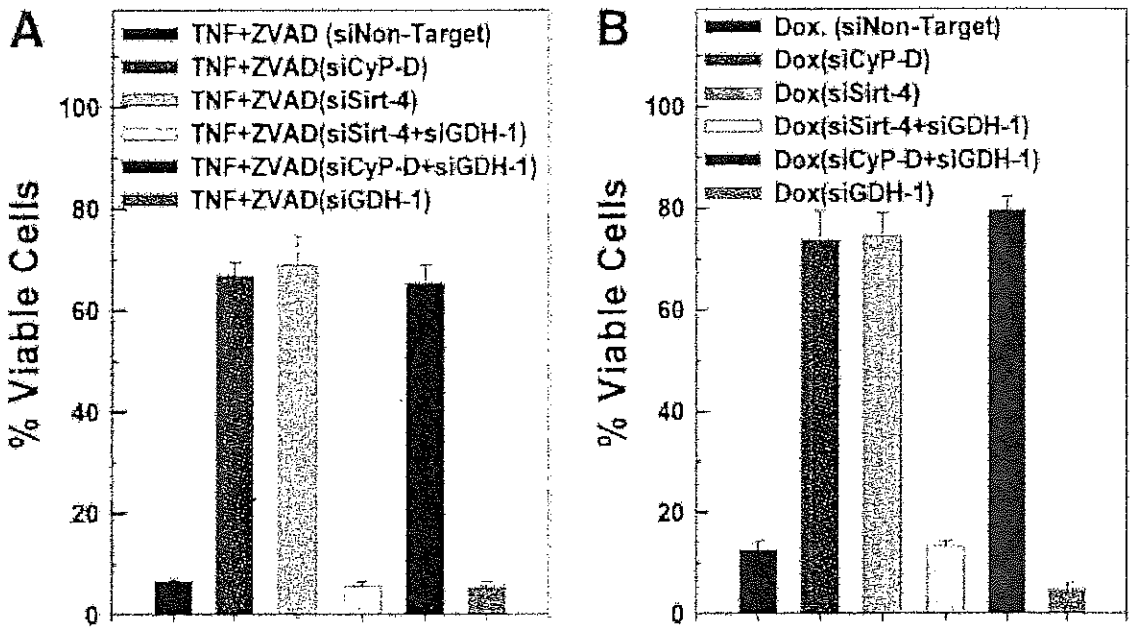

(A) and (B). HeLa cells were transfected with 50 nM of a non-targeting control siRNA or siRNAs targeting sirt-4 or CyP-D, separately or in tandem with siRNA targeting GDH-1 or siGDH-1 alone. Following 48 hours incubation, the cells were incubated with 20 ng/ml of TNFα in the presence of 20 μM of ZVAD, or treated with 10 μM of doxorubicin. After 24 hours, the cells were harvested and cell viability assessed utilizing propidium iodide as described in Materials and methods. Values are the means of three independent experiments with the error bars indicating standard deviations.

Discussion:

The present study demonstrates that sirt-4 modulates sensitivity to PTP induction and that this may be mediated partly through regulation of glutamate dehydrogenase-1. Depletion of sirt-4 prevented PTP induction brought about by Ca^{2+} or PAO. Additionally, sirt-4 expression mediated sensitivity to PTP dependent cell death, with suppression of sirt-4 levels preventing TNF + ZVAD and doxorubicin induced cytotoxicity. Importantly, inhibition of PTP sensitivity by down-regulation of sirt-4 is dependent on GDH-1 expression. Depletion of GDH-1 negated the protective effect exerted by suppressing sirt-4 levels against PTP induction brought about by Ca^{2+} and PAO, and also prevented sirt-4 suppression from inhibiting TNF + ZVAD or doxorubicin induced cytotoxicity. By contrast, suppression of PTP induction or inhibition of PTP dependent cytotoxicity by down-regulating CyP-D was insensitive to GDH-1 levels. Moreover, pre-treatment with the GDH-1 allosteric activator, leucine, prevented PTP induction, with depletion of GDH-1 reversing the protective effect of leucine. These data suggest that by negatively regulating GDH-1, sirt-4 increases sensitivity to PTP induction and that when sirt-4 levels are suppressed, activation of GDH-1 promotes resistance to PTP induction and subsequent cytotoxicity.

The regulation of GDH-1 activity by ADP-ribosylation was noted before the identification of sirt-4 as the enzyme responsible for the modification (Choi et al., 2005; Herrero-Yraola et al., 2001). GDH-1 is active as a homohexamer, but the stoichiometry between incorporated ADP-ribose and GDH-1 subunits indicates that ADP-ribosylation of one subunit of the hexameric complex maybe all that is needed for its inactivation (Karaca et al., 2011). The cysteine residue at position 119 is the site ADP-ribosylated by

sirt-4, but curiously is thought not to be directly involved in GDH-1 catalysis, as cysteine residue 323 has been shown to be. In addition to ADP-ribosylation, GDH-1 is controlled by a number of allosteric effectors including ADP, ATP, GDP, GTP and leucine (Li et al., 2012; Tomita et al., 2011).

Sirt-4 is localized to the mitochondrial matrix but possesses no deacetylase activity. Rather, sirt-4 ADP-ribosylates GDH-1, thereby inhibiting its activity and provoking a number of metabolic alterations (Haigis et al., 2006). In pancreatic β cells, suppression of sirt-4 resulted in activation of GDH-1 that in turn provoked an increase in insulin secretion in response to glucose (Ahuja et al., 2007). The ability of GDH-1 to promote insulin secretion was also identified in dominant mutations of GDH-1 that cause reduced GTP inhibition of the enzyme, resulting in a syndrome of hyperinsulinism and hyperammonemia (Kapoor et al., 2009). Sirt-4 has also been shown to interact with insulin degrading enzyme (IDE) and adenine nucleotide translocase 2 (ANT-2). ANT-2 mediates the uptake of ATP from the cytosol into the mitochondria and exhibits increased expression in highly glycolytic cancer cells (Chevrollier et al., 2005; Chevrollier et al., 2011). Expression of ANT-2 is associated with inhibition of apoptosis, although the exact mechanism by which it exerts this effect is unclear. However down-regulating ANT-2 or IDE had no effect on the ability of sirt-4 to modulate sensitivity to PTP induction (results not shown). Intriguingly, mutations of the pancreatic duodenal homeobox gene-1 (Pdx-1) cause heritable diabetes in humans and mice, brought about by increased pancreatic beta cell death mediated by onset of the PTP, suggesting that in pancreatic beta cells, sirt-4 may contribute to regulation of the PTP (Fujimoto et al., 2010a; Fujimoto et al., 2010b).

The mechanism by which suppression of sirt-4 inhibits PTP induction is unclear. The dependence on GDH-1 expression may indicate that it involves metabolic alterations in mitochondrial metabolism. In an anapleurotic reaction, increased GDH-1 activity funnels glutamate into the tricarboxylic acid cycle via α-ketoglutarate dehydrogenase, resulting in an elevation of NADPH, NADH and ATP production; all of which increase the threshold for PTP induction. (Karaca et al., 2011). Alternatively, once activated, GDH-1 in its hexameric configuration may interact with a component of the PTP to inhibit assembly of the pore complex. Interestingly, before the concept of a permeability transition pore emerged, it was shown that ADP-ribosylation controlled sensitivity to the mitochondrial permeability transition (Frei and Richter, 1988; Masmoudi et al., 1988; Richter and Frei, 1988; Richter et al., 1983). Mono-ADP-ribosylation of mitochondrial proteins is stimulated by pro-oxidants and is associated with loss of mitochondrial membrane integrity. It is possible that the ADP-ribosyltransferase activity responsible for this phenomenon is partly mediated by sirt-4. Indeed, it maybe that sirt-4 ADP-ribosylates and modulates multiple targets that impact sensitivity to PTP induction.

In summary, the present study provides evidence indicating that sirt-4 modulates sensitivity to mitochondrial PTP induction and PTP dependent cytotoxicity that is in part dependent on GDH-1 (Fig. 31).

Figure 31. Control of mitochondrial permeability transition pore sensitivity by sirt4. Sirtuin 4 modulates the activity of GDH-1 which in turn inhibits PTP opening and loss of cell viability

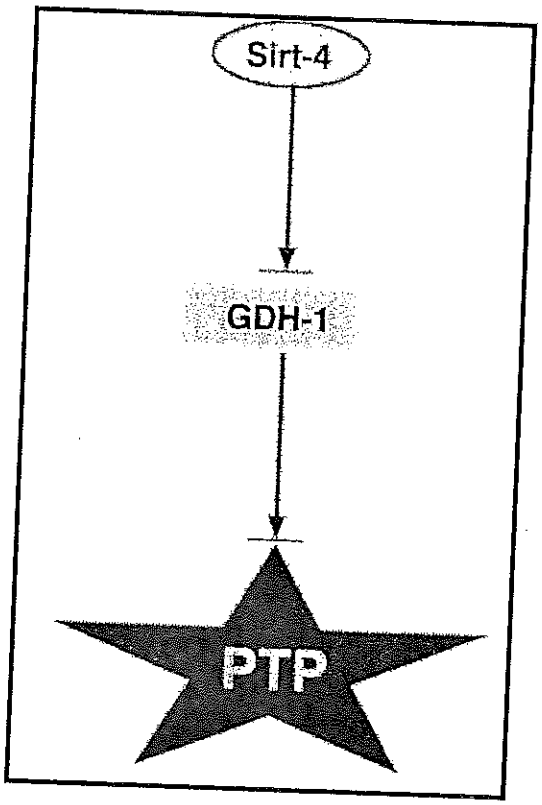

Summary and Conclusions

Summary and Conclusions:

A) Sirtuin 3 modulates Bax/Bak dependent apoptosis.

In this study I was able to show that sirtuin 3 is a mitochondrial localized tumor suppressor.

i) In intact mitochondria, knock down of Sirt3 by siRNA prevented Mcl-1 and Bcl-X_L knockdown induced cell death (fig. 6B) which was also prevented by knock down of Bax and Bak (fig 6B)

ii) Knock down of Mcl-1 and Bcl-X_L induced activation of Bax and Bak. Simultaneous knock down of Mcl-1, Bcl-X_L and Sirt3 prevented Bax and Bak activation (fig. 7A and 7B)

iii) Sirt3 or Bax/Bak knockdown prevent mitochondrial injury (fig 8A), ROS generation (fig. 8B) or caspase activation (fig 9A)

iv) In permeabilized cells, depletion of Sirt3 prevented t-Bid induced mitochondrial depolarization which was depended hexokinase II binding on the OMM.

v) Expression of Sirt3 modulated sensitivity to cisplatin. Knockdown of Sirt3 prevented cisplatin induced cytotoxicity, whereas, over expression of Sirt3 wild type but not the mutant (H248Y) sensitized tumor cells to cisplatin.

B) Sirtuin 4 modulates sensitivity to induction of permeability transition pore (mPTP).

In this study I was able to shown that sirtuin 4 modulates the opening of mPTP

i) Knock down Sirt4 prevented Ca^{2+} or PAO induced mitochondrial depolarization and ROS generation

ii) Knockdown of Sirt4 and GDH-1 simultaneously reversed Sirt4 knockdown mediated protection against Ca2+ and PAO indicating that GDH-1 activity negatively regulated PTP induction.

iii) Also knockdown of GDH-1 alone sensitized cells to PTP induction (fig 25 A and B) whereas stimulation of GDH-1 activity by L-leucine prevented PTP induction (fig 26 A and B)

iv) Knockdown of Sirt4 prevented TNF and doxorubicin induced cytotoxicity which was reversed by simultaneous knock down of Sirt4 and GDH-1 (fig 30 A and B)

REFERENCES

Abu-Hamad, S., Zaid, H., Israelson, A., Nahon, E. and Shoshan-Barmatz, V. (2008). Hexokinase-I protection against apoptotic cell death is mediated via interaction with the voltage-dependent anion channel-1: mapping the site of binding. *The Journal of biological chemistry* **283**, 13482–90.

Adachi, M., Higuchi, H., Miura, S., Azuma, T., Inokuchi, S., Saito, H., Kato, S. and Ishii, H. (2004). Bax interacts with the voltage-dependent anion channel and mediates ethanol-induced apoptosis in rat hepatocytes. *American journal of physiology. Gastrointestinal and liver physiology* **287**, G695–705.

Adrain, C., Slee, E. A., Harte, M. T. and Martin, S. J. (1999). Regulation of apoptotic protease activating factor-1 oligomerization and apoptosis by the WD-40 repeat region. *The Journal of biological chemistry* **274**, 20855–60.

Ahmed, E. A., Sfeir, A., Takai, H. and Scherthan, H. (2013). Ku70 and non-homologous end joining protect testicular cells from DNA damage. *Journal of cell science* **126**, 3095–104.

Ahn, B.-H., Kim, H.-S., Song, S., Lee, I. H., Liu, J., Vassilopoulos, A., Deng, C.-X. and Finkel, T. (2008). A role for the mitochondrial deacetylase Sirt3 in regulating energy homeostasis. *Proceedings of the National Academy of Sciences of the United States of America* **105**, 14447–52.

Ahuja, N., Schwer, B., Carobbio, S., Waltregny, D., North, B. J., Castronovo, V., Maechler, P. and Verdin, E. (2007). Regulation of insulin secretion by SIRT4, a mitochondrial ADP-ribosyltransferase. *The Journal of biological chemistry* **282**, 33583–92.

Alhazzazi, T. Y., Kamarajan, P., Joo, N., Huang, J.-Y., Verdin, E., D'Silva, N. J. and Kapila, Y. L. (2011a). Sirtuin-3 (SIRT3), a novel potential therapeutic target for oral cancer. *Cancer* **117**, 1670–8.

Alhazzazi, T. Y., Kamarajan, P., Verdin, E. and Kapila, Y. L. (2011b). SIRT3 and cancer: tumor promoter or suppressor? *Biochimica et biophysica acta* **1816**, 80–8.

Allison, S. J. and Milner, J. (2007). SIRT3 is pro-apoptotic and participates in distinct basal apoptotic pathways. *Cell cycle (Georgetown, Tex.)* **6**, 2669–77.

Ashkenazi, A. and Dixit, V. M. (1998). Death receptors: signaling and modulation. *Science (New York, N.Y.)* **281**, 1305–8.

Ashraf, N., Zino, S., Macintyre, A., Kingsmore, D., Payne, A. P., George, W. D. and Shiels, P. G. (2006). Altered sirtuin expression is associated with node-positive breast cancer. *British journal of cancer* **95**, 1056–61.

Azoulay-Zohar, H., Israelson, A., Abu-Hamad, S. and Shoshan-Barmatz, V. (2004). In self-defence: hexokinase promotes voltage-dependent anion channel closure and prevents mitochondria-mediated apoptotic cell death. *The Biochemical journal* **377**, 347–55.

Baines, C. P., Kaiser, R. A., Purcell, N. H., Blair, N. S., Osinska, H., Hambleton, M. A., Brunskill, E. W., Sayen, M. R., Gottlieb, R. A., Dorn, G. W., et al. (2005). Loss of cyclophilin D reveals a critical role for mitochondrial permeability transition in cell death. *Nature* **434**, 658–62.

Baines, C. P., Kaiser, R. A., Sheiko, T., Craigen, W. J. and Molkentin, J. D. (2007). Voltage-dependent anion channels are dispensable for mitochondrial-dependent cell death. *Nature cell biology* **9**, 550–5.

Balaban, R. S., Nemoto, S. and Finkel, T. (2005). Mitochondria, oxidants, and aging. *Cell* **120**, 483–95.

Barger, J. L., Walford, R. L. and Weindruch, R. (2003). The retardation of aging by caloric restriction: its significance in the transgenic era. *Experimental gerontology* **38**, 1343–51.

Basso, E., Fante, L., Fowlkes, J., Petronilli, V., Forte, M. A. and Bernardi, P. (2005). Properties of the permeability transition pore in mitochondria devoid of Cyclophilin D. *The Journal of biological chemistry* **280**, 18558–61.

Bell, E. L., Emerling, B. M., Ricoult, S. J. H. and Guarente, L. (2011). SirT3 suppresses hypoxia inducible factor 1α and tumor growth by inhibiting mitochondrial ROS production. *Oncogene* **30**, 2986–96.

Bernardi, P. (1992). Modulation of the mitochondrial cyclosporin A-sensitive permeability transition pore by the proton electrochemical gradient. Evidence that the pore can be opened by membrane depolarization. *The Journal of biological chemistry* **267**, 8834–9.

Bernardi, P., Vassanelli, S., Veronese, P., Colonna, R., Szabó, I. and Zoratti, M. (1992). Modulation of the mitochondrial permeability transition pore. Effect of protons and divalent cations. *The Journal of biological chemistry* **267**, 2934–9.

Boffa, D. J., Waka, J., Thomas, D., Suh, S., Curran, K., Sharma, V. K., Besada, M., Muthukumar, T., Yang, H., Suthanthiran, M., et al. (2005). Measurement of apoptosis of intact human islets by confocal optical sectioning and stereologic analysis of YO-PRO-1-stained islets. *Transplantation* **79**, 842–5.

Bowlby, S. C., Thomas, M. J., D'Agostino, R. B. and Kridel, S. J. (2012). Nicotinamide phosphoribosyl transferase (Nampt) is required for de novo lipogenesis in tumor cells. *PloS one* **7**, e40195.

Brachmann, C. B., Sherman, J. M., Devine, S. E., Cameron, E. E., Pillus, L. and Boeke, J. D. (1995). The SIR2 gene family, conserved from bacteria to humans, functions in silencing, cell cycle progression, and chromosome stability. *Genes & development* **9**, 2888–902.

Bradham, C. A., Qian, T., Streetz, K., Trautwein, C., Brenner, D. A. and Lemasters, J. J. (1998). The mitochondrial permeability transition is required for tumor necrosis factor alpha-mediated apoptosis and cytochrome c release. *Molecular and cellular biology* **18**, 6353–64.

Bratton, D. L., Fadok, V. A., Richter, D. A., Kailey, J. M., Guthrie, L. A. and Henson, P. M. (1997). Appearance of phosphatidylserine on apoptotic cells requires calcium-mediated nonspecific flip-flop and is enhanced by loss of the aminophospholipid translocase. *The Journal of biological chemistry* **272**, 26159–65.

Brenner, D. and Mak, T. W. (2009). Mitochondrial cell death effectors. *Current opinion in cell biology* **21**, 871–7.

Cardoso, S., Santos, R. X., Carvalho, C., Correia, S., Pereira, G. C., Pereira, S. S., Oliveira, P. J., Santos, M. S., Proença, T. and Moreira, P. I. (2008). Doxorubicin increases the susceptibility of brain mitochondria to Ca(2+)-induced permeability transition and oxidative damage. *Free radical biology & medicine* **45**, 1395–402.

Cardus, A., Uryga, A. K., Walters, G. and Erusalimsky, J. D. (2013). SIRT6 protects human endothelial cells from DNA damage, telomere dysfunction, and senescence. *Cardiovascular research* **97**, 571–9.

Chan, C.-H., Lee, S.-W., Wang, J. and Lin, H.-K. (2010). Regulation of Skp2 expression and activity and its role in cancer progression. *TheScientificWorldJournal* **10**, 1001–15.

Charitou, P. and M Th Burgering, B. (2012). Forkhead Box(O) in Control of Reactive Oxygen Species and Genomic Stability to Ensure Healthy Lifespan. *Antioxidants & redox signaling*.

Chen, D. and Guarente, L. (2007). SIR2: a potential target for calorie restriction mimetics. *Trends in molecular medicine* **13**, 64–71.

Chen, W. Y., Wang, D. H., Yen, R. C., Luo, J., Gu, W. and Baylin, S. B. (2005). Tumor suppressor HIC1 directly regulates SIRT1 to modulate p53-dependent DNA-damage responses. *Cell* **123**, 437–48.

Chen, J., Chan, A. W. H., To, K.-F., Chen, W., Zhang, Z., Ren, J., Song, C., Cheung, Y.-S., Lai, P. B. S., Cheng, S.-H., et al. (2013). SIRT2 overexpression in hepatocellular carcinoma mediates epithelial to mesenchymal transition via akt/GSK-3β/β-catenin signaling (revised version). *Hepatology (Baltimore, Md.)*.

Cheng, E. H. Y., Sheiko, T. V, Fisher, J. K., Craigen, W. J. and Korsmeyer, S. J. (2003). VDAC2 inhibits BAK activation and mitochondrial apoptosis. *Science (New York, N.Y.)* **301**, 513–7.

Chevrollier, A., Loiseau, D., Chabi, B., Renier, G., Douay, O., Malthièry, Y. and Stepien, G. (2005). ANT2 isoform required for cancer cell glycolysis. *Journal of bioenergetics and biomembranes* **37**, 307–16.

Chevrollier, A., Loiseau, D., Reynier, P. and Stepien, G. (2011). Adenine nucleotide translocase 2 is a key mitochondrial protein in cancer metabolism. *Biochimica et biophysica acta* **1807**, 562–7.

Chipuk, J. E., Bouchier-Hayes, L. and Green, D. R. (2006). Mitochondrial outer membrane permeabilization during apoptosis: the innocent bystander scenario. *Cell death and differentiation* **13**, 1396–402.

Choi, M.-M., Huh, J.-W., Yang, S.-J., Cho, E. H., Choi, S. Y. and Cho, S.-W. (2005). Identification of ADP-ribosylation site in human glutamate dehydrogenase isozymes. *FEBS letters* **579**, 4125–30.

Cohen, G. M. (1997). Caspases: the executioners of apoptosis. *The Biochemical journal* **326 (Pt 1**, 1–16.

Cohen, H. Y., Lavu, S., Bitterman, K. J., Hekking, B., Imahiyerobo, T. A., Miller, C., Frye, R., Ploegh, H., Kessler, B. M. and Sinclair, D. A. (2004a). Acetylation of the C terminus of Ku70 by CBP and PCAF controls Bax-mediated apoptosis. *Molecular cell* **13**, 627–38.

Cohen, H. Y., Miller, C., Bitterman, K. J., Wall, N. R., Hekking, B., Kessler, B., Howitz, K. T., Gorospe, M., de Cabo, R. and Sinclair, D. A. (2004b). Calorie restriction promotes mammalian cell survival by inducing the SIRT1 deacetylase. *Science (New York, N.Y.)* **305**, 390–2.

Colman, R. F. and Frieden, C. (1966). On the role of amino groups in the structure and function of glutamate dehydrogenase. I. Effect of acetylation on catalytic and regulatory properties. *The Journal of biological chemistry* **241**, 3652–60.

Crompton, M. and Costi, A. (1988). Kinetic evidence for a heart mitochondrial pore activated by Ca2+, inorganic phosphate and oxidative stress. A potential mechanism for mitochondrial dysfunction during cellular Ca2+ overload. *European journal of biochemistry / FEBS* **178**, 489–501.

Crompton, M., Ellinger, H. and Costi, A. (1988). Inhibition by cyclosporin A of a Ca2+-dependent pore in heart mitochondria activated by inorganic phosphate and oxidative stress. *The Biochemical journal* **255**, 357–60.

Csibi, A., Fendt, S.-M., Li, C., Poulogiannis, G., Choo, A. Y., Chapski, D. J., Jeong, S. M., Dempsey, J. M., Parkhitko, A., Morrison, T., et al. (2013). The mTORC1 Pathway Stimulates Glutamine Metabolism and Cell Proliferation by Repressing SIRT4. *Cell* **153**, 840–54.

Davids, M. S. and Letai, A. (2012). Targeting the B-cell lymphoma/leukemia 2 family in cancer. *Journal of clinical oncology : official journal of the American Society of Clinical Oncology* **30**, 3127–35.

Dehennaut, V. and Leprince, D. (2009). Implication of HIC1 (Hypermethylated In Cancer 1) in the DNA damage response. *Bulletin du cancer* **96**, E66–72.

Dewson, G., Kratina, T., Czabotar, P., Day, C. L., Adams, J. M. and Kluck, R. M. (2009). Bak activation for apoptosis involves oligomerization of dimers via their alpha6 helices. *Molecular cell* **36**, 696–703.

Di Lisa, F., Menabò, R., Canton, M., Barile, M. and Bernardi, P. (2001). Opening of the mitochondrial permeability transition pore causes depletion of mitochondrial and cytosolic NAD+ and is a causative event in the death of myocytes in postischemic reperfusion of the heart. *The Journal of biological chemistry* **276**, 2571–5.

Du, C., Fang, M., Li, Y., Li, L. and Wang, X. (2000). Smac, a mitochondrial protein that promotes cytochrome c-dependent caspase activation by eliminating IAP inhibition. *Cell* **102**, 33–42.

Du, J., Zhou, Y., Su, X., Yu, J. J., Khan, S., Jiang, H., Kim, J. H., Woo, J., Choi, B. H., He, B., et al. (2011). Sirt5 is a NAD-dependent protein lysine demalonylase and desuccinylase. *Science (New York, N.Y.)* **334**, 806–9.

Eliseev, R. A., Malecki, J., Lester, T., Zhang, Y., Humphrey, J. and Gunter, T. E. (2009). Cyclophilin D interacts with Bcl2 and exerts an anti-apoptotic effect. *The Journal of biological chemistry* **284**, 9692–9.

Elrod, J. W., Wong, R., Mishra, S., Vagnozzi, R. J., Sakthievel, B., Goonasekera, S. A., Karch, J., Gabel, S., Farber, J., Force, T., et al. (2010). Cyclophilin D controls mitochondrial pore-dependent Ca(2+) exchange, metabolic flexibility, and propensity for heart failure in mice. *The Journal of clinical investigation* **120**, 3680–7.

Eskes, R., Desagher, S., Antonsson, B. and Martinou, J. C. (2000). Bid induces the oligomerization and insertion of Bax into the outer mitochondrial membrane. *Molecular and cellular biology* **20**, 929–35.

Finley, L. W. S., Haas, W., Desquiret-Dumas, V., Wallace, D. C., Procaccio, V., Gygi, S. P. and Haigis, M. C. (2011a). Succinate dehydrogenase is a direct target of sirtuin 3 deacetylase activity. *PloS one* **6**, e23295.

Finley, L. W. S., Carracedo, A., Lee, J., Souza, A., Egia, A., Zhang, J., Teruya-Feldstein, J., Moreira, P. I., Cardoso, S. M., Clish, C. B., et al. (2011b). SIRT3 opposes reprogramming of cancer cell metabolism through HIF1α destabilization. *Cancer cell* **19**, 416–28.

Frei, B. and Richter, C. (1988). Mono(ADP-ribosylation) in rat liver mitochondria. *Biochemistry* **27**, 529–35.

Frey, N., Katus, H. A., Olson, E. N. and Hill, J. A. (2004). Hypertrophy of the heart: a new therapeutic target? *Circulation* **109**, 1580–9.

Frye, R. A. (1999). Characterization of five human cDNAs with homology to the yeast SIR2 gene: Sir2-like proteins (sirtuins) metabolize NAD and may have protein ADP-ribosyltransferase activity. *Biochemical and biophysical research communications* **260**, 273–9.

Frye, R. A. (2000). Phylogenetic classification of prokaryotic and eukaryotic Sir2-like proteins. *Biochemical and biophysical research communications* **273**, 793–8.

Fu, Z. and Tindall, D. J. (2008). FOXOs, cancer and regulation of apoptosis. *Oncogene* **27**, 2312–9.

Fujimoto, K., Chen, Y., Polonsky, K. S. and Dorn, G. W. (2010a). Targeting cyclophilin D and the mitochondrial permeability transition enhances beta-cell survival and prevents diabetes in Pdx1 deficiency. *Proceedings of the National Academy of Sciences of the United States of America* **107**, 10214–9.

Fujimoto, K., Ford, E. L., Tran, H., Wice, B. M., Crosby, S. D., Dorn, G. W. and Polonsky, K. S. (2010b). Loss of Nix in Pdx1-deficient mice prevents apoptotic and necrotic β cell death and diabetes. *The Journal of clinical investigation* **120**, 4031–9.

Furtado, C. M., Marcondes, M. C., Sola-Penna, M., de Souza, M. L. S. and Zancan, P. (2012). Clotrimazole preferentially inhibits human breast cancer cell proliferation, viability and glycolysis. *PloS one* 7, e30462.

Gall, J. M., Wong, V., Pimental, D. R., Havasi, A., Wang, Z., Pastorino, J. G., Bonegio, R. G. B., Schwartz, J. H. and Borkan, S. C. (2011). Hexokinase regulates Bax-mediated mitochondrial membrane injury following ischemic stress. *Kidney international* **79**, 1207–16.

Galluzzi, L., Vitale, I., Abrams, J. M., Alnemri, E. S., Baehrecke, E. H., Blagosklonny, M. V, Dawson, T. M., Dawson, V. L., El-Deiry, W. S., Fulda, S., et al. (2012a). Molecular definitions of cell death subroutines: recommendations of the Nomenclature Committee on Cell Death 2012. *Cell death and differentiation* **19**, 107–20.

Galluzzi, L., Kepp, O. and Kroemer, G. (2012b). Mitochondria: master regulators of danger signalling. *Nature Reviews Molecular Cell Biology* **13**, 780–788.

García-Ruiz, C., Colell, A., Morales, A., Calvo, M., Enrich, C. and Fernández-Checa, J. C. (2002). Trafficking of ganglioside GD3 to mitochondria by tumor necrosis factor-alpha. *The Journal of biological chemistry* **277**, 36443–8.

George, N. M., Evans, J. J. D. and Luo, X. (2007). A three-helix homo-oligomerization domain containing BH3 and BH1 is responsible for the apoptotic activity of Bax. *Genes & development* **21**, 1937–48.

Gil, R., Barth, S., Kanfi, Y. and Cohen, H. Y. (2013). SIRT6 exhibits nucleosome-dependent deacetylase activity. *Nucleic acids research*.

Giralt, A. and Villarroya, F. (2012). SIRT3, a pivotal actor in mitochondrial functions: metabolism, cell death and aging. *The Biochemical journal* **444**, 1–10.

Gwak, G.-Y., Yoon, J.-H., Kim, K. M., Lee, H.-S., Chung, J. W. and Gores, G. J. (2005). Hypoxia stimulates proliferation of human hepatoma cells through the induction of hexokinase II expression. *Journal of hepatology* **42**, 358–64.

Hafner, A. V, Dai, J., Gomes, A. P., Xiao, C.-Y., Palmeira, C. M., Rosenzweig, A. and Sinclair, D. a (2010). Regulation of the mPTP by SIRT3-mediated deacetylation of CypD at lysine 166 suppresses age-related cardiac hypertrophy. *Aging* **2**, 914–23.

Haigis, M. C., Mostoslavsky, R., Haigis, K. M., Fahie, K., Christodoulou, D. C., Murphy, A. J., Valenzuela, D. M., Yancopoulos, G. D., Karow, M., Blander, G., et al. (2006). SIRT4 inhibits glutamate dehydrogenase and opposes the effects of calorie restriction in pancreatic beta cells. *Cell* **126**, 941–54.

Haigis, M. C., Deng, C.-X., Finley, L. W. S., Kim, H.-S. and Gius, D. (2012a). SIRT3 is a mitochondrial tumor suppressor: a scientific tale that connects aberrant cellular ROS, the Warburg effect, and carcinogenesis. *Cancer research* **72**, 2468–72.

Haigis, M. C., Deng, C.-X., Finley, L. W. S., Kim, H.-S. and Gius, D. (2012b). SIRT3 Is a Mitochondrial Tumor Suppressor: A Scientific Tale That Connects Aberrant Cellular ROS, the Warburg Effect, and Carcinogenesis. *Cancer research* **72**, 2468–72.

Halestrap, A. P., Connern, C. P., Griffiths, E. J. and Kerr, P. M. (1997). Cyclosporin A binding to mitochondrial cyclophilin inhibits the permeability transition pore and protects hearts from ischaemia/reperfusion injury. *Molecular and cellular biochemistry* **174**, 167–72.

Halestrap, A. P., Kerr, P. M., Javadov, S. and Woodfield, K. Y. (1998). Elucidating the molecular mechanism of the permeability transition pore and its role in reperfusion injury of the heart. *Biochimica et biophysica acta* **1366**, 79–94.

Halestrap, A. P., Clarke, S. J. and Javadov, S. A. (2004). Mitochondrial permeability transition pore opening during myocardial reperfusion--a target for cardioprotection. *Cardiovascular research* **61**, 372–85.

Hall, J. A., Dominy, J. E., Lee, Y. and Puigserver, P. (2013). The sirtuin family's role in aging and age-associated pathologies. *The Journal of clinical investigation* **123**, 973–9.

Hallows, W. C., Yu, W., Smith, B. C., Devries, M. K., Devires, M. K., Ellinger, J. J., Someya, S., Shortreed, M. R., Prolla, T., Markley, J. L., et al. (2011). Sirt3 promotes the urea cycle and fatty acid oxidation during dietary restriction. *Molecular cell* **41**, 139–49.

Hamanaka, R. B. and Chandel, N. S. (2010). Mitochondrial reactive oxygen species regulate cellular signaling and dictate biological outcomes. *Trends in biochemical sciences* **35**, 505–13.

He, X., Nie, H., Hong, Y., Sheng, C., Xia, W. and Ying, W. (2012). SIRT2 activity is required for the survival of C6 glioma cells. *Biochemical and biophysical research communications* **417**, 468–72.

Hengartner, M. O., Ellis, R. E. and Horvitz, H. R. (1992). Caenorhabditis elegans gene ced-9 protects cells from programmed cell death. *Nature* **356**, 494–9.

Herranz, D. and Serrano, M. (2010). SIRT1: recent lessons from mouse models. *Nature reviews. Cancer* **10**, 819–23.

Herrero-Yraola, A., Bakhit, S. M., Franke, P., Weise, C., Schweiger, M., Jorcke, D. and Ziegler, M. (2001). Regulation of glutamate dehydrogenase by reversible ADP-ribosylation in mitochondria. *The EMBO journal* **20**, 2404–12.

Hirschey, M. D., Shimazu, T., Goetzman, E., Jing, E., Schwer, B., Lombard, D. B., Grueter, C. A., Harris, C., Biddinger, S., Ilkayeva, O. R., et al. (2010). SIRT3 regulates mitochondrial fatty-acid oxidation by reversible enzyme deacetylation. *Nature* **464**, 121–5.

Hirschey, M. D., Shimazu, T., Capra, J. A., Pollard, K. S. and Verdin, E. (2011a). SIRT1 and SIRT3 deacetylate homologous substrates: AceCS1,2 and HMGCS1,2. *Aging* **3**, 635–42.

Hirschey, M. D., Shimazu, T., Jing, E., Grueter, C. A., Collins, A. M., Aouizerat, B., Stančáková, A., Goetzman, E., Lam, M. M., Schwer, B., et al. (2011b). SIRT3

deficiency and mitochondrial protein hyperacetylation accelerate the development of the metabolic syndrome. *Molecular cell* **44**, 177–90.

Horvitz, H. R. (1999). Genetic control of programmed cell death in the nematode Caenorhabditis elegans. *Cancer research* **59**, 1701s–1706s.

Hsu, H., Xiong, J. and Goeddel, D. V (1995). The TNF receptor 1-associated protein TRADD signals cell death and NF-kappa B activation. *Cell* **81**, 495–504.

Hsu, Y. T., Wolter, K. G. and Youle, R. J. (1997). Cytosol-to-membrane redistribution of Bax and Bcl-X(L) during apoptosis. *Proceedings of the National Academy of Sciences of the United States of America* **94**, 3668–72.

Huffman, D. M., Grizzle, W. E., Bamman, M. M., Kim, J., Eltoum, I. A., Elgavish, A. and Nagy, T. R. (2007). SIRT1 is significantly elevated in mouse and human prostate cancer. *Cancer research* **67**, 6612–8.

Hunter, D. R. and Haworth, R. A. (1979). The Ca2+-induced membrane transition in mitochondria. I. The protective mechanisms. *Archives of biochemistry and biophysics* **195**, 453–9.

Hunter, D. R., Haworth, R. A. and Southard, J. H. (1976). Relationship between configuration, function, and permeability in calcium-treated mitochondria. *The Journal of biological chemistry* **251**, 5069–77.

Hüttemann, M., Pecina, P., Rainbolt, M., Sanderson, T. H., Kagan, V. E., Samavati, L., Doan, J. W. and Lee, I. (2011). The multiple functions of cytochrome c and their regulation in life and death decisions of the mammalian cell: From respiration to apoptosis. *Mitochondrion* **11**, 369–381.

Iborra, M., Moret, I., Rausell, F., Bastida, G., Aguas, M., Cerrillo, E., Nos, P. and Beltrán, B. (2011). Role of oxidative stress and antioxidant enzymes in Crohn's disease. *Biochemical Society transactions* **39**, 1102–6.

Idziorek, T., Estaquier, J., De Bels, F. and Ameisen, J. C. (1995). YOPRO-1 permits cytofluorometric analysis of programmed cell death (apoptosis) without interfering with cell viability. *Journal of immunological methods* **185**, 249–58.

Igney, F. H. and Krammer, P. H. (2002). Death and anti-death: tumour resistance to apoptosis. *Nature reviews. Cancer* **2**, 277–88.

Imai, S., Armstrong, C. M., Kaeberlein, M. and Guarente, L. (2000). Transcriptional silencing and longevity protein Sir2 is an NAD-dependent histone deacetylase. *Nature* **403**, 795–800.

Inuzuka, H., Gao, D., Finley, L. W. S., Yang, W., Wan, L., Fukushima, H., Chin, Y. R., Zhai, B., Shaik, S., Lau, A. W., et al. (2012). Acetylation-Dependent Regulation of Skp2 Function. *Cell* **150**, 179–193.

Jacobs, K. M., Pennington, J. D., Bisht, K. S., Aykin-Burns, N., Kim, H.-S., Mishra, M., Sun, L., Nguyen, P., Ahn, B.-H., Leclerc, J., et al. (2008). SIRT3 interacts with the daf-16 homolog FOXO3a in the mitochondria, as well as increases FOXO3a dependent gene expression. *International journal of biological sciences* **4**, 291–9.

Jeong, S. M., Xiao, C., Finley, L. W. S., Lahusen, T., Souza, A. L., Pierce, K., Li, Y.-H., Wang, X., Laurent, G., German, N. J., et al. (2013). SIRT4 Has Tumor-Suppressive Activity and Regulates the Cellular Metabolic Response to DNA Damage by Inhibiting Mitochondrial Glutamine Metabolism. *Cancer Cell*.

Jia, G., Su, L., Singhal, S. and Liu, X. (2012). Emerging roles of SIRT6 on telomere maintenance, DNA repair, metabolism and mammalian aging. *Molecular and cellular biochemistry* **364**, 345–50.

Jourdain, A. and Martinou, J.-C. (2009). Mitochondrial outer-membrane permeabilization and remodelling in apoptosis. *The international journal of biochemistry & cell biology* **41**, 1884–9.

Kaeberlein, M., McVey, M. and Guarente, L. (1999). The SIR2/3/4 complex and SIR2 alone promote longevity in Saccharomyces cerevisiae by two different mechanisms. *Genes & development* **13**, 2570–80.

Kamarajan, P., Alhazzazi, T. Y., Danciu, T., D'silva, N. J., Verdin, E. and Kapila, Y. L. (2012). Receptor-interacting protein (RIP) and Sirtuin-3 (SIRT3) are on opposite sides of anoikis and tumorigenesis. *Cancer*.

Kapoor, R. R., Flanagan, S. E., Fulton, P., Chakrapani, A., Chadefaux, B., Ben-Omran, T., Banerjee, I., Shield, J. P., Ellard, S. and Hussain, K. (2009). Hyperinsulinism-hyperammonaemia syndrome: novel mutations in the GLUD1 gene and genotype-phenotype correlations. *European journal of endocrinology / European Federation of Endocrine Societies* **161**, 731–5.

Karaca, M., Frigerio, F. and Maechler, P. (2011). From pancreatic islets to central nervous system, the importance of glutamate dehydrogenase for the control of energy homeostasis. *Neurochemistry international* **59**, 510–7.

Kawahara, T. L. A., Michishita, E., Adler, A. S., Damian, M., Berber, E., Lin, M., McCord, R. A., Ongaigui, K. C. L., Boxer, L. D., Chang, H. Y., et al. (2009). SIRT6 links histone H3 lysine 9 deacetylation to NF-kappaB-dependent gene expression and organismal life span. *Cell* **136**, 62–74.

Kendrick, A. a, Choudhury, M., Rahman, S. M., McCurdy, C. E., Friederich, M., Van Hove, J. L. K., Watson, P. A., Birdsey, N., Bao, J., Gius, D., et al. (2011). Fatty liver is associated with reduced SIRT3 activity and mitochondrial protein hyperacetylation. *The Biochemical journal* **433**, 505–14.

Kerr, J. F., Wyllie, A. H. and Currie, A. R. (1972). Apoptosis: a basic biological phenomenon with wide-ranging implications in tissue kinetics. *British journal of cancer* **26**, 239–57.

Kim, S. C., Sprung, R., Chen, Y., Xu, Y., Ball, H., Pei, J., Cheng, T., Kho, Y., Xiao, H., Xiao, L., et al. (2006). Substrate and functional diversity of lysine acetylation revealed by a proteomics survey. *Molecular cell* **23**, 607–18.

Kim, H., Tu, H.-C., Ren, D., Takeuchi, O., Jeffers, J. R., Zambetti, G. P., Hsieh, J. J.-D. and Cheng, E. H.-Y. (2009). Stepwise activation of BAX and BAK by tBID, BIM, and PUMA initiates mitochondrial apoptosis. *Molecular cell* **36**, 487–99.

Kim, H.-S., Patel, K., Muldoon-Jacobs, K., Bisht, K. S., Aykin-Burns, N., Pennington, J. D., van der Meer, R., Nguyen, P., Savage, J., Owens, K. M., et al. (2010). SIRT3 is a mitochondria-localized tumor suppressor required for maintenance of mitochondrial integrity and metabolism during stress. *Cancer cell* **17**, 41–52.

Kojima, K., Ohhashi, R., Fujita, Y., Hamada, N., Akao, Y., Nozawa, Y., Deguchi, T. and Ito, M. (2008). A role for SIRT1 in cell growth and chemoresistance in prostate cancer PC3 and DU145 cells. *Biochemical and biophysical research communications* **373**, 423–8.

Korge, P., Goldhaber, J. I. and Weiss, J. N. (2001). Phenylarsine oxide induces mitochondrial permeability transition, hypercontracture, and cardiac cell death. *American journal of physiology. Heart and circulatory physiology* **280**, H2203–13.

Krauskopf, A., Eriksson, O., Craigen, W. J., Forte, M. A. and Bernardi, P. (2006). Properties of the permeability transition in VDAC1(-/-) mitochondria. *Biochimica et biophysica acta* **1757**, 590–5.

Kroemer, G., Galluzzi, L. and Brenner, C. (2007). Mitochondrial membrane permeabilization in cell death. *Physiological reviews* **87**, 99–163.

Lai, C.-C., Lin, P.-M., Lin, S.-F., Hsu, C.-H., Lin, H.-C., Hu, M.-L., Hsu, C.-M. and Yang, M.-Y. (2013). Altered expression of SIRT gene family in head and neck squamous cell carcinoma. *Tumour biology : the journal of the International Society for Oncodevelopmental Biology and Medicine*.

Landry, J., Sutton, A., Tafrov, S. T., Heller, R. C., Stebbins, J., Pillus, L. and Sternglanz, R. (2000). The silencing protein SIR2 and its homologs are NAD-

dependent protein deacetylases. *Proceedings of the National Academy of Sciences of the United States of America* **97**, 5807–11.

Lazarou, M., Stojanovski, D., Frazier, A. E., Kotevski, A., Dewson, G., Craigen, W. J., Kluck, R. M., Vaux, D. L. and Ryan, M. T. (2010). Inhibition of Bak activation by VDAC2 is dependent on the Bak transmembrane anchor. *The Journal of biological chemistry* **285**, 36876–83.

Lenartowicz, E., Bernardi, P. and Azzone, G. F. (1991). Phenylarsine oxide induces the cyclosporin A-sensitive membrane permeability transition in rat liver mitochondria. *Journal of bioenergetics and biomembranes* **23**, 679–88.

Letai, A., Bassik, M. C., Walensky, L. D., Sorcinelli, M. D., Weiler, S. and Korsmeyer, S. J. (2002). Distinct BH3 domains either sensitize or activate mitochondrial apoptosis, serving as prototype cancer therapeutics. *Cancer cell* **2**, 183–92.

Li, Y., Johnson, N., Capano, M., Edwards, M. and Crompton, M. (2004). Cyclophilin-D promotes the mitochondrial permeability transition but has opposite effects on apoptosis and necrosis. *The Biochemical journal* **383**, 101–9.

Li, S., Banck, M., Mujtaba, S., Zhou, M.-M., Sugrue, M. M. and Walsh, M. J. (2010). p53-induced growth arrest is regulated by the mitochondrial SirT3 deacetylase. *PloS one* **5**, e10486.

Li, Y., Matsumori, H., Nakayama, Y., Osaki, M., Kojima, H., Kurimasa, A., Ito, H., Mori, S., Katoh, M., Oshimura, M., et al. (2011). SIRT2 down-regulation in HeLa can induce p53 accumulation via p38 MAPK activation-dependent p300 decrease, eventually leading to apoptosis. *Genes to cells : devoted to molecular & cellular mechanisms* **16**, 34–45.

Li, M., Li, C., Allen, A., Stanley, C. A. and Smith, T. J. (2012). The structure and allosteric regulation of mammalian glutamate dehydrogenase. *Archives of biochemistry and biophysics* **519**, 69–80.

Lin, D.-T. and Lechleiter, J. D. (2002). Mitochondrial targeted cyclophilin D protects cells from cell death by peptidyl prolyl isomerization. *The Journal of biological chemistry* **277**, 31134–41.

Lin, S. J., Defossez, P. A. and Guarente, L. (2000). Requirement of NAD and SIR2 for life-span extension by calorie restriction in Saccharomyces cerevisiae. *Science (New York, N.Y.)* **289**, 2126–8.

Lin, S.-J., Ford, E., Haigis, M., Liszt, G. and Guarente, L. (2004). Calorie restriction extends yeast life span by lowering the level of NADH. *Genes & development* **18**, 12–6.

Liszt, G., Ford, E., Kurtev, M. and Guarente, L. (2005). Mouse Sir2 homolog SIRT6 is a nuclear ADP-ribosyltransferase. *The Journal of biological chemistry* **280**, 21313–20.

Locksley, R. M., Killeen, N. and Lenardo, M. J. (2001). The TNF and TNF receptor superfamilies: integrating mammalian biology. *Cell* **104**, 487–501.

Lombard, D. B., Alt, F. W., Cheng, H., Bunkenborg, J., Streeper, R. S., Mostoslavsky, R., Kim, J., Yancopoulos, G., Valenzuela, D., Murphy, A., et al. (2007). Mammalian Sir2 homolog SIRT3 regulates global mitochondrial lysine acetylation. *Molecular and cellular biology* **27**, 8807–14.

López-Otín, C., Blasco, M. A., Partridge, L., Serrano, M. and Kroemer, G. (2013). The hallmarks of aging. *Cell* **153**, 1194–217.

Luo, J., Nikolaev, A. Y., Imai, S., Chen, D., Su, F., Shiloh, A., Guarente, L. and Gu, W. (2001). Negative control of p53 by Sir2alpha promotes cell survival under stress. *Cell* **107**, 137–48.

Machida, K., Ohta, Y. and Osada, H. (2006). Suppression of apoptosis by cyclophilin D via stabilization of hexokinase II mitochondrial binding in cancer cells. *The Journal of biological chemistry* **281**, 14314–20.

Majewski, N., Nogueira, V., Robey, R. B. and Hay, N. (2004a). Akt inhibits apoptosis downstream of BID cleavage via a glucose-dependent mechanism involving mitochondrial hexokinases. *Molecular and cellular biology* **24**, 730–40.

Majewski, N., Nogueira, V., Bhaskar, P., Coy, P. E., Skeen, J. E., Gottlob, K., Chandel, N. S., Thompson, C. B., Robey, R. B. and Hay, N. (2004b). Hexokinase-mitochondria interaction mediated by Akt is required to inhibit apoptosis in the presence or absence of Bax and Bak. *Molecular cell* **16**, 819–30.

Majno, G. and Joris, I. (1995). Apoptosis, oncosis, and necrosis. An overview of cell death. *The American journal of pathology* **146**, 3–15.

Mao, Z., Hine, C., Tian, X., Van Meter, M., Au, M., Vaidya, A., Seluanov, A. and Gorbunova, V. (2011). SIRT6 promotes DNA repair under stress by activating PARP1. *Science (New York, N.Y.)* **332**, 1443–6.

Marfe, G., Tafani, M., Indelicato, M., Sinibaldi-Salimei, P., Reali, V., Pucci, B., Fini, M. and Russo, M. A. (2009). Kaempferol induces apoptosis in two different cell lines via Akt inactivation, Bax and SIRT3 activation, and mitochondrial dysfunction. *Journal of cellular biochemistry* **106**, 643–50.

Marín-Hernández, A., Gallardo-Pérez, J. C., Ralph, S. J., Rodríguez-Enríquez, S. and Moreno-Sánchez, R. (2009). HIF-1alpha modulates energy metabolism in

cancer cells by inducing over-expression of specific glycolytic isoforms. *Mini reviews in medicinal chemistry* **9**, 1084–101.

Masmoudi, A., Islam, F. and Mandel, P. (1988). ADP-ribosylation of highly purified rat brain mitochondria. *Journal of neurochemistry* **51**, 188–93.

Mathupala, S. P., Rempel, A. and Pedersen, P. L. (2001). Glucose catabolism in cancer cells: identification and characterization of a marked activation response of the type II hexokinase gene to hypoxic conditions. *The Journal of biological chemistry* **276**, 43407–12.

McCubrey, J. and Demidenko, Z. (2012). Recent discoveries in the cycling, growing and aging of the p53 field. *Aging* **4**, 887–93.

Michishita, E., Park, J. Y., Burneskis, J. M., Barrett, J. C. and Horikawa, I. (2005). Evolutionarily conserved and nonconserved cellular localizations and functions of human SIRT proteins. *Molecular biology of the cell* **16**, 4623–35.

Montaigne, D., Marechal, X., Preau, S., Baccouch, R., Modine, T., Fayad, G., Lancel, S. and Neviere, R. (2011). Doxorubicin induces mitochondrial permeability transition and contractile dysfunction in the human myocardium. *Mitochondrion* **11**, 22–6.

Morris, S. M. (2002). Regulation of enzymes of the urea cycle and arginine metabolism. *Annual review of nutrition* **22**, 87–105.

Mostoslavsky, R., Chua, K. F., Lombard, D. B., Pang, W. W., Fischer, M. R., Gellon, L., Liu, P., Mostoslavsky, G., Franco, S., Murphy, M. M., et al. (2006). Genomic instability and aging-like phenotype in the absence of mammalian SIRT6. *Cell* **124**, 315–29.

Nakagawa, T., Shimizu, S., Watanabe, T., Yamaguchi, O., Otsu, K., Yamagata, H., Inohara, H., Kubo, T. and Tsujimoto, Y. (2005). Cyclophilin D-dependent mitochondrial permeability transition regulates some necrotic but not apoptotic cell death. *Nature* **434**, 652–8.

Nakagawa, T., Lomb, D. J., Haigis, M. C. and Guarente, L. (2009). SIRT5 Deacetylates carbamoyl phosphate synthetase 1 and regulates the urea cycle. *Cell* **137**, 560–70.

Nakamura, Y., Ogura, M., Ogura, K., Tanaka, D. and Inagaki, N. (2012). SIRT5 deacetylates and activates urate oxidase in liver mitochondria of mice. *FEBS letters* **586**, 4076–81.

Naqvi, A., Hoffman, T. A., DeRicco, J., Kumar, A., Kim, C.-S., Jung, S.-B., Yamamori, T., Kim, Y.-R., Mehdi, F., Kumar, S., et al. (2010). A single-

nucleotide variation in a p53-binding site affects nutrient-sensitive human SIRT1 expression. *Human molecular genetics* **19**, 4123–33.

Nemoto, S., Fergusson, M. M. and Finkel, T. (2004). Nutrient availability regulates SIRT1 through a forkhead-dependent pathway. *Science (New York, N.Y.)* **306**, 2105–8.

North, B. J. and Verdin, E. (2004). Sirtuins: Sir2-related NAD-dependent protein deacetylases. *Genome biology* **5**, 224.

North, B. J., Marshall, B. L., Borra, M. T., Denu, J. M. and Verdin, E. (2003). The human Sir2 ortholog, SIRT2, is an NAD+-dependent tubulin deacetylase. *Molecular cell* **11**, 437–44.

Ogura, M., Nakamura, Y., Tanaka, D., Zhuang, X., Fujita, Y., Obara, A., Hamasaki, A., Hosokawa, M. and Inagaki, N. (2010). Overexpression of SIRT5 confirms its involvement in deacetylation and activation of carbamoyl phosphate synthetase 1. *Biochemical and biophysical research communications* **393**, 73–8.

Ota, H., Tokunaga, E., Chang, K., Hikasa, M., Iijima, K., Eto, M., Kozaki, K., Akishita, M., Ouchi, Y. and Kaneki, M. (2006). Sirt1 inhibitor, Sirtinol, induces senescence-like growth arrest with attenuated Ras-MAPK signaling in human cancer cells. *Oncogene* **25**, 176–85.

Palacios, O. M., Carmona, J. J., Michan, S., Chen, K. Y., Manabe, Y., Ward, J. L., Goodyear, L. J. and Tong, Q. (2009). Diet and exercise signals regulate SIRT3 and activate AMPK and PGC-1alpha in skeletal muscle. *Aging* **1**, 771–83.

Park, S.-H., Zhu, Y., Ozden, O., Kim, H.-S., Jiang, H., Deng, C.-X., Gius, D. and Vassilopoulos, A. (2012). SIRT2 is a tumor suppressor that connects aging, acetylome, cell cycle signaling, and carcinogenesis. *Translational cancer research* **1**, 15–21.

Pastorino, J. G. and Hoek, J. B. (2008). Regulation of hexokinase binding to VDAC. *Journal of bioenergetics and biomembranes* **40**, 171–82.

Pastorino, J. G., Simbula, G., Yamamoto, K., Glascott, P. A., Rothman, R. J. and Farber, J. L. (1996). The cytotoxicity of tumor necrosis factor depends on induction of the mitochondrial permeability transition. *The Journal of biological chemistry* **271**, 29792–8.

Pastorino, J. G., Shulga, N. and Hoek, J. B. (2002). Mitochondrial binding of hexokinase II inhibits Bax-induced cytochrome c release and apoptosis. *The Journal of biological chemistry* **277**, 7610–8.

Pedersen, P. L. (1999). Mitochondrial events in the life and death of animal cells: a brief overview. *Journal of bioenergetics and biomembranes* **31**, 291–304.

Pedersen, P. L. (2007). Warburg, me and Hexokinase 2: Multiple discoveries of key molecular events underlying one of cancers' most common phenotypes, the "Warburg Effect", i.e., elevated glycolysis in the presence of oxygen. *Journal of bioenergetics and biomembranes* **39**, 211–22.

Pellegrini, L., Pucci, B., Villanova, L., Marino, M. L., Marfe, G., Sansone, L., Vernucci, E., Bellizzi, D., Reali, V., Fini, M., et al. (2012). SIRT3 protects from hypoxia and staurosporine-mediated cell death by maintaining mitochondrial membrane potential and intracellular pH. *Cell death and differentiation* 1–11.

Pfister, J. A., Ma, C., Morrison, B. E. and D'Mello, S. R. (2008). Opposing effects of sirtuins on neuronal survival: SIRT1-mediated neuroprotection is independent of its deacetylase activity. *PloS one* **3**, e4090.

Pfluger, P. T., Herranz, D., Velasco-Miguel, S., Serrano, M. and Tschöp, M. H. (2008). Sirt1 protects against high-fat diet-induced metabolic damage. *Proceedings of the National Academy of Sciences of the United States of America* **105**, 9793–8.

Picklo, M. J. (2008). Ethanol intoxication increases hepatic N-lysyl protein acetylation. *Biochemical and biophysical research communications* **376**, 615–9.

Rai, N. K., Tripathi, K., Sharma, D. and Shukla, V. K. (2005). Apoptosis: a basic physiologic process in wound healing. *The international journal of lower extremity wounds* **4**, 138–44.

Reitman, Z. J. and Yan, H. (2010). Isocitrate dehydrogenase 1 and 2 mutations in cancer: alterations at a crossroads of cellular metabolism. *Journal of the National Cancer Institute* **102**, 932–41.

Richter, C. and Frei, B. (1988). Ca2+ release from mitochondria induced by prooxidants. *Free radical biology & medicine* **4**, 365–75.

Richter, C., Winterhalter, K. H., Baumhüter, S., Lötscher, H. R. and Moser, B. (1983). ADP-ribosylation in inner membrane of rat liver mitochondria. *Proceedings of the National Academy of Sciences of the United States of America* **80**, 3188–92.

Riddle, S. R., Ahmad, A., Ahmad, S., Deeb, S. S., Malkki, M., Schneider, B. K., Allen, C. B. and White, C. W. (2000). Hypoxia induces hexokinase II gene expression in human lung cell line A549. *American journal of physiology. Lung cellular and molecular physiology* **278**, L407–16.

Roos, N., Benz, R. and Brdiczka, D. (1982). Identification and characterization of the pore-forming protein in the outer membrane of rat liver mitochondria. *Biochimica et biophysica acta* **686**, 204–14.

Roy, S. S., Ehrlich, A. M., Craigen, W. J. and Hajnóczky, G. (2009). VDAC2 is required for truncated BID-induced mitochondrial apoptosis by recruiting BAK to the mitochondria. *EMBO reports* **10**, 1341–7.

Saelens, X., Festjens, N., Walle, L. Vande, Gurp, M. van, Loo, G. van and Vandenabeele, P. (2004). Toxic proteins released from mitochondria in cell death. *Oncogene* **23**, 2861–2874.

Sastre-Serra, J., Nadal-Serrano, M., Gabriel Pons, D., Valle, A., Garau, I., García-Bonafé, M., Oliver, J. and Roca, P. (2013). The oxidative stress in breast tumors of postmenopausal women is ERα/ERβ Ratio dependent. *Free radical biology & medicine*.

Savill, J. and Fadok, V. (2000). Corpse clearance defines the meaning of cell death. *Nature* **407**, 784–8.

Schubert, A. and Grimm, S. (2004). Cyclophilin D, a component of the permeability transition-pore, is an apoptosis repressor. *Cancer research* **64**, 85–93.

Schumacker, P. T. (2011). SIRT3 controls cancer metabolic reprogramming by regulating ROS and HIF. *Cancer cell* **19**, 299–300.

Schwer, B. and Verdin, E. (2008). Conserved metabolic regulatory functions of sirtuins. *Cell metabolism* **7**, 104–12.

Schwer, B., Bunkenborg, J., Verdin, R. O., Andersen, J. S. and Verdin, E. (2006). Reversible lysine acetylation controls the activity of the mitochondrial enzyme acetyl-CoA synthetase 2. *Proceedings of the National Academy of Sciences of the United States of America* **103**, 10224–9.

Schwer, B., Eckersdorff, M., Li, Y., Silva, J. C., Fermin, D., Kurtev, M. V, Giallourakis, C., Comb, M. J., Alt, F. W. and Lombard, D. B. (2009). Calorie restriction alters mitochondrial protein acetylation. *Aging cell* **8**, 604–6.

Sebastián, C., Zwaans, B. M. M., Silberman, D. M., Gymrek, M., Goren, A., Zhong, L., Ram, O., Truelove, J., Guimaraes, A. R., Toiber, D., et al. (2012). The histone deacetylase SIRT6 is a tumor suppressor that controls cancer metabolism. *Cell* **151**, 1185–99.

Semenza, G. L. (2009). Regulation of cancer cell metabolism by hypoxia-inducible factor 1. *Seminars in cancer biology* **19**, 12–6.

Shackelford, R., Hirsh, S., Henry, K., Abdel-Mageed, A., Kandil, E. and Coppola, D. (2013). Nicotinamide Phosphoribosyltransferase and SIRT3 Expression Are Increased in Well-differentiated Thyroid Carcinomas. *Anticancer research* **33**, 3047–52.

Sharov, V. G., Todor, A., Khanal, S., Imai, M. and Sabbah, H. N. (2007). Cyclosporine A attenuates mitochondrial permeability transition and improves mitochondrial respiratory function in cardiomyocytes isolated from dogs with heart failure. *Journal of molecular and cellular cardiology* **42**, 150–8.

Shimazu, T., Hirschey, M. D., Hua, L., Dittenhafer-Reed, K. E., Schwer, B., Lombard, D. B., Li, Y., Bunkenborg, J., Alt, F. W., Denu, J. M., et al. (2010). SIRT3 deacetylates mitochondrial 3-hydroxy-3-methylglutaryl CoA synthase 2 and regulates ketone body production. *Cell metabolism* **12**, 654–61.

Shoshan-Barmatz, V., Zakar, M., Rosenthal, K. and Abu-Hamad, S. (2009). Key regions of VDAC1 functioning in apoptosis induction and regulation by hexokinase. *Biochimica et biophysica acta* **1787**, 421–30.

Shulga, N. and Pastorino, J. G. (2010). Ethanol sensitizes mitochondria to the permeability transition by inhibiting deacetylation of cyclophilin-D mediated by sirtuin-3. *Journal of cell science* **123**, 4117–27.

Shulga, N., Wilson-Smith, R. and Pastorino, J. G. (2009). Hexokinase II detachment from the mitochondria potentiates cisplatin induced cytotoxicity through a caspase-2 dependent mechanism. *Cell cycle (Georgetown, Tex.)* **8**, 3355–64.

Shulga, N., Wilson-Smith, R. and Pastorino, J. G. (2010). Sirtuin-3 deacetylation of cyclophilin D induces dissociation of hexokinase II from the mitochondria. *Journal of cell science* **123**, 894–902.

Sinclair, D. A. and Guarente, L. (1997). Extrachromosomal rDNA circles--a cause of aging in yeast. *Cell* **91**, 1033–42.

Slee, E. A., Adrain, C. and Martin, S. J. (2001). Executioner caspase-3, -6, and -7 perform distinct, non-redundant roles during the demolition phase of apoptosis. *The Journal of biological chemistry* **276**, 7320–6.

Someya, S., Yu, W., Hallows, W. C., Xu, J., Vann, J. M., Leeuwenburgh, C., Tanokura, M., Denu, J. M. and Prolla, T. A. (2010). Sirt3 mediates reduction of oxidative damage and prevention of age-related hearing loss under caloric restriction. *Cell* **143**, 802–12.

Storz, P. (2011). Forkhead homeobox type O transcription factors in the responses to oxidative stress. *Antioxidants & redox signaling* **14**, 593–605.

Strasser, A., Harris, A. W., Bath, M. L. and Cory, S. (1990). Novel primitive lymphoid tumours induced in transgenic mice by cooperation between myc and bcl-2. *Nature* **348**, 331–3.

Sun, Y., Sun, D., Li, F., Tian, L., Li, C., Li, L., Lin, R. and Wang, S. (2007). Downregulation of Sirt1 by antisense oligonucleotides induces apoptosis and enhances radiation sensitization in A549 lung cancer cells. *Lung cancer (Amsterdam, Netherlands)* **58**, 21–9.

Sundaresan, N. R., Gupta, M., Kim, G., Rajamohan, S. B., Isbatan, A. and Gupta, M. P. (2009). Sirt3 blocks the cardiac hypertrophic response by augmenting Foxo3a-dependent antioxidant defense mechanisms in mice. *The Journal of clinical investigation* **119**, 2758–71.

Suzuki, Y., Imai, Y., Nakayama, H., Takahashi, K., Takio, K. and Takahashi, R. (2001). A serine protease, HtrA2, is released from the mitochondria and interacts with XIAP, inducing cell death. *Molecular cell* **8**, 613–21.

Szabó, I., Bernardi, P. and Zoratti, M. (1992). Modulation of the mitochondrial megachannel by divalent cations and protons. *The Journal of biological chemistry* **267**, 2940–6.

Tait, S. W. G. and Green, D. R. (2010). Mitochondria and cell death: outer membrane permeabilization and beyond. *Nature reviews. Molecular cell biology* **11**, 621–32.

Tait, S. W. G. and Green, D. R. (2012). Mitochondria and cell signalling. *Journal of Cell Science* **125**, 807–815.

Tajeddine, N., Galluzzi, L., Kepp, O., Hangen, E., Morselli, E., Senovilla, L., Araujo, N., Pinna, G., Larochette, N., Zamzami, N., et al. (2008). Hierarchical involvement of Bak, VDAC1 and Bax in cisplatin-induced cell death. *Oncogene* **27**, 4221–32.

Tanny, J. C., Dowd, G. J., Huang, J., Hilz, H. and Moazed, D. (1999). An enzymatic activity in the yeast Sir2 protein that is essential for gene silencing. *Cell* **99**, 735–45.

Tanveer, A., Virji, S., Andreeva, L., Totty, N. F., Hsuan, J. J., Ward, J. M. and Crompton, M. (1996). Involvement of cyclophilin D in the activation of a mitochondrial pore by Ca2+ and oxidant stress. *European journal of biochemistry / FEBS* **238**, 166–72.

Tao, R., Coleman, M. C., Pennington, J. D., Ozden, O., Park, S.-H., Jiang, H., Kim, H.-S., Flynn, C. R., Hill, S., Hayes McDonald, W., et al. (2010). Sirt3-mediated deacetylation of evolutionarily conserved lysine 122 regulates MnSOD activity in response to stress. *Molecular cell* **40**, 893–904.

Tomita, T., Kuzuyama, T. and Nishiyama, M. (2011). Structural basis for leucine-induced allosteric activation of glutamate dehydrogenase. *The Journal of biological chemistry* **286**, 37406–13.

Trump, B. F., Berezesky, I. K., Chang, S. H. and Phelps, P. C. (1997). The pathways of cell death: oncosis, apoptosis, and necrosis. *Toxicologic pathology* **25**, 82–8.

Tsujimoto, Y., Yunis, J., Onorato-Showe, L., Erikson, J., Nowell, P. C. and Croce, C. M. (1984). Molecular cloning of the chromosomal breakpoint of B-cell lymphomas and leukemias with the t(11;14) chromosome translocation. *Science (New York, N.Y.)* **224**, 1403–6.

Van Meter, M., Mao, Z., Gorbunova, V. and Seluanov, A. (2011a). Repairing split ends: SIRT6, mono-ADP ribosylation and DNA repair. *Aging* **3**, 829–35.

Van Meter, M., Mao, Z., Gorbunova, V. and Seluanov, A. (2011b). SIRT6 overexpression induces massive apoptosis in cancer cells but not in normal cells. *Cell cycle (Georgetown, Tex.)* **10**, 3153–8.

Vaux, D. L., Cory, S. and Adams, J. M. (1988). Bcl-2 gene promotes haemopoietic cell survival and cooperates with c-myc to immortalize pre-B cells. *Nature* **335**, 440–2.

Vitale, I., Galluzzi, L., Castedo, M. and Kroemer, G. (2011). Mitotic catastrophe: a mechanism for avoiding genomic instability. *Nature reviews. Molecular cell biology* **12**, 385–92.

Vyssokikh, M. Y., Zorova, L., Zorov, D., Heimlich, G., Jürgensmeier, J. J. and Brdiczka, D. (2002). Bax releases cytochrome c preferentially from a complex between porin and adenine nucleotide translocator. Hexokinase activity suppresses this effect. *Molecular biology reports* **29**, 93–6.

Wallace, D. C. (2012). Mitochondria and cancer. *Nature Reviews Cancer* **12**, 685–698.

Wang, X., Carlsson, Y., Basso, E., Zhu, C., Rousset, C. I., Rasola, A., Johansson, B. R., Blomgren, K., Mallard, C., Bernardi, P., et al. (2009). Developmental shift of cyclophilin D contribution to hypoxic-ischemic brain injury. *The Journal of neuroscience : the official journal of the Society for Neuroscience* **29**, 2588–96.

Wang, Q., Zhang, Y., Yang, C., Xiong, H., Lin, Y., Yao, J., Li, H., Xie, L., Zhao, W., Yao, Y., et al. (2010). Acetylation of metabolic enzymes coordinates carbon source utilization and metabolic flux. *Science (New York, N.Y.)* **327**, 1004–7.

Wei, M. C., Lindsten, T., Mootha, V. K., Weiler, S., Gross, A., Ashiya, M., Thompson, C. B. and Korsmeyer, S. J. (2000). tBID, a membrane-targeted death ligand, oligomerizes BAK to release cytochrome c. *Genes & development* **14**, 2060–71.

Wei, M. C., Zong, W. X., Cheng, E. H., Lindsten, T., Panoutsakopoulou, V., Ross, A. J., Roth, K. A., MacGregor, G. R., Thompson, C. B. and Korsmeyer, S. J. (2001). Proapoptotic BAX and BAK: a requisite gateway to mitochondrial dysfunction and death. *Science (New York, N.Y.)* **292**, 727–30.

Willis, S. N., Chen, L., Dewson, G., Wei, A., Naik, E., Fletcher, J. I., Adams, J. M. and Huang, D. C. S. (2005). Proapoptotic Bak is sequestered by Mcl-1 and Bcl-xL, but not Bcl-2, until displaced by BH3-only proteins. *Genes & development* **19**, 1294–305.

Yamamoto, H., Schoonjans, K. and Auwerx, J. (2007). Sirtuin functions in health and disease. *Molecular endocrinology (Baltimore, Md.)* **21**, 1745–55.

Yang, Y., Hou, H., Haller, E. M., Nicosia, S. V and Bai, W. (2005). Suppression of FOXO1 activity by FHL2 through SIRT1-mediated deacetylation. *The EMBO journal* **24**, 1021–32.

Yang, H., Yang, T., Baur, J. A., Perez, E., Matsui, T., Carmona, J. J., Lamming, D. W., Souza-Pinto, N. C., Bohr, V. A., Rosenzweig, A., et al. (2007). Nutrient-sensitive mitochondrial NAD+ levels dictate cell survival. *Cell* **130**, 1095–107.

Yu, W., Dittenhafer-Reed, K. E. and Denu, J. M. (2012). SIRT3 protein deacetylates isocitrate dehydrogenase 2 (IDH2) and regulates mitochondrial redox status. *The Journal of biological chemistry* **287**, 14078–86.

Zamzami, N., Marchetti, P., Castedo, M., Zanin, C., Vayssière, J. L., Petit, P. X. and Kroemer, G. (1995). Reduction in mitochondrial potential constitutes an early irreversible step of programmed lymphocyte death in vivo. *The Journal of experimental medicine* **181**, 1661–72.

Zamzami, N., Hirsch, T., Dallaporta, B., Petit, P. X. and Kroemer, G. (1997). Mitochondrial implication in accidental and programmed cell death: apoptosis and necrosis. *Journal of bioenergetics and biomembranes* **29**, 185–93.

Zancan, P., Sola-Penna, M., Furtado, C. M. and Da Silva, D. (2010). Differential expression of phosphofructokinase-1 isoforms correlates with the glycolytic efficiency of breast cancer cells. *Molecular genetics and metabolism* **100**, 372–8.

Zhang, C. Z., Liu, L., Cai, M., Pan, Y., Fu, J., Cao, Y. and Yun, J. (2012). Low SIRT3 Expression Correlates with Poor Differentiation and Unfavorable Prognosis in Primary Hepatocellular Carcinoma. *PloS one* **7**, e51703.

Zhong, L., D'Urso, A., Toiber, D., Sebastian, C., Henry, R. E., Vadysirisack, D. D., Guimaraes, A., Marinelli, B., Wikstrom, J. D., Nir, T., et al. (2010). The histone deacetylase Sirt6 regulates glucose homeostasis via Hif1alpha. *Cell* **140**, 280–93.

Zhou, S., Starkov, A., Froberg, M. K., Leino, R. L. and Wallace, K. B. (2001). Cumulative and irreversible cardiac mitochondrial dysfunction induced by doxorubicin. *Cancer research* **61**, 771–7.

Zou, H., Henzel, W. J., Liu, X., Lutschg, A. and Wang, X. (1997). Apaf-1, a human protein homologous to C. elegans CED-4, participates in cytochrome c-dependent activation of caspase-3. *Cell* **90**, 405–13.

ABBREVIATIONS

AceCS2- acetyl-CoA synthetase 2

ADP- Adenosine diphosphate

AIF- Apoptosis Inducing Factor

AMPK- 5' AMP-activated protein kinase

ANT- Adenine nucleotide translocator

ATP- Adenosine-5'-triphosphate

Bak- Bcl-2 homologous antagonist/killer

Bax- Bcl-2–associated X protein

Bcl-2- B-cell Lymphoma 2

Bxl-xL- Bcl2 Like 1

CPS1- Carbamoyl phosphate synthetase 1

CR- Calorie restriction

CsA- Cyclosporin A

CTZ- Clotrimazole

CyP-D- Cyclophilin d

DISC- Death Inducing Signaling Complex

DNA- Deoxyribonucleic acid

ERCs-Extrachromosomal rDNA circles

ERK- Extracellular-signal Regulated Kinase

ETC- Electron Transport Chain

FADD- Fas-Associated protein with Death Domain

FOXO- Forkhead box protein subclass O

GDH- Glutamate dehydrogenase

GSK-3β- Glycogen synthase kinase 3β

H3K56- Histone 3 lysine 56

H3K9- Histone 3 lysine 9

HDACs- Histone deacetylases

HIC1- Hypermethylated in cancer 1

HIF1α- Hypoxia Inducible Factor 1α

HKII- Hexokinase II

HMGCS2- 3-hydroxy-3-methylglutaryl-CoA synthase 2

IDE- Insulin degrading enzyme

IDH2- Isocitrate Dehydrogenase 2

IMM- Inner Mitochondrial Membrane

IMS- Intermembrane space

LCAD- Long-chain acyl-CoA dehydrogenase

MAPK- Mitogen-activated protein kinase

Mcl-1- myeloid cell leukemia sequence 1

MEF- Mouse embryonic fibroblast

MMP- Mitochondrial membrane permeabilization

MnSOD2- Manganese Superoxide Dismutase 2

MOMP- Mitochondrial outer membrane permeabilization

MPT- Mitochondrial Permeability Transition

MPTP- mitochondrial Permeability Transition Pore

NAD- Nicotinamide adenine dinucleotide

NAM- Nicotinamide

NAMPT- Nicotinamide phosphoribosyltransferase

OMM- Outer Mitochondrial Membrane

PAO- Phenyl arsine Oxide

PARP1- Poly [ADP-ribose] polymerase 1

PEPCK- Phosphoenolpyruvate carboxykinase

PGC1α- Peroxisome proliferator-activated receptor gamma coactivator 1α

RIP- Receptor interacting protein

ROS- Reactive Oxygen Species

Sir2-Silent information regulator 2

siRNA- short interfering ribonucleic acid

Sirt1-7- Sirtuin 1-7

TCA- Tricarboxylic acid

TNF- Tumor Necrosis Factor

TRADD- TNF receptor type 1-associated Death Domain protein

TRAIL- TNF-related apoptosis-inducing ligand

VDAC- Voltage Dependent Anion Channel

ATTRIBUTES

Attributes:

Figure 1: from ref (North and Verdin, 2004)

Figure 2: from ref (Frye, 2000)

Figure 3: from ref (Yamamoto et al., 2007)

Figure 4: adapted from ref (Schwer and Verdin, 2008)

Figure 5: from ref (Hamanaka and Chandel, 2010)

Figure 6: A and C- Nataly Shulga

B- Manish Verma

Figure 7: A-Nataly Shulga

B-Manish Verma

Figure 8: A and B- Manish Verma

Figure 9: A (Insert)- Nataly Shulga

A and B- Manish Verma

Figure 10: A to D- Manish Verma

Figure 11: A to C- Manish Verma

Figure 12: A to C- Manish Verma

Figure 13: A to C- Manish Verma

Figure 14: A to D- Manish Verma

E- Nataly Shulga

Figure 15: A- Nataly Shulga

B- Manish Verma

Figure 16: A and B- Nataly Shulga

Figure 17: A to F- Manish Verma

Figure 18: A- Manish Verma

B to D- Nataly Shulga

Figure 19: Dr. J.G. Pastorino

Figure 20: A and B- Manish Verma

Figure 21: A- Nataly Shulga

B and C- Manish Verma

Figure 22: A to C- Manish Verma

Figure 23: A and B- Manish Verma

Figure 24: A to C- Manish Verma

Figure 25: A and B- Manish Verma

Figure 26: A and B- Manish Verma

Figure 27: A and B- Manish Verma

Figure 28: Manish Verma

Figure 29: A to C- Manish Verma

Figure 30: A and B- Nataly Shulga

Figure 31: Dr. J. G. Pastorino